Design of an Alternative Glaucoma Drainage Device Using CFD Tools

M.Sc. Thesis

in

Mechanical Engineering

University of Gaziantep

Supervisor

Assist. Prof. Dr. A. İhsan KUTLAR

by

Emre KARA

August 2008

T.C.
GAZİANTEP UNIVERSITY
GRADUATE SCHOOL OF
NATURAL & APPLIED SCIENCES
MECHANICAL ENGINEERING

Name of the thesis: Design of an Alternative Glaucoma Drainage Device Using CFD Tools
Name of the student: Emre KARA
Exam date: 05.08.08

Approval of the Graduate School of Natural and Applied Sciences

Prof. Dr. Sadettin ÖZYAZICI
Director

I certify that this thesis satisfies all the requirements as a thesis for the degree of Master of Science.

Prof. Dr. Sedat BAYSEÇ
Head of Department

This is to certify that we have read this thesis and that in our opinion it is fully adequate, in scope and quality, as a thesis for the degree of Master of Science.

Assist. Prof. Dr. A. İhsan KUTLAR
Supervisor

Examining Committee Members

Prof. Dr. Mehmet D. ÖNER _____

Prof. Dr. Melda ÇARPINLIOĞLU _____

Prof. Dr. Ali Rıza TEKİN _____

Assoc. Prof. Dr. Kıvanç GÜNGÖR _____

Assist. Prof. Dr. A. İhsan KUTLAR _____

ABSTRACT

DESIGN OF AN ALTERNATIVE GLAUCOMA DRAINAGE DEVICE USING CFD TOOLS

KARA, Emre

M.Sc. in Mechanical Engineering

Supervisor: Assist. Prof. Dr. A. İhsan KUTLAR

August 2008, 144 pages

Glaucoma is an eye disorder in which the optic nerve is damaged over time due to a sustained elevation of the intraocular pressure. Being the second leading cause of blindness according to the reports of the World Health Organization, glaucoma is not only a serious ocular disease that threatens individuals, but a community health problem as well. The available contemporary approaches to the treatment of the disease are the medication, surgery and implants. In recent years, great improvement has been achieved in the technology of implants used in the treatment of the disease. Despite the great effort dedicated to the design and implementation of the Glaucoma drainage devices, the implants still have unsolved problems and weaknesses. The Venturi valve device designed by and named after Mateen Ahmed, is a commonly used device. This device has advantages such as compactness, durability, superior drainage mechanism over the others. However, it has a major disadvantage of undesirably coarse pressure control.

At first, the Computational Fluid Dynamics (CFD) analysis of commercially available Ahmed Glaucoma Valve (AGV) is accomplished. In the light of the results, alternative micro-valves are examined and functionally the most appropriate one is integrated into the new designed device. Subsequently, CFD analysis of the new device and AGV are realized by stressing on the superiorities of the new design. Comparison of CFD analyses and experimentally obtained data existing in literature are made. Finally,

improvements on the performance characteristics of the new design are discussed; conclusions are reached and suggestions for future work are presented.

Keywords: CFD analysis, Glaucoma Drainage Device

ÖZET

HAD ARAÇLARI KULLANARAK ALTERNATİF BİR GLOKOM DRENAJ CİHAZI TASARIMI

KARA, Emre
Yüksek Lisans Tezi, Makine Mühendisliği Bölümü
Tez Yöneticisi: Yrd. Doç. Dr. A. İhsan KUTLAR
Ağustos 2008, 144 sayfa

Glokom, göz içi basınçtaki sürekli basınç artışı nedeniyle optik sinirin zaman içinde zarar görmesi ile oluşan bir göz bozukluğudur. Dünya Sağlık Örgütü'nün raporlarına göre körlüğün ikinci sıradaki nedeni olmasıyla, glokom sadece bireyleri tehdit eden ciddi bir göz hastalığı değil, aynı zamanda bir toplum sağlığı sorunudur. Hastalığın tedavisine uygun modern yaklaşımlar ilaç tedavisi, cerrahi müdahale ve implantlardır. Son yıllarda, hastalığın tedavisinde kullanılan implantların teknolojisinde büyük ilerleme kaydedilmiştir. Glokom drenaj implantlarının (GDD) tasarım ve yapımında harcanan büyük çabaya rağmen, implantların hala çözülmemiş sorunları ve zayıflıkları vardır. Mateen Ahmed tarafından tasarlanan ve ondan adını alan Venturi valflı cihaz, sıklıkla kullanılan bir cihazdır. Bu cihazın küçüklük, dayanıklılık, diğerlerinden üstün drenaj mekanizması gibi avantajları vardır. Ancak düşük hassasiyetli basınç kontrolü dezavantajına sahiptir.

İlk olarak piyasada bulunan Ahmed Glokom Valfi'nin (AGV) Hesaplamalı Akışkanlar Dinamiği (HAD) analizi başarılmıştır. Sonuçların ışığında, alternatif mikrovalfler incelenmiş, işlevsel olarak en uygun olanı yeni tasarlanmış cihaza dahil edilmiştir. Daha sonra, yeni tasarımın ve AGV'nin HAD analizleri yeni tasarımın üstünlüklerine önem verilerek gerçekleştirilmiştir. Literatürde bulunan deneysel yöntemlerle elde edilmiş verilerle HAD analizi karşılaştırması yapılmıştır. Son olarak,

yeni tasarımın performans karakteristiğindeki iyileştirmeler tartışılmış; sonuçlara varılmış ve gelecekte yapılabilecek işler için öneriler sunulmuştur.

Anahtar Kelimeler: HAD Analizi, Glokom Drenaj İmplantı

ACKNOWLEDGMENTS

The satisfaction and happiness that accompanies the successful completion of any task would be incomplete without the expression of gratitude and appreciation to the people who made this task possible.

I would like to express my profound gratitude to my advisor, Dr. A. İhsan Kutlar, for his advices, comments, and encouragement during my dissertation research. Observing his critical thinking skills and erudite knowledge has improved me not only professionally, but also more importantly, personally.

I would like to thank medical advisor Dr. Kıvanç Güngör for making this project possible. This thesis would not have taken the shape and progressed without the support of Dr. Güngör. I also thank Dr. Temurhan Kara for being there whenever I feel the lack of medical background.

I also wish to express my sincere appreciation to Prof. Melda Çarpınlıoğlu, and Dr. M. Yaşar Gündoğdu for their support and guidance to improve my skills in the field of fluid mechanics during my study at the University of Gaziantep. I would like to thank Dr. Tolgay Kara for providing academic guidance.

My eternal gratitude goes to my mother for her prayers, love, patience and support. I owe Güler an immeasurable debt of gratitude for her unending patience, endearing encouragement during this master thesis.

Finally, I would like to thank ANOVA company for making FLUENT and GAMBIT software available and Thermodynamics Department for providing the software license through ANOVA.

CONTENTS

page

LIST OF TABLES

page

LIST OF FIGURES

page

NOMENCLATURE

a : The radius/half-edge length of the membrane, mm

A : The cross-sectional area of the flow duct, mm^2

$\bar{a}$: Half of the average width of the flat membrane, mm

C_1 : Geometry and model dependent dimensionless constant

C_2 : Geometry and model dependent dimensionless constant

d : The diameter of the pipe, mm

D_h : Hydraulic diameter, mm

E : Young's modulus of the membrane, Pa

f_F : Fanning friction factor

h : The deflection height, mm

l : The length of the pipe, mm

L : The length of the membrane, m

L_{FD} : Entrance length, mm

n : Aspect ratio

Q : Flow rate of aqueous humor, $\mu l / \min$

p : Applied pressure, Pa

Δp : The pressure drop between the entrance and the exit of the pipe, Pa

P : The wetted perimeter of the duct, mm

Po : Poiseuille Number

r : Radius of the pipe, mm

R : Resistance, Pa-s / m^3

Re : Steady flow Reynolds Number

Re_{crit} : Critical Reynolds Number

t : Thickness of the membrane, mm

V_r : Radial velocity, mm/s

V_θ : Tangential velocity, mm/s

V_z : Axial velocity, mm/s

$V_{z,max}$: Maximum axial velocity, mm/s

$\bar{V}_z$: Average axial velocity, mm/s

y : Deflection of the membrane, mm

Greek Letters

μ : Absolute (dynamic) viscosity of aqueous humor, kg/m.s

ν : Poisson's ratio

ρ : Density of aqueous humor, kg/m^3

σ_o : Internal stress of the membrane, Pa

τ_w : The wall shear stress, Pa

$\overline{\tau_w}$: The perimeter averaged wall shear stress, Pa

ABBREVIATIONS

2ddp	Two-dimensional&double-precision
3ddp	Three-dimensional&double-precision
AC	Anterior chamber
AGFID	Advanced Glaucoma Filtration Implant Device
AGV	Ahmed Glaucoma Valve
AH	Aqueous Humor
CATIA	Computer Aided Three-Dimensional Interactive Application
CFD	Computational Fluid Dynamics
FEM	Finite Element Method
GDD	Glaucoma Drainage Device
GFS	Glaucoma Filtration Surgery
IOP	Intraocular Pressure
MEMS	Micro-Electro-Mechanical-Systems
PC	Phosphorylchlorine
PP	Polypropylene
PI	Polyimide
PMMA	Polymethylmethacrylate
RVK	Reynolds-Von Karman
TUI	Text User Interface
UDC	User Defined Code
UDF	User Defined Function
WHO	World Health Organization

CHAPTER 1

INTRODUCTION

1.1 BACKGROUND AND MOTIVATION

Glaucoma is a group of eye diseases, most often caused by the rise of the pressure within the eye above the normal limits. This increased pressure is usually caused by some form of blocking of the passageways that allow aqueous flow. If it is left untreated, glaucoma can cause blindness. The disease gradually steals sight without warning.

Glaucoma is the second leading cause of blindness in the world according to the World Health Organization (WHO) [1]. About 2% of the world's population between the ages of 40 and 50 and 8% of those over 70 suffers from glaucoma. Although elder people are at a higher risk of glaucoma, approximately one in 10,000 babies is born with the disease. It is estimated that approximately half of the patients suffering glaucoma are not aware of the fact that they already have the disease. Worldwide, there are 67 million estimated cases of glaucoma [1].

Glaucoma can be treated by one of the following means: Medical therapy, surgical treatment and drainage implants [2]. Although none of these methods give utterly satisfactory results, glaucoma implant surgery has lead to gradual success rates with design improvements in the last decade.

The development of glaucoma drainage devices (GDDs) dates back to the beginning of the 20^{th} century [3]. First drainage device was a horse hair placed through the cornea to drain the liquid externally [2]. From horsehair to valved shunting devices, the use of GDDs has come a long way. Most of the current employed devices are very simple and have a major problem of clogging. New

techniques have been devised to overcome the clogging and to improve patient's comfort. One of the new techniques is the Venturi valve device, which was developed by Mateen Ahmed in 1993. The device has advantages such as compactness, durability, and superiority of drainage. However, it has a major deficiency of providing a coarse interval of pressure control. Namely, causing the pressure in the eye to become too high before allowing the fluid drainage thus bringing the risk of further damaging of the optical nerves in one end; and becoming too late to restrict the outflow, therefore, causing over-reduction of the eye pressure which risks the collapse of cornea on the other end [2]. Consequently, it is clear that an improved implant should be designed to eliminate this shortcoming.

An ideal drainage device has to be easy to implant, consistent in operating pressure range, avoid the complications, biomaterially inert, and functional during patient's lifetime. Another design issue of a glaucoma implant is the cost factor. As an example, Ahmed Glaucoma Valve (AGV) is sold at a price of $275 which is quite higher than the other commercially available glaucoma drainage devices. Nevertheless, the cost of the drainage device gives only a slight increase to the total treatment cost. A drainage device functions for patient's lifetime whereas the alternative procedures such as medical, laser and surgical modalities are utilized for a limited period of time. A successful treatment is highly priced. One or more specific operations must be scheduled to implant a device so the cost of the device is less significant by the total cost of the treatment. Thus, the cost factor is not one of the leading problems that should be dealt with. Briefly, the design issues are:

- Ease of implantation
- Effective operation in the pre-specified pressure range
- Use of suitable biomaterials

1.2 OBJECTIVE OF THE THESIS

The primary aim of this thesis is to explore the pitfall of the previous GDDs in order to develop a novel implant by employing Computational Fluid Dynamics (CFD) techniques. When it comes into designing an eye implant, the care should be paid, since the eye is a very delicate organ having a critical role in human body. Even a small mistake in design can be vital.

The studies to improve GDDs were mainly experimental until the last decade. They all use microfluidic test setups and simulate the flow. In order to assist the development of GDDs very few workgroups used CFD technology, but the use of it increases from day-to-day. Newly developed branch of microfluidic studies on GDDs using CFD analysis is a powerful tool and there are rare published articles about the modeling and characterization of the flow through the GDDs using CFD [4-6]. The common points in the CFD simulations are the verification technique of the pressure measurements made in the test setup and trade mark of the simulated part (AGV). The main advantage of CFD is that the results are obtained without the need to construct of the required implant prototype. But this advantage may become a disadvantage if there are no prior validations on the similar cases exist. To overcome this difficulty, validation tests are applied on previously studied cases available in literature.

A further step of this study should be the production of a model implant and carrying the clinical tests on it to prove its reliability and durability.

1.3 OUTLINE OF THE THESIS

In chapter 2 a summary of medical background and review of current GDDs are given. It also examines the implications for drainage device design. Attention then turned to the existing drainage devices that are currently used in clinical practice, together with the problems that can arise in using these devices and some new developments that are already in progress.

Computational models of the AGV and proposed design are the subjects of Chapter 3. The chapter starts with the analytical and CFD models of the pipe flow, as the integral part of all GDDs. Then, the CFD analysis of the flow using GAMBIT and FLUENT software packages for AGV is presented. In the light of the results, the critical part is decided to be the improvement of the valve. Alternative microvalves are reviewed with their beneficial and detrimental effects. A microvalve suiting the operational restrictions to the best is decided and adapted in the new design. Afterwards, the new device is constructed virtually in CATIA and analyzed by using CFD softwares (GAMBIT and FLUENT).

Chapter 4 covers the comparisons of the outputs obtained from the CFD analysis of the new design with the results from that of the AGV design at the same operational range. The same results are also compared with the experimental studies available on AGV in literature. The chapter is followed by the discussion about the feasibility of the new design and the conclusions. Finally, in Chapter 5, a discussion part is included together with conclusions reached and suggestions for future work.

CHAPTER 2

THE EYE AND GLAUCOMA

2.1 INTRODUCTION

The patient with glaucoma is usually asymptomatic until the disease reaches to an advanced stage. Most of the glaucoma patients do not have any clue about the progression of the disease. As the starting point, it is necessary to know about the structure and function of the eye to understand the mechanism of the disease and its progression.

2.2 THE EYE ANATOMY

The eye (Figure 2.1) is a soft tissue organ that is divided into three chambers [7]. The anterior chamber (AC) consists of clear cornea and aqueous humor (AH). The posterior chamber contains the white colored sclera and at the back of the lens, the vitreous body contains gel-like vitreous inside.

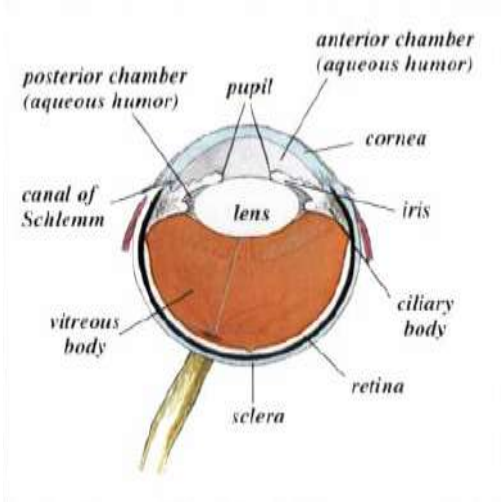

Figure 2.1: Anatomy of the eye [7]

Containing no bone, the eye's shape is maintained by the action of fluid pressure. The vitreous body is filled with a transparent, gel like material called the vitreous. The vitreous body helps to maintain the general shape of the eye. AC is

located behind the cornea and in front of the iris. The posterior chamber is behind the iris and in front of the lens and ciliary bodies. The posterior and anterior chambers are filled with a transparent liquid called the aqueous humor (AH). In addition to providing structure, the AH also supplies the cells of the lens with nutrients and carries away metabolic waste products. Blood, which is normally responsible for this task, is not present in these tissues, since its opaque nature would prevent light from passing through the eye [7]. Some properties of the eye are given in Table 2.1.

Table 2.1: Properties of the eye parts [8]

Eye region	Thermal Conductivity (W/m.K)	Density (kg/m^3)	Heat Capacity (J/kg.K)	Dynamic Viscosity (kg/m.s)	Volume Expansion Coefficient (1/K)
Aqueous Humor	0.58	1000	4200	0.001	0.0003
Cornea	0.58	1000	4200	-	-
Lens	0.40	1000	4200	-	-
Iris	0.58	1000	4200	-	-
Ciliary Body	0.58	1000	4200	-	-

2.2.1 Composition of aqueous humor

Relative to plasma AH has the following properties [9]:

- Slight hypertonicity and acidity (pH 7.2 in AC)
- Marked excess of ascorbate (15 times greater than arterial plasma)
- Marked deficit of protein (0.02% in aqueous vs. 7% in plasma)
- Slight excess of chloride and lactic acid
- Slight deficit of sodium, bicarbonate, carbon dioxide, and glucose
- Protein and antibodies in aqueous equilibrate with those in serum when a plasmoid aqueous occurs with an anterior uveitis
- Albumin/globulin ratio is similar to plasma, although there is less gamma globulin.

The properties of AH are very close to those of water. In the light of the properties given above, the AH is assumed to be a linear viscous liquid similar to water [10].

2.2.2 The mechanism of ocular fluid pressure regulation

Aqueous humor is produced by the ciliary body at a rate of 2-3 μl/min, and flows from posterior chamber through pupil into the AC. This colorless liquid continually drains from the AC both by passing through the porous connecting tissue known as the trabecular meshwork (three dimensional set of diagonally-crossing collagen fibers) before entering the Schlemm's Canal (Figure 2.2) and by uveoscleral outflow (Figure 2.3), resulting in a relatively constant intraocular pressure (IOP). IOP is the fluid pressure inside the AC of the eye. In the normal eye this pressure is around 2000 Pa gage pressure whereas it can increase up to 8000 Pa in eyes suffering the disease of glaucoma [8]. AH is absorbed into the bloodstream after the canal of Schlemm [11]. The average value of IOP in a healthy individual is 2000 Pa, with a ranging from 1600 to 2666 Pa. The aqueous outflow system is structurally organized to act as a mechanical pump, and is part of a vascular circulatory loop, but all other vascular circulatory loops return fluids to the heart by pumping mechanisms.

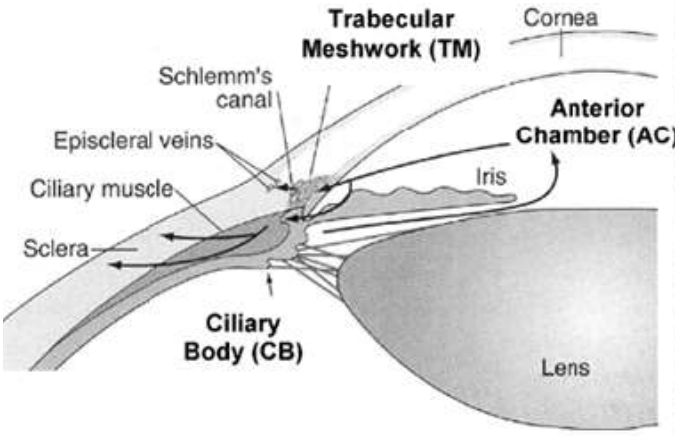

Figure 2.2: A close-up view of the aqueous humor outflow pathway [11]

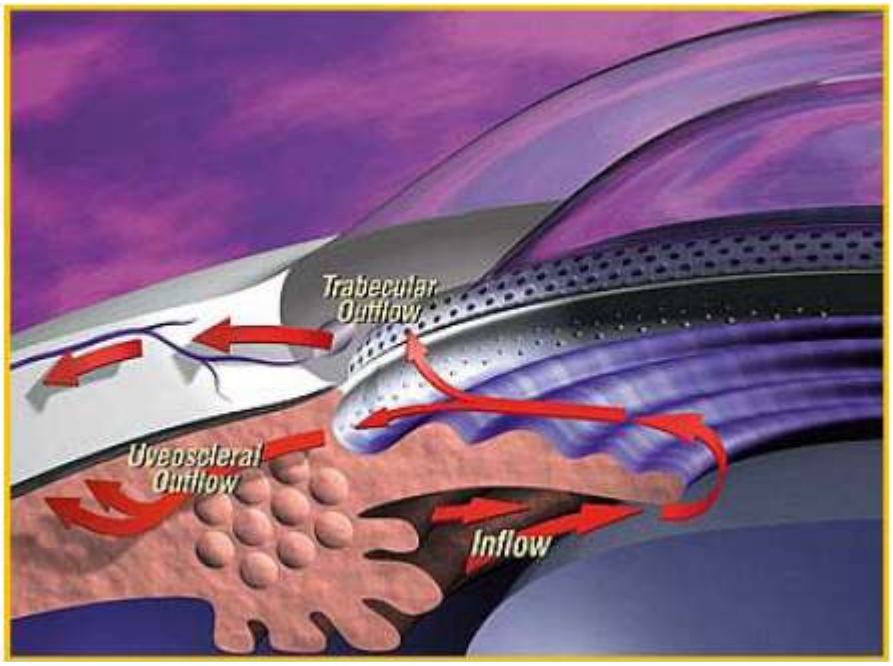

Figure 2.3: Outflow system of human eye [10]

2.2.3 Main mechanism of aqueous humor outflow

The blood circulation in the iris and the ciliary body maintains the temperature of these tissues at the body temperature (37 °C). The outer surface of the cornea (0.6 mm thick) is generally maintained at 32-33 °C by the tear film evaporation. The inner corneal surface is at a lower temperature, which is only 2-4 °C below the body temperature as a result of the thermal resistance provided by the corneal tissues. However, this small temperature difference across the AC is believed to be the dominant mechanism driving the fluid flow in the AC of the eye [8].

2.3 THE GLAUCOMA

Glaucoma is an eye disorder in which the optic nerve is damaged over time due to a sustained elevation of the IOP. Mostly glaucoma develops when the AH drainage pathways become partially or fully blocked, and IOP is elevated due to the increasing resistance to normal outflow. IOP is related to AH flow (Q) and flow resistance (R) by:

$$IOP = Q.R \tag{2.1}$$

This elevated pressure causes irreparable damage to the optic nerve, possibly by inhibiting blood flow in capillaries of the optic nerve, thus preventing nutrients from reaching the individual neurons [12]. If the IOP is permitted to remain above 2666 Pa for an extended period of time, the vision is progressively impaired and blindness eventually results. In extreme cases where IOP can be as high as 8000 or 9000 Pa, blindness may occur within days or even hours [6].

2.3.1 Types of glaucoma

- Primary open angle glaucoma: Primary open angle glaucoma is the most common type of glaucoma and is responsible for approximately 90% of the glaucoma cases. This type of glaucoma develops slowly. As an example, pigmentary glaucoma is a type of primary open angle glaucoma and is caused by pigments from the iris and other eye structures that obstruct the outflow of the AH.

- Low tension glaucoma: Low tension, or normal tension glaucoma causes damage to the optic nerve even though the IOP is normal or low. This is more common in older adults. In the case of low tension glaucoma, even IOP values of 2000–2666 Pa can cause optic nerve damage [13].

- Closed angle glaucoma: Closed angle glaucoma is less common and has severe symptoms. The drainage area is less visible on inspection and is blocked by the iris rotating toward the cornea and causing the folded iris to block the outflow of AH. IOP usually exceeds 8000 Pa in closed angle glaucoma.

- Juvenile glaucoma: Juvenile glaucoma occurs in new-borns whose IOP is high at birth or during the first months of life.

- Secondary glaucoma: Secondary glaucoma occurs as a result of eye deformities, inflammation, or trauma.

- Neovascular glaucoma: Neovascular glaucoma occurs when abnormal blood vessels grow into the AC of the eye and block the drainage channel [7].

2.3.2 Management of glaucoma

Glaucoma treatments can be classified into three groups. These are the medical therapy, surgical treatment and the drainage implants [2].

All current medical therapies for glaucoma are designed to lower IOP. Oral medication can control IOP. Medications constrict the pupil and flatten the iris so that aqueous fluid flows through the canal of Schlemm. In other words, the medications act to reduce the production of AH and increase the outflow of AH. The medications used to treat glaucoma are:

- Miotics - Increase the outflow of AH from the eye
- Epinephrine compounds - Increase the outflow of AH from the eye
- Beta-blockers - Reduce the amount of AH produced in the eye
- Carbonic anhydrase inhibitors and alpha-adrenergic agonists - Reduce the amount of AH produced in the eye. They are the most common among the medications.
- Prostaglandin analogs - Work near the drainage area of the eye to increase the secondary route of AH outflow to lower IOP [14].

Glaucoma, in the majority of patients, can be controlled by medical treatment only. However, about one third of the patients with glaucomatous damage need filtration surgery. The medications also fail frequently. Some common side effects of the medications are redness of the eye, burning and stinging on installation, and allergic reactions of the eye [7].

For some patients, surgery might be the best option. Surgery may be performed first or after attempts to lower IOP with medication. Several types of surgery are available to treat patients with glaucoma. The type and the severity of the glaucoma, the patient's other eye problems, and the patient's health condition are all considerations in selecting the type of operation. Surgery may be performed by using laser or with more conventional approaches, such as incisional surgery, or shunt placement [14].

Glaucoma filtration surgery (GFS) has been shown to be more effective at preventing disease progression than other primary treatment modalities in open angle

glaucoma. Complications associated with poor flow control prevent primary GFS from being offered more widely [2].

- Laser Treatment (Trabeculoplasty): Trabeculoplasty is most often used for patients with open-angle glaucoma. It is performed to create a hole in the iris or the trabecular meshwork that allows for an increased flow of AH within the eye. Unfortunately, the effectiveness falls with time and after 5 years, up to two-thirds fail.

- Trabeculectomy: If laser trabeculoplasty does not control glaucoma, a trabeculectomy is performed. Trabeculectomy is a technique where a drainage channel is constructed between the AC and subconjuctival space.

- Other Surgical Procedures: If a trabeculectomy fails to control glaucoma, other surgical procedures are attempted. An example is the cyclodestructive surgery performed using a laser or cryoprobe to damage the ciliary body to alter the production of aqueous fluid.

Risks associated with these surgical procedures include infection, cataracts, bleeding, and hypotony. Even if the surgery is initially successful, scarring may close the drainage channels at the surface layers in the course of months to a year [14].

Because of the risk of causing visual damage to an eye with normal visual acuity, surgery is usually reserved for cases not responding to medical treatment or patients with advanced disease. Another method to surgically correct glaucoma includes the insertion of a GDD into the AC to drain AH from the eye to lower the IOP.

2.4 GLAUCOMA DRAINAGE DEVICES

Glaucoma is becoming an increasingly important cause of blindness as the world's population ages. New statistics gathered by the WHO in 2002 show that glaucoma is now the second leading cause of blindness worldwide, after cataracts [1]. However, glaucoma presents perhaps an even greater public health challenge than cataracts because the blindness it causes is irreversible. Therefore, WHO

officials are searching for ways to prevent the glaucoma in a definite way [14]. In the treatment of glaucoma, GDDs are the first to manage the problem effectively. The devices have changed considerably in design in the last decade.

2.4.1 Commercial implants

Glaucoma drainage devices are being used more frequently in the treatment of glaucoma that is not responding to medications and trabeculectomy operations. All modern GDDs consist of a tube that shunts AH to an end plate located in the equatorial region of the globe [15-18]. The tubes are all silicone with inside diameter 0.3 mm and outside diameter typically 0.64 mm unless otherwise stated.

Only a handful of glaucoma drainage implant types are commercially available and in common use. Comparisons between the various implant types are, however, difficult because most clinical data are derived from retrospective studies with different study populations, small sample size, limited follow-up, and varied criteria for defining successful outcomes. Tube and plate devices still dominate the contemporary GDD market. Prominent examples, in chronological order, are the Molteno, Schocket, Krupin, Baerveldt, Ahmed, and OptiMed GDDs [2]. These drainage implants differ in their design with respect to the size, shape, and material from which the end plate is manufactured. With a course categorization, two main types of contemporary GDDs are available: the non-valved devices (*e.g.*, the Molteno implant, the Schocket implant, the Baerveldt implant, and the OptiMed implant) and the valved devices (*e.g.*, the Krupin implant, the Ahmed Valve, and Joseph implant) [19]. From Molteno to the newly developed AGV, the comparison is given in the Table 2.2.

Among available GDDs, the Schocket, the OptiMed, and the Joseph implants lack literature review at the present time and will not be considered for modification [20].

All implants are long-tube implants based on the original Molteno design. The Molteno implant, the Baerveldt implant, and the AGV are the GDDs used most commonly, and collectively they have been the subject of several studies that have established their efficiency and safety in clinical use.

Table 2.2: The comparison of contemporary GDDs [2, 14-18]

GDD	Shape	Material	Advantages	Disadvantages
Molteno	Round, dog dish shaped	PP	Concept of tube&plate GDD	Uncontrolled flow mechanism
				Small reduction in IOP
				Hypotony
Schocket	Retinal encircling element	Silicone	Large drainage reservoir	Surgical complications
				Micromotion
Baerveldt	Kidney shaped	Silicone	Easy to modify	Micromotion
			Flexible	Bulky device
			Low profile	Hypotony
			Fenestrations	Diplopia
				Scar deformation
Krupin	Oval shaped	Silicone	Unidirectional slit valve	Bulky device
			Minimal contact with muscles	Valve malfunction
			Flexible	Small surface area
				High profile
OptiMed	Bench of 180 microtubes	PMMA & Silicone	Uniform flow	Occlusion
			Flow restricting model	Bulky device
				Not in business
AGV	Pearl Shaped	PP & Silicone	Simple valve	Valve malfunction
			Venturi Flow	
			Easy to implant	Micromotion
			Minimal contact with muscles	Inflammation
				High profile

The Molteno tube consists of a long, non-valved silicone rubber tube attached to a polypropylene (PP) plate, given in Figure 2.4. Inserted into the eye, the tube facilitates drainage as a product of the pressure differential on either side of the plate [15]. A double-plate form of the Molteno device, introduced in the early 1980s, allows greater IOP control in the postoperative hypertensive phase, and is generally more effective in reducing IOP. Another modification is pressure ridge that is designed to limit the initial drainage area by dividing the top portion of the end plate into two spaces with the help of a V-shaped ridge. The complications such as hypotony or overfiltration are not prevented by the pressure ridge mechanism as Ayyala et al. experienced [20]. The effect appears to be due to the enhanced plate area. These drainage tubes, however, may lead to complications. Molteno devices routinely produce post-operative hypotony. Despite associated complications, the Molteno continues to function as the benchmark against which all subsequent devices are measured [21].

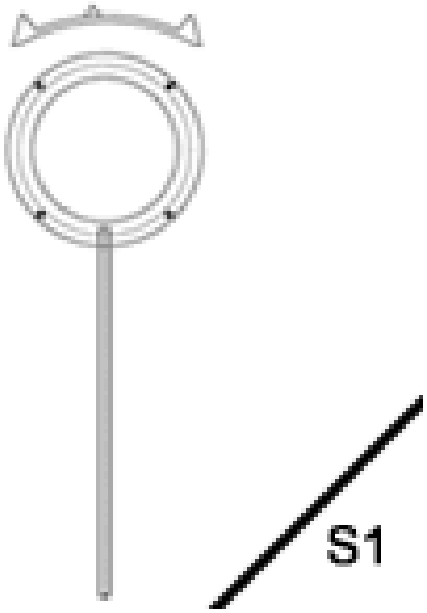

Figure 2.4: Single plate Molteno® implant (S1) [16]

The Baerveldt implant, developed in the early 1990s, consists of a long silicone rubber tube that inserts into a ridge at the anterior aspect of a barium implanted silicone plate, as shown in Figure 2.5. Baerveldt has developed the implant to provide easy placement of large end plate. It is a silicone tube attached to a soft, pliable, barium-impregnated silicone end plate of various sizes (250, 350 or 425

mm^2). The implant may be inserted into a single quadrant, unlike the Molteno device, and is easily secured onto the globe through large fixation holes. The primary advantages of the Baerveldt implant consist of its affordance of larger plate size (and associated increases in IOP reduction) with minimally invasive and relatively simple surgery. The placement of the end plate wings underneath the eye muscles can result in disturbing diplopia. The design has some modifications such as fenestrations in the end plate that may allow limiting fibrous capsule overgrowth [20].

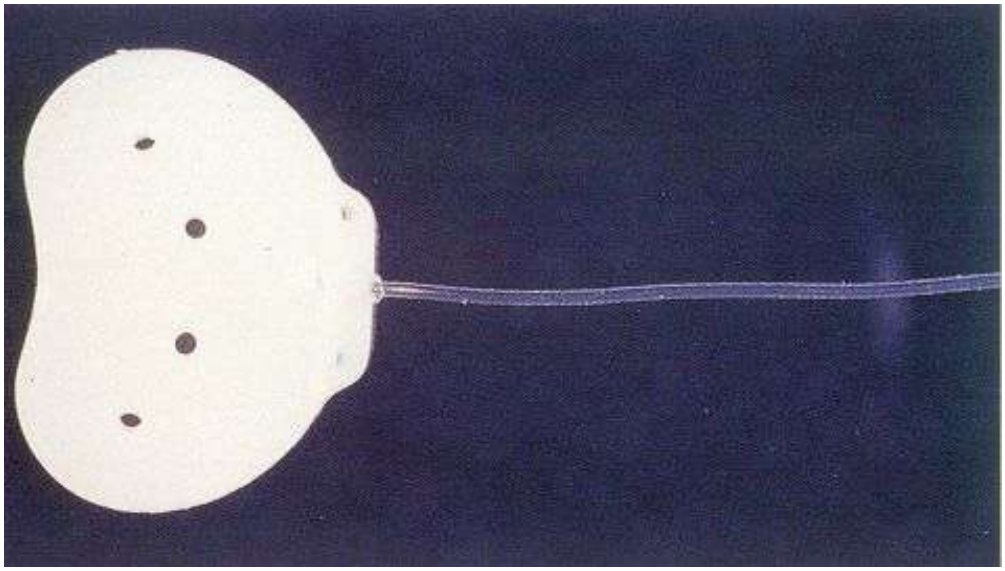

Figure 2.5: Baerveldt glaucoma implant [17]

The Molteno, Schocket, and Baerveldt implants are non-valved. Neither the Baerveldt nor the Schocket implant solves the problem of non-valved drainage devices evident in the first Molteno device. All devices without valves are associated with high risk of hypotony. To address this concern, some tubes without valves were implanted in a two-stage process, with the plate inserted first and the tube later, to prevent the immediate outflow of fluid. This also allows AH reaching the plate surface, resulting in a decreased hypertensive phase and a thinner, more functional bleb. The downside of this tactic was that IOP could not be immediately reduced [22].

Krupin device uses a slit valve at the end of the tube to regulate AH flow (Figure 2.6). The flappers of tubing that form the slit-valve fold completely open even under low pressure. In this scenario, flow resistance would be due only to the tube, making the device similar to the Baerveldt and Molteno designs [23, 25].

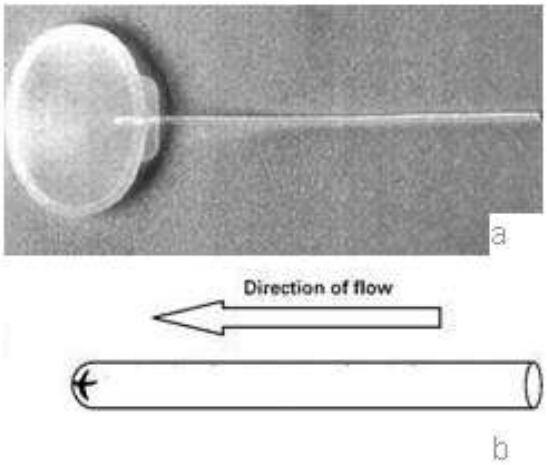

Figure 2.6: Schematics of a) top view of Krupin eye implant and b) Krupin slit valve showing the crossed slit elements [25]

The Ahmed implant (AGV) consists of a silicone tube connected to a silicone sheet valve held in a PP body (Figure 2.7). The valve consists of thin silicone elastomer membranes and creates a Venturi-shaped chamber. The valve is designed to open at an IOP of 1066 Pa, thus avoiding hypotony. The valves on the Ahmed implant are far from perfect and clinical results do not always support manufacturer specification for valve function [26].

Figure 2.7: Ahmed Glaucoma Valve [25]

The major advantage of the valved implant is reduced postoperative hypotony in most cases. Valve blockage, occurring early or late following implantation is the

main disadvantage. Both circumstances result in a failure of aqueous drainage. The valve systems of the Krupin and Ahmed devices are designed to open at 1466 and 1066 Pa, respectively; however, this is not always the case, and hypotony can still occur with these valved implants. Another disadvantage of valved implants is a more intense hypertensive phase and subsequent thicker bleb with less pressure lowering [22].

2.4.2 Published studies on implants

There are numerous literatures that document the effectiveness of various drainage devices in stabilizing IOP where medical therapy, laser treatment, and other surgery proved ineffective. GDDs are the most effective means of reducing IOP and produce the lowest IOPs in eyes with complicated glaucoma [27]. Definitive evidence does not exist that one type of implant is substantially more effective than another. Hong et al. [26] performed a literature review that compares Molteno, Baerveldt, Krupin and Ahmed Implants. They did not find statistically significant differences in either surgical success rate or postoperative IOP in their review of 52 studies. An earlier review by Lim et al. [2] is similarly inconclusive. Implants in general, however, do appear to effectively manage IOP in complicated cases. Due to hypotony (problematically low IOP) complications, implants are predominantly still an option of last resort. In certain complicated cases, implantation of GDDs is becoming a primary operation [28].

Wilson et al. [29] state that the valve system substantially reduces incidence of hypotony, where the AGV has been used as an alternative to traditional filtration surgery. Complication rates in the two procedures appear comparable within a limited period of follow-up. Overall rates of success (as measured by IOP < 2933 Pa) are also comparable across the two procedures. However, at least one study shows that implantation of the AGV fails to control IOP spikes (for 82% of cases) in the first six months of the postoperative period (hypertensive phase) without medical or surgical intervention [30]. The hypertensive phase is less common with trabeculectomy, suggesting that the AGV as a trabeculectomy alternative is less appropriate for patients with advanced optic nerve damage in immediate need of IOP [30]. The hypertensive phase has been documented with double-plate Molteno devices [31] and Krupin discs [32] as well. It may be less frequent with Baerveldt

implants, which have larger surface explants and thus greater drainage potential [30]. Hong et al. [26] provide a comprehensive discussion of device features and their impact on IOP control. Due to the wide variety of study methods and often limited sample sizes, researchers still lack definitive evidence for the effectiveness of particular features.

Table 2.3: Literature summary of the GDDs [14-18]

	Molteno Without Pressure Ridge	**Molteno With Pressure Ridge**	**Baerveldt**	**Ahmed Glaucoma Valve**	**Krupin Valve**
Number of published studies	6	27	9	8	2
Preoperative IOP (Pa)	5612.9	4546.3	4106.3	4519.6	4839.6
Postoperative IOP (Pa)	2279.8	2213.1	1906.5	1906.5	1839.8
Change in IOP (%)	59	51	54	51	62
Surgical success (%)	75	77	75	**79**	72
Transient hypotony (%)	26	12	15	14	17
Chronic hypotony (%)	5	6	6	**2**	2
Diplopia (%)	Not Encountered	2	9	3	7
Suprachoroidal hemorrhage	Not Encountered	4	5	3	8

In summary, the literature reviews conclude that all four devices (Molteno, Baerveldt, Ahmed, and Krupin) appear to be effective in controlling the IOP and preventing the vision loss. So the results of the published articles can be summarized as in Table 2.3, to have a better understanding of strengths and weaknesses of the devices with respect to each other.

The performance results of the GDDs in published literature are very close in the surgical success, IOP management success, preoperative and postoperative IOP. They also have close complication rates (such as diplopia, suprachoroidal hemorrhage). Besides, AGV shows itself as the one with the best performance as a result of its superior hypotony management. Consequently, among the devices which aim to set the initial IOP level by incorporating a non-adjustable resistance mechanism, most effective one is the AGV. The next section focuses on the AGV.

2.4.3 Ahmed Glaucoma Valve

The Ahmed Glaucoma Valve was introduced in 1993. The valved GDD is developed to reduce the incidence of postoperative hypotony. AGV consists of a silicone tube connected to a silicone Venturi valve and the valve is connected to an oblong-shaped PP-made end plate (Figure 2.8). The AGV directs AH flow through the silicone tube and between the membranes of the tapered chamber valve (Figure 2.9) which is designed to provide resistance to aqueous flow [19].

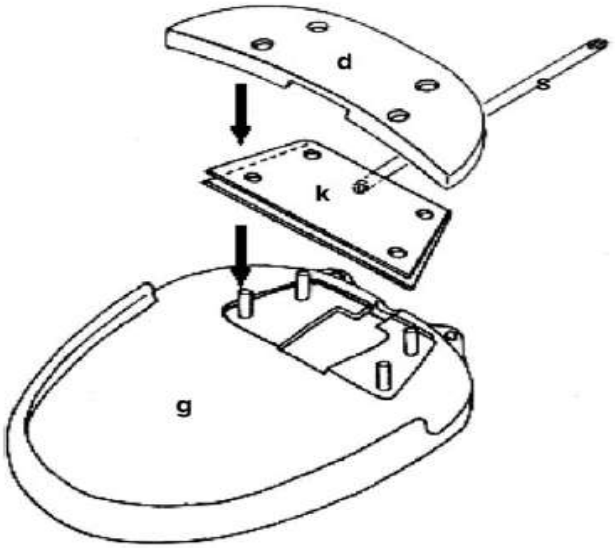

Figure 2.8: AGV assembly

The valve is constructed from two opposed deformable silastic sheets pinned together along the side walls, which run parallel to the direction of AH flow. When AH passes through the channel formed by the two membranes, the fluid pressure pushes the two opposing sheets apart with its free edge forming a one way outlet.

The valve creates a Venturi-shaped chamber. The inlet cross-section of the chamber is wider than the outlet (Bernoulli Principle) and there is a pressure difference between the AC and the bleb that develops on the end-plate. If the AH flow rate increases, the valve leaflets move farther apart. The valve will open at a specific level of IOP, thus reducing the chance of hypotony in the early postoperative period [2]. The AGV that is studied in the present thesis is the model S2 (Figure 2.9).

In vitro studies, the AGV demonstrated a sublinear pressure drop response to increased flow rate, an effect hypothesized to be due to the flexibility of the valve material and the geometry of the valve. The hypothesis tested by this study was that the pressure drop vs. flow-rate curve for the AGV is nonlinear because the valve leaflets continue to deform for increased flow rate, in other words increased upstream pressure. The relatively narrow range of pressure drops that result from a relatively large range of AH flow is, in part, the reason for the AGVs increased popularity. AGV is compared with the other two commercial implants in Table 2.4.

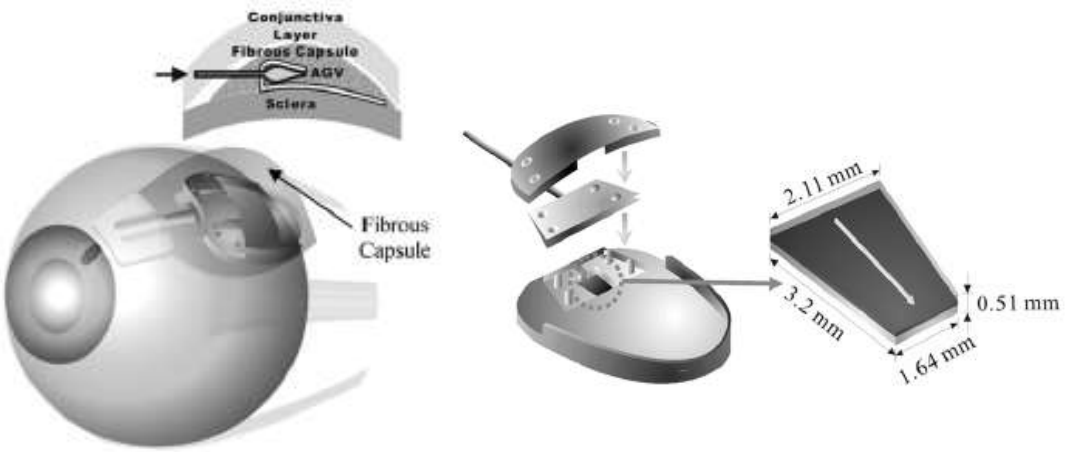

(a) *(b)*

Figure 2.9: Schematics of (a) a standard GDD implanted on an eye with fibrous capsule formed around and (b) discrete components for assembling the AGV Model S2 and dimensions [6]

2.4.3.1 Mechanics of the Ahmed Glaucoma Valve

The main mechanism of AGV is through the tapered valve chamber. The mechanism called Venturi-Flo is to reduce internal friction within the valve system. In that system the AGV utilizes a specially designed, tapered trapezoidal chamber to

create a Venturi effect to help aqueous flow through the device. As can be demonstrated by Bernoulli's equation, the inlet velocity of aqueous entering the larger port of the Venturi-shaped chamber increases significantly as it exits the smaller outlet port of the tapered chamber (Figures 2.10, 2.11). In an AGV this increased exit velocity greatly helps in evacuating aqueous from the valve, thereby helping to reduce valve friction [24].

Table 2.4: Comparison of AGV with other commercially available drainage devices [24]

Product	**Drainage Device**	**Surface Area**	**Valved/Non-Valved**
Ahmed Glaucoma Valve	Model S3	96 mm^2	Valved
	Model S2	184 mm^2	Valved
	Bi-Plate	364 mm^2	Valved
Baerveldt	BG-103-250	250 mm^2	Non-Valved
	BG-101-350	350 mm^2	Non-Valved
	BG-103-425	425 mm^2	Non-Valved
Molteno	Single-Plate	135 mm^2	Non-Valved
	Double-Plate	270 mm^2	Non-Valved
Type	**Ahmed Glaucoma Valve**	**Baerveldt**	**Molteno**
Success Rate (Lowering IOP)	95%	72%	60%
Visual Acuity	82%	62%	70%
Hypotony (Occurrence)	9%	26%	14.6%

Non-obstructive, self-regulating mechanism is the second trademark mechanism of AGV. For the flow to be non-obstructive, a particle large enough to pass through the hole of the tube should easily pass through a much larger opening of the Venturi-Flow chamber. The elastic membranes help to regulate fluid flow at all

times, consistently by changing their shape. The tension on these membranes is responsible for reducing hypotony [24].

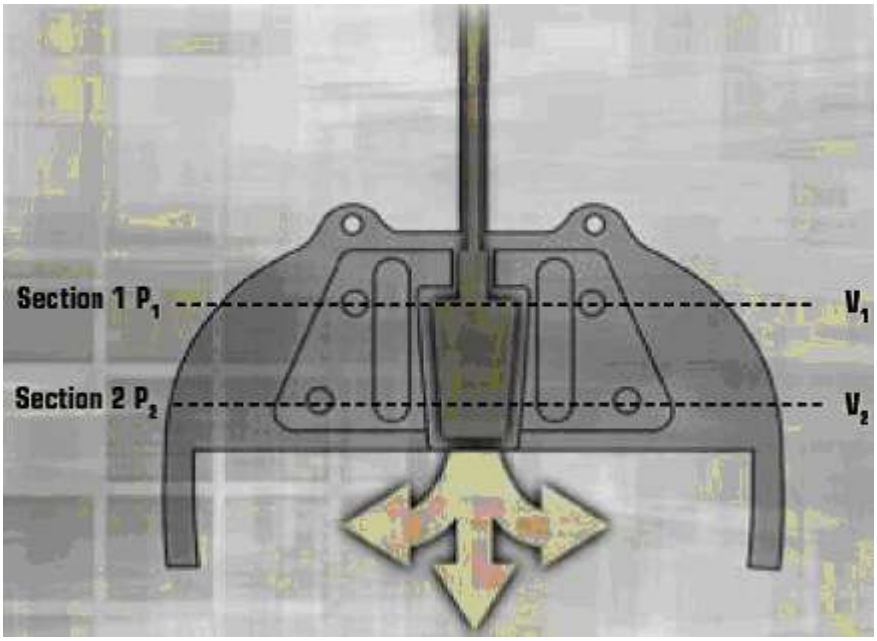

Figure 2.10: Flow path inside the AGV [24]

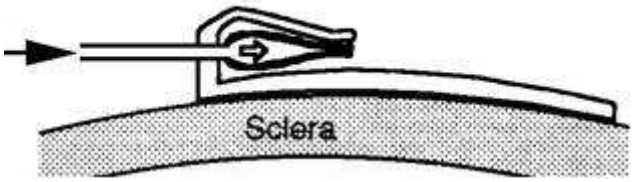

Figure 2.11: Schematic drawing of the resistance mechanism of the AGV [25]

2.4.3.2 Main Problems with AGV

Design issue is the most important problem of AGV. For all GDDs, after the device is implanted, the body reacts to this foreign object and begins to encapsulate it with fibrous tissue, forming a bleb. This bleb is extremely important in the operation of the device, because it is the principal source of resistance to the flow of AH through the device. The bleb must grow to a suitable size to regulate the pressure acceptably and this is a major feature in the success or failure of individual cases. Pearl-shaped end plate of AGV is surrounded by a high-degree bleb encapsulation around it.

The valve functioning is not so well in AGV system. AGV has a higher risk in the first week after shunt implantation, probably due to poor valve function. AGV has a significantly greater risk of developing a hypertensive phase (83.5%) compared with the double-plate Molteno (43.5%) [33]. The AGV is reported not to eliminate the risk of other complications associated with ocular hypotony, such as AC flattening and choroidal detachment [38]. The valves in the AGV implant function as flow-restriction devices or regulators rather than as valves that truly open and close in response to pressure change after immersion in fluid [35]. Although the manufacturers claim that the device has true valve, the valve appears to not close after initial opening in perfusion tests at physiological flow rates (i.e. 2-3 μl/min) [36]. The valves may not always open when they should, may not always close when the pressure drops and may have varying opening set points. These results may indicate problems both in design and in manufacture and claims may be overstated for commercial reasons.

Another problem of AGV is the oblong shape. The potential for micromotion may be more pronounced with implants like the AGV that have an oblong-shape and positioned in an anterioposterior direction. The patient is not comfortable with this micromotion so that the ergonomics is another issue to be considered [35].

Frictional effects are negligible in AGV as in the case of other implants. According to a study by Francis, et al. [36], the pressure drop of the AGV is independent of the flow rate in the 0 to 100 μl/min range. This implies that at physiological flow rate (2.5 μl/min) the pressure drop due to the friction is negligible. Therefore, it is the pressure drop across the valve (in other words, the pressure needed to keep the two leafs of the silicone elastomer membrane apart to create the path for the AH outflow) that dominates the total pressure drop.

2.4.4 Novel implants

Current GDDs have low flow performance, less biocompatibility and some design flaws. Some adaptations and modifications for the existing GDDs are developed for better flow control, low leakage, etc. These devices are not commercially available worldwide or they have no studies in vivo. Newly developed implants can only be a reference to the model that is to be designed.

2.4.4.1 The Advanced Glaucoma Filtration Implant Device (AGFID)

The Advanced Glaucoma Filtration Implant Device (AGFID) is designed to eliminate the leakage (Figure 2.12). The device is coated with phosphoryl chlorine (PC), which has been demonstrated to reduce protein adhesion. The novel GDD has a small diameter hole to provide the required resistance and a larger diameter hole for large flow rate needs. They adapted existing methods of evaluating GDD flow performance in an examination of internal flow control using single small diameters as flow resistors [37]. The device is not commercially available and there are no articles about the device, positive or negative.

Figure 2.12: AGFID drainage device [37]

2.4.4.2 The Ex-PRESS mini glaucoma shunt

There is another GDD that is newly developed and will soon be in the market. The most recently introduced device, the Ex-PRESS Mini Glaucoma Shunt, is explicitly designed to replace trabeculectomy as an initial surgical intervention. The Ex-PRESS Mini Glaucoma Shunt (Optonol, Neve Ilan, Israel), made of implantable stainless steel, is a non-valved glaucoma drainage implant that resembles a small arrowhead [38]. It shunts aqueous humor from anterior chamber to the episcleral space directly (Figure 2.13).

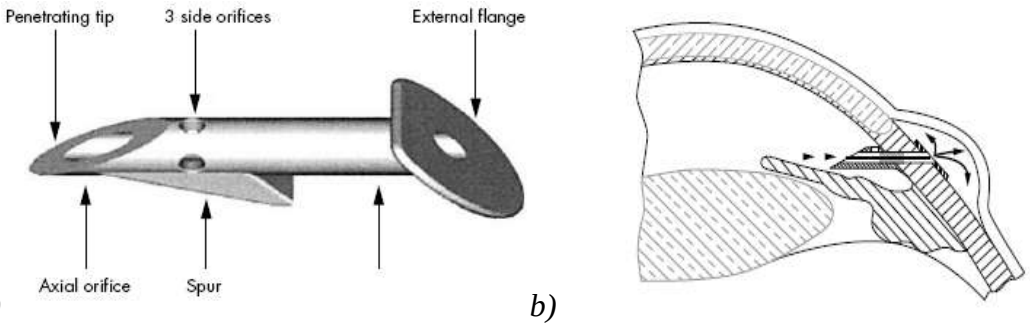

a) *b)*

Figure 2.13: Schematic drawing of a) the Ex-PRESS miniature implant (3 mm long, 400-micron outer diameter) [39] and b) the Ex-PRESS implant in situ [38]

The advantages of Ex-PRESS implant, being a shunt device, are results of its simplicity. Its size is intended to make insertion simple and avoid surgical trauma to ocular tissue associated with trabeculectomy. A combination of design and biomaterial improvements coupled with an easier, more rapid and less traumatic implantation technique. The Ex-PRESS implant, which is made of stainless steel, offers better biocompatibility characteristics than polymers [39].

Long-term complications associated with the Ex-PRESS shunt include shunt erosion through the conjunctiva, and device malposition and rotation [34]. The correct positioning of the implant is the most crucial consideration for preventing complications [38]. The Ex-PRESS implant is explicitly designed to replace trabeculectomy as an initial surgical intervention, but it is not functional. Recent reports on the miniature Ex-PRESS implant support its effectiveness in controlling IOP in complicated glaucomas resistant to other treatments. As Wamsley et al. [41] stated, complications in this area have raised serious concerns about the safety of the device, despite its ability to control IOP in difficult cases. Also, experimental comparative trials have not yet appeared.

2.4.4.3 SmartFlow glaucoma stent

An MIT Project, The SmartFlow glaucoma implant [42], is designed to increase and maintain the fluid outflow from the eye in order to decrease the IOP and prevent damage to the optic nerve. The usage of current glaucoma implants serve to reduce pressure and prevent further damage to the optical nerve, however, damage to the optical nerve head is permanent and vision will not improve with any current or research device. Since it has been recently developed, there are no available reports on the device in literature. The device seems to be very functional but further information is needed.

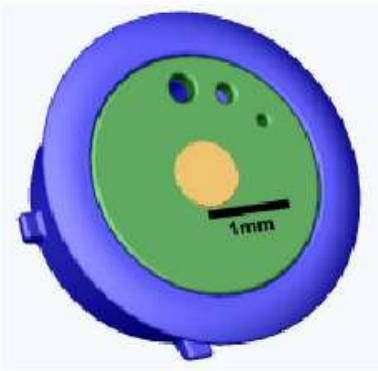

Figure 2.14: SmartFlow implant [42]

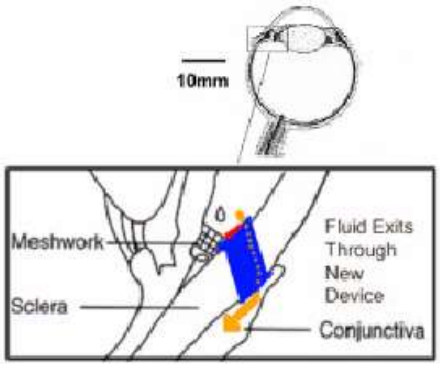

Figure 2.15: Device inserted into eye [42]

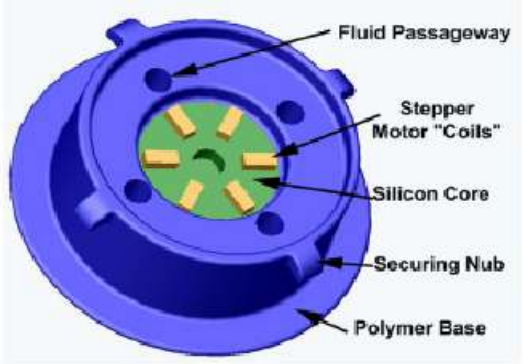

Figure 2.16: Internal view of device [42]

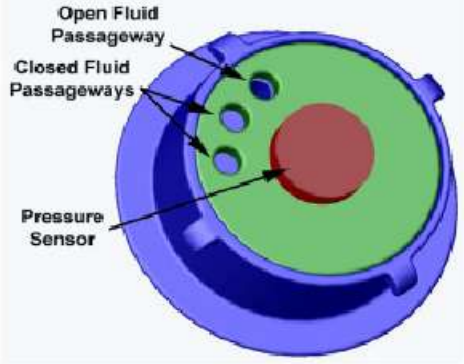

Figure 2.17: Rear view of device [42]

After all the advantages and disadvantages of the commercially available GDDs are revealed, the AGV is concluded to be the most efficient device. The implant has some malfunctions as mentioned in section 2.4.3.2. Microfluidic characterization of GDDs in CFD will be applied on AGV to get rid of these malfunctions and to design a better implant. This new analysis technique has been applied previously by a researcher group as a part of research project. In 2003, Pan et al. [4] reported on the microfluidic characterization of a valved GDD (AGV). They ended up with three-dimensional mechanical and fluidic models that were numerically solved using ANSYS and FLUENT softwares. Two years after this study, Pan et al. [5] developed a new Finite Element Method (FEM) simulation, based on the Lubrication-Von Karman model. They used that model to analyze the valve's mechanical and fluidic performances at the same time. They ended up with a required IOP limit for a healthy eye. In late 2005, a fluid-solid analysis of flow through the Ahmed GDD was maintained using FEM [6]. Coupled fluid-solid physics of the AGV was used to reduce the difficulty of solving three-dimensional Navier-Stokes and solid equilibrium relations on the deforming domain (valve part). All three studies reveal the significance of the effects of the modulus and yield strength of the valve membranes on the resistance to flow. In light of the results they have obtained, Pan et al. [5] have concluded that for given a fixed pressure drop and viscosity, the flow rate is proportional to the pressure drop and the channel height inside the valve membranes. The constants and variables used in these three studies are compared in Table 2.5.

Table 2.5: Comparison of the constant and variables of the studies [4, 5, 6]

Article / **Property**	Pan et al. [4]	Pan et al. [5]	Pan et al. [6]
Aqueous Flow Rate (μl/min)	2.5 μl/min	2.5 μl/min	1.6 μl/min
Pressure Drop (Pa)	1066-1200 Pa	933-1066 Pa	640-746 Pa
Valve Membrane Modulus (MPa)	4.2 MPa	26.65 MPa	4.2 MPa
Valve Membrane Poisson's Ratio	0.45	0.45	0.45
Model Name	Coupled Solid-Fluid Analysis	Von Karman Plate Model	Reynolds-Von Karman (RVK) Model

The constants and variables given above were obtained using a unique mathematical model that correlates the leaflet deformation of the AGV and the flow through the valve. The leaflets of the AGV are modeled using the Von Karman plate theory coupled to a lubrication theory model of the aqueous flow through the valve. The resulting two-dimensional coupled steady-state partial differential equation system is solved using the FEM.

Researchers working on GDDs have developed computational models to have a better understanding of the operating principle and dynamics of the microfluidic flow inside the devices. In recent years, the development of new CFD softwares and high-speed computers has given the opportunity to do simulations and obtain reliable numerical test results without conducting empirical tests or clinical studies. Unfortunately, the method is quite new and many researches lack of the qualification to use the softwares in these respects. In Turkey, engineers are not very interested in modeling the microfluidic systems. Worldwide, there are only a few worked models about newly developed GDDs [37, 39, 42].

As a unique mathematical model that correlates the leaflet deformation of the AGV and the flow through the valve, Pan et al. [4] used FEM simulations, based on the lubrication-von Karman model, and then analyzed the valve's mechanical and fluidic performance. They modeled the leaflets of the AGV using the von Karman

plate theory coupled to a Reynolds lubrication theory model of the AH flow through the valve. In other words, they used the coupled solid-fluid model to analyze the flow of AH through AGV. The resulting two-dimensional coupled steady-state partial differential equation system is solved by FEM [5]. They analyzed AGV both experimentally and computationally, but they have not developed a new design as the result of their simulations and verifications. In the present thesis, the method used by Pan et al. [4] constitutes the starting point. A new design is proposed in the light of the simulation results on AGV.

CHAPTER 3

THREE DIMENSIONAL MODELING

3.1 MATHEMATICAL MODEL

In order to describe the flow regime (i.e. laminar or turbulent) in a closed conduit such as a pipe or a valve as in the object of the thesis, the Reynolds number must be calculated as the first critical criteria. For pipe flows, the Reynolds number is larger than the critical Reynolds number (Re_{crit}~2300), the flow turns out to be in the turbulent regime. As soon as the regime is reversed (i.e. reducing the Reynolds number), the flow turns back to laminar flow. In the case of microchannels and micromachined fluid systems (e.g. micropumps and microvalves), the dimensions are in orders of mm and μm, which make the Reynolds number well below the critical threshold. Therefore, the flows in microfluidic devices are generally accepted as laminar [37]. Laminar flow is an advantage to study, since the flow is easier to understand and manipulate than the turbulent flow. In the following sections, the fundamentals of microfluidics are described.

3.2 MICROFLUIDIC THEORY

In a microscale fluidic channel, the scaling down effect makes some physical parameters (i.e. inertia, gravity) less important than parameters such as viscosity. Basic fluid mechanics can still be applied to microfluidics, but with some assumptions. Fluid flows in microchannels and micromachined fluid systems (e.g. micropumps and microvalves) are analyzed using the Navier-Stokes equations. However, a number of publications have shown that the flows on the microscale are different from that on the macroscale and that the Navier-Stokes equations alone are incapable of modeling the occurring phenomena [43]. In order to design such microdevices effectively, the fluid flow on the microscale must be well understood.

Several effects, which are normally neglected when considering macroscale flow, may be significant at the microscale. The first of these microscale phenomena are the 2D and 3D transport effects. As the characteristic lengths are reduced to the same order of magnitude as the hydrodynamic boundary layer thickness, momentum transfer in directions other than the streamwise direction can increase significantly. Other effects that may play a more significant role at the microscale include temperature variations, viscosity variation near the solid surface, slip flow at the boundary and the micropolar fluid effects [43].

3.2.1 Hagen-Poiseuille Flow

Consider the fully developed laminar flow of an incompressible viscous liquid in a pipe. In the cylindrical coordinate system, the viscous flow velocity profile through the cross-section of the circular pipe for two-dimensional, steady and incompressible laminar flow is given in Figure 3.1.

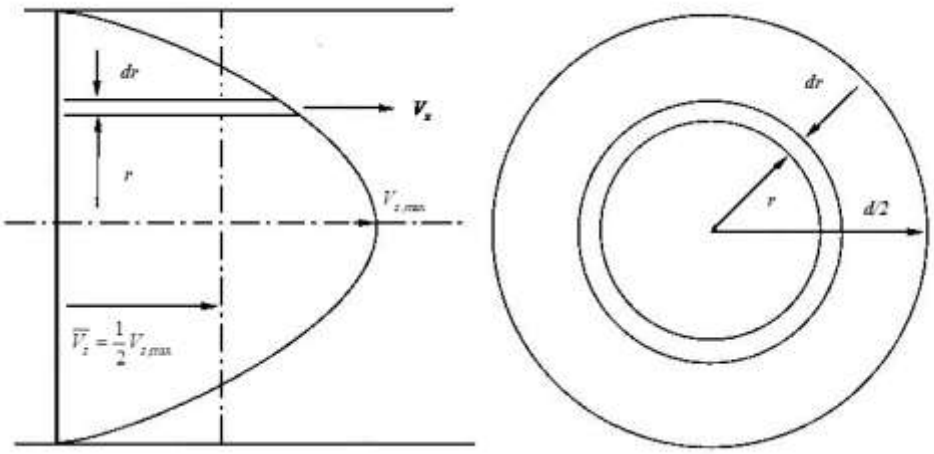

Figure 3.1: Viscous flow in a circular pipe

For the steady flow of an incompressible fluid with constant viscosity in the absence of body forces in a circular pipe, the Navier-Stokes equations in the cylindrical coordinate system are given as follows [44],

$$V_r \frac{\partial V_r}{\partial r} + \frac{V_\theta}{r}\frac{\partial V_r}{\partial \theta} + V_z \frac{\partial V_r}{\partial z} = -\frac{1}{\rho}\frac{\partial p}{\partial r} + \frac{\mu}{\rho}\left[\frac{1}{r}\frac{\partial}{\partial r}\left(r\frac{\partial V_r}{\partial r}\right) + \frac{1}{r^2}\frac{\partial^2 V_r}{\partial \theta^2} + \frac{\partial^2 V_r}{\partial z^2} - \frac{V_r}{r^2} - \frac{2}{r^2}\frac{\partial V_\theta}{\partial \theta}\right] \tag{3.1a}$$

$$V_r\frac{\partial V_\theta}{\partial r}+\frac{V_\theta}{r}\frac{\partial V_\theta}{\partial \theta}+V_z\frac{\partial V_\theta}{\partial z}+\frac{V_rV_\theta}{r}=-\frac{1}{\rho r}\frac{\partial p}{\partial \theta}+\frac{\mu}{\rho}\left[\begin{array}{l}\frac{1}{r}\frac{\partial}{\partial r}\left(r\frac{\partial V_\theta}{\partial r}\right)+\frac{1}{r^2}\frac{\partial^2 V_\theta}{\partial \theta^2}\\ +\frac{\partial^2 V_\theta}{\partial z^2}-\frac{V_\theta}{r^2}+\frac{2}{r^2}\frac{\partial V_r}{\partial \theta}\end{array}\right] \tag{3.1b}$$

$$V_r\frac{\partial V_z}{\partial r}+\frac{V_\theta}{r}\frac{\partial V_z}{\partial \theta}+V_z\frac{\partial V_z}{\partial z}=-\frac{1}{\rho}\frac{\partial p}{\partial z}+\frac{\mu}{\rho}\left[\frac{1}{r}\frac{\partial}{\partial r}\left(r\frac{\partial V_z}{\partial r}\right)+\frac{1}{r^2}\frac{\partial^2 V_z}{\partial \theta^2}+\frac{\partial^2 V_z}{\partial z^2}\right] \tag{3.1c}$$

The flow through a straight pipe of circular cross-section is the case with rotational symmetry which corresponds to the case of two-dimensional flow through a channel. The velocity components in the tangential and radial directions are zero, since the flow is axisymmetric. The velocity component parallel to axis, denoted by V_z, depends on *r* alone, and the pressure is constant in every cross-section [44]. Since the flow is fully developed, then $\frac{\partial V_z}{\partial z}$ is zero at every point of the flow field, and $\frac{\partial^2 V_z}{\partial z^2}$ is also zero everywhere. Of the three Navier-Stokes equations in cylindrical coordinates, eqns. 3.1, only one for the axial direction remains, and it simplifies to,

$$\frac{1}{r}\frac{\partial}{\partial r}\left(r\frac{\partial V_z}{\partial r}\right)=\frac{1}{\mu}\frac{\partial p}{\partial z} \tag{3.2}$$

Eqn. 3.2 holds for steady, isothermal, incompressible, fully developed laminar flow of Newtonian fluids through constant cross-section pipes. Boundary conditions are,

$$\text{at}\qquad r=0\qquad\qquad \frac{\partial V_z}{\partial r}=0 \tag{3.3}$$

$$\text{at}\qquad r=\frac{d}{2}\qquad\qquad V_z=0 \tag{3.4}$$

where *d* is the diameter of the pipe. Integrating the equation with respect to *r* twice gives,

$$V_z = \frac{1}{4\mu}\left[r^2 - \frac{d^2}{4}\right]\frac{dp}{dz} \tag{3.5}$$

It is easy to determine the volumetric flow rate Q through the pipe,

$$Q = \int_0^{2\pi}\int_0^{\frac{d}{2}} V_z \; r \; rd\theta dr \tag{3.6a}$$

$$= -\frac{\pi d^4}{128\mu}\frac{dp}{dz} \tag{3.6b}$$

$$= -\frac{\pi d^4}{128\mu}\frac{\Delta p}{l} \tag{3.6c}$$

where $\Delta p = p_2 - p_1$ is the pressure drop between the entrance and the exit, μ is the dynamic viscosity at atmospheric temperature and l is the length of the pipe [43]. If the mean velocity, $\overline{V_z} = \frac{1}{2}V_{z,\max}$ over the cross-section is introduced, eqn. 3.6 can be rewritten as,

$$\Delta p = -32\mu\frac{l}{d^2}\overline{V_z} \tag{3.7}$$

Eqn. 3.7 is the so-called Hagen-Poiseuille equation for a laminar flow through a pipe [44].

3.2.1.1 Flow characterization

Microfluidics is concerned with the flow of fluids in micromachined devices of which hydraulic diameter, D_h, is defined as [43],

$$D_h = \frac{4A}{P} \tag{3.8}$$

where A is the cross-sectional area of the flow duct and P is the wetted perimeter of the duct.

In small structures flow may be characterized by the Fanning friction factor, f_F, the Reynolds number, *Re*, and their product, the Poiseuille number, *Po* [43],

$$f_F \mathrm{Re} = Po \tag{3.9}$$

$$f_F = \frac{2\bar{\tau}_w}{\rho \bar{V}_z^{\,2}} \tag{3.10}$$

$$\mathrm{Re} = \frac{\rho D_h \bar{V}_z}{\mu} \tag{3.11}$$

The wall shear stress, τ_w, is defined as,

$$\tau_w = -\mu \left(\frac{\partial V_z}{\partial r} \right)_w \tag{3.12a}$$

Integrating the eqn. 3.12 with eqns. 3.5 and 3.8 gives the perimeter averaged shear stress,

$$\bar{\tau}_w = -\frac{D_h}{4} \frac{\partial p}{\partial z} \tag{3.12b}$$

Combining the eqns. 3.7, 3.8, 3.9, 3.10, 3.11 and 3.12, the equation yields the Poiseuille number through the length, *l*:

$$Po = \frac{A D_h^{\,2} \Delta p}{2 \mu Q l} \tag{3.13}$$

The Poiseuille number is a dimensionless constant which is independent of fluid properties, velocity, and duct size. It is solely a function of the duct shape. *Po* may be calculated directly from equations given above for simple geometries, such as circular ducts $Po = 16$ or infinite parallel plates $Po = 24$. For complicated shapes, Poiseuille number is calculated numerically [43].

3.2.2 Ahmed implant model

Among the commercially available GDDs constant resistance is expected for the Molteno and Baerveldt drainage devices since their designs do not include valves. Resistance in these devices, due solely to flow through the pipe, can be estimated with Poiseuille's law for steady laminar flow in a rigid pipe. But the Ahmed implant consists of a silicone pipe connected to a silicone Venturi valve and the valve is connected to an oblong-shaped end plate. So it can be analyzed in two parts, first one is a silicone pipe, and the flow inside. It can be computed by the Hagen-Poiseuille equation. Second one (AGV) is more complicated, but it can be analyzed by adding the results of the load deformation of the valve membranes.

As AH moves through the AGV, the leaflets move apart, and for a given steady-state flow an equilibrium pressure drop forms across the length of the channel. If the AH flow rate increases, the equilibrium pressure increases, and the elastic leaflets displace farther. The pressure does not rise as high as it would if the leaflets were fixed, since increased parting of the leaflets increases the channel height and decreases channel resistance. Thus, coupled fluid-solid interactions between the valve leaflet and the AH flow generate a resistance that is a function of the flow rate through the valve. Since AH is Newtonian and incompressible, the fluid mechanics of the AGV are governed by the Navier–Stokes equations, suggesting that the AGV fluid and solid domains are thin and planar. [6, 39]

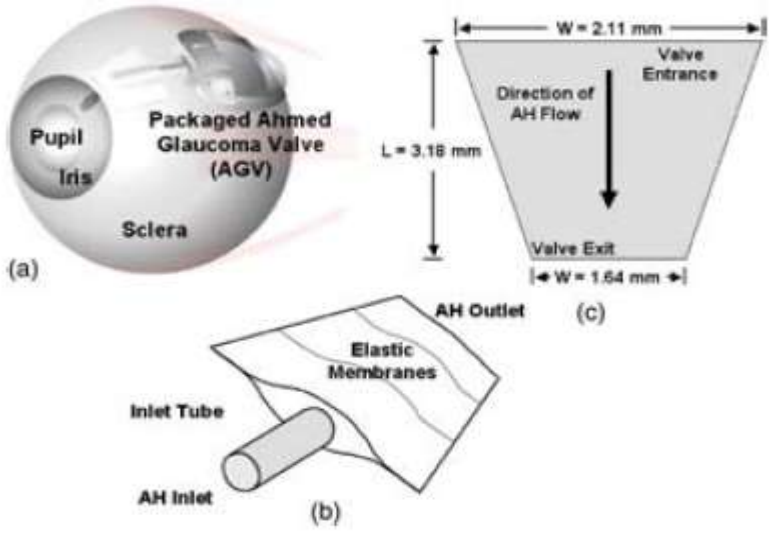

Figure 3.2: a) The attached AGV to the eye, b) basic AGV components construction, c) the dimensions of the two-dimensional channel formed by the silastic sheets [45]

3.2.2.1 Pipe model

In microfluidic devices, due to the low flow velocity and the micron size channels, the Reynolds number is generally low. This means that the viscosity plays a dominant role in microchannels rather than inertia, and turbulence can not exist in such a flow. For the microfluidic system, the fluid inside microchannel or the pipe, flow is under the instantly changed pressure. So, the inertia of the fluid in the channels should be considered in the dynamic modeling of fluid flow in micropipes. Although the micropipe flow can be considered as the laminar, the Reynolds number can be calculated for a better understanding of the flow characteristics. The required parameters are obtained from the datasheet of the AGV [24]. The parameters are given as,

$l = 25mm$ $d = 0.305mm$ $\rho = 1000kg/m^3$

$\mu = 10^{-3} Pas$ $Q = 2.5\mu l/\min$

where l is the length of the pipe, d is the diameter of the pipe (also equal to the characteristic length D_h), ρ is the density of the AH, μ is the dynamic viscosity of the AH and Q is the volumetric flow rate through the micropipe. The average fluid velocity component in the z direction ($\overline{V_z}$) is calculated by averaging the volumetric flow rate (Q) in the cross-sectional area of the micropipe such as [44],

$$\overline{V_z} = \frac{Q}{A} = \frac{4Q}{\pi d^2} \tag{3.14}$$

Calculation gives the $\overline{V_z}$ value as 0.57 mm/s. Inserting the dimensions of the pipe and the average velocity, Re_d is computed as,

$$\mathrm{Re}_d = \frac{(1000kg/m^3)\dfrac{(0.57mm/s)}{(1000mm/m)}\dfrac{(0.305mm)}{(1000mm/m)}}{10^{-3}kg/m.s} = 0.174 \tag{3.15}$$

Also, the entry length must be calculated for a fully developed laminar pipe flow. The relation for a microfluidic flow is given as [44],

$$\frac{L_{FD}}{d} = \frac{0.6}{1+0.035\,\mathrm{Re}_d} + 0.056\,\mathrm{Re}_d = 0.606 \tag{3.16}$$

The entrance length, L_{FD}, is about 0.73 % of the entire pipe length. Since the entrance length is very small, the flow can be accepted as a fully developed flow throughout.

The flow Reynolds number is much lower than Re_{crit}, so the flow is laminar. Furthermore, at $\mathrm{Re} \ll 1$ laminar flow always occurs and there will never exist any turbulence in low Reynolds number flow. The flow field can be taken as steady, laminar, and Newtonian, with one fluid. The inertia dies off following the Navier-Stokes equation, and gives the governing equation at such low Reynolds number as,

$$\mu \nabla^2 u = \nabla p \tag{3.17}$$

For this special case, the nonlinear partial differential Navier-Stokes equation reduces to a linear equation. It indicates that the velocity is determined only by the pressure distribution and all motion is symmetric in time at low Reynolds number, since there are no time derivatives. This type of flows are given different names such as “Stokes flows”, “Creeping flows”, “Potential flows” or “Low Reynolds number flows” [43]. For a steady, fully developed laminar flow in a circular cross-section pipe, the equation is exactly the same equation with Hagen-Poiseuille equation, eqn. 3.7.

Hagen-Poiseuille equation is actually an expression governing laminar flow of liquids through cylindrical pipes. In general, researchers are more inclined to apply this law to AH flow rather than blood flow, because the aqueous is a noncellular low-protein content liquid which should behave in a Newtonian fashion [46].

The normal IOP is in the range 1500 to 2660 Pa above atmospheric pressure and the average is around 2000 Pa. A glaucomatous eye typically has a pressure of up to 3 times the average value, but it is possible that glaucoma develops for lower IOP values and people with higher IOP may not suffer glaucoma. It is considered

that in patients with glaucoma, the IOP has values in the range of 1800 to 9100 Pa with a standard deviation of 1500 Pa. The mean pre-surgical IOP is 4866 Pa. The success in surgical glaucoma treatment is achieved when there is a reduction in IOP to less than 2900 Pa, but not below 700 to 1300 Pa. The failure of the surgical treatment is for an uncontrolled IOP higher than 2900 Pa [47]. So the desired IOP range is,

$$1300Pa \le IOP \le 2900Pa \tag{3.18}$$

Combining the eqns. 3.7 and 3.14, for the constant flow rate and viscosity of AH, and the given length and diameter of the pipe, the pressure drop through the micropipe can be calculated as,

$$\Delta p = -\frac{128Q\mu l}{\pi d^4} \tag{3.19a}$$

$$= -\frac{128\dfrac{(2.5\,\mu l/\min)}{\left(10^9\,\dfrac{\mu l}{m^3}\right)\left(60\,\dfrac{s}{\min}\right)}(10^{-3}\,kg/m.s)\dfrac{(25\,mm)}{\left(10^3\,\dfrac{mm}{m}\right)}}{\pi\left[\dfrac{(0.305\,mm)}{\left(10^3\,\dfrac{mm}{m}\right)}\right]^4} \tag{3.19b}$$

$$= -4.904\,Pa \tag{3.19c}$$

So the pressure drop across the micropipe is negligible when it is compared to the normal IOP (~2250 Pa). In the GDD pipe model, *Po* is calculated directly from eqn. 3.13. The calculation is given as:

$$Po = \frac{\left[\dfrac{\pi\ \ 0.305x10^{-3}\ ^2}{4}\right]\ 0.305x10^{-3}\ ^2\ \ 4.904}{2\ \ 0.001\quad 4.16x10^{-11}\quad 25x10^{-3}} = 16.02 \tag{3.20}$$

The pipe model has the same number as the default value of *Po* in circular ducts. So, *Po* number can be a reference for the micropipe models, as it is for the macro systems.

The micropipe does not act as a flow restriction element, significantly, for the eye fluid drainage. The micropipe acts only as a transport mechanism from the AC to the sclera. The real flow restrictor is the valve of AGV, in other words the main design consideration is the valve element.

3.2.2.2 Valve model

The deflecting membrane is used in AGV to adjust a pressure difference within critical limit of 1000 to 3000 Pa over atmospheric pressure at flow rates, 1 to 3 μl/min. So the deflection of the flexible membrane acts as a valve to adjust the AH drainage. However, the valve operates with some problems: The valve may not always open when they should, may not always close when the pressure drops and may have varying opening set points (not exactly within 1000 Pa and 3000 Pa limits). These malfunctions signal problems involved both in design and in manufacture processes. The valve geometry is the basic problem to obtain the desired pressure drop, and the volumetric flow rate.

In the following section, the AH drainage through the microvalve channel is estimated by means of analytical equations. The pressure-deflection relationship is studied at the first part, and the pressure drop across the microvalve is calculated for a simple geometry (elliptical cross-section). Properties of the original AGV material, the silicone elastomer, are used for the study of valve behavior for its biocompatibility and flexibility.

3.3 Analytical model

The membrane deflection by the effect of applied pressure was modeled using the load-deflection methods on the flat membranes [48, 49]. For small deflections, the relationship between pressure and deflection is linear, where only the bending of the membrane occurs. In classical mechanics, the linear theory for membranes made of homogeneous, linear elastic materials can be derived based on the following simplified assumptions: (1) the thickness, *t*, is small compared with the other dimensions of the membrane, (2) deflection of the membrane, *y*, is small compared

with the thickness [43]. The non-linearity which occurs for deflections above 25% of the membrane thickness, regardless of its radius, is the result of tensile stress caused by the stretching of the membrane. If large initial stress is present in the membrane, due to deposition process parameters and packaging, the effect of bending can be ignored, and a new first order term is introduced [48, 49].

The relationship between the pressure, *p*, and the deflection height, *h*, is shown in the following equation [48]:

$$p = \frac{C_1 t}{a^2}\sigma_o h + \frac{C_2 t}{a^4} E h^3 \tag{3.21}$$

where *p* is the applied pressure on the cross-section, *h* is the center deflection, *a* is the radius/half-edge length of the membrane, *t* is the thickness, *E* is the Young's Modulus of the membrane, σ_o is the internal stress. The dimensionless constants C_1 and C_2 are geometry and model dependent, they both are determined by the membrane shape (aspect ratio, *n*) and the Poisson's ratio, *v*. The obtained load deflection relationship of a rectangular membrane is [43],

$$C_1 = \frac{\pi^4(1+n^2)}{64} \tag{3.22}$$

$$C_2 = \frac{\pi^6}{24(1-v^2)}\left\{\frac{9(1+2n^2+n^4)}{16} + \frac{(4+n^2+n^4+3v(1+n^2))^2}{8(1-v)} + \frac{3(1+n^2)(4+n^2+n^4+3v(1+n^2))}{4(1-v)} + \frac{3(1+n^2)^2}{2(1-v)}\right\} \tag{3.23}$$

where *n* is the aspect ratio of the average width of the flat membrane ($2\bar{a}$) to the length of the membrane (*L*) assuming that the membrane is not tilted along its length. So, *n* is calculated as,

$$n = \frac{2\bar{a}}{L} = \frac{2\dfrac{(0.82+1.05)}{2}}{3.18} = 0.588 \tag{3.24}$$

The second parameter in constants C_1 and C_2, ν is the Poisson's ratio and is a property of the selected membrane material. For AGV model, ν is taken as 0.45 for silicone elastomer membrane. Inserting ν and *n* values into the eqns. 3.22 and 3.23, C_1 and C_2 are calculated to be 2.0482 and 1.0389, respectively [45].

For the AGV, other parameters in eqn. 3.21 are,

$$\sigma_o = 0$$
$$E = 750000\,Pa$$
$$t = 0.125\,mm$$

Before the start of the valve functioning, the center deflection *h* and the radius/half-edge length of the membrane *a* vary within the following limits,

$$0.318\,mm \le h \le 0\,mm \tag{3.25a}$$

$$0.32\,mm \le a \le 1.95\,mm \tag{3.25b}$$

At no flow condition, the variation of the applied pressure, *p*, along the length of the value, L, is calculated in eqn. 3.21 by using the constants and dimensions given above and presented in graphical form in Figure 3.3. The figure shows that the flow just starts when 2500 Pa of AH pressure is applied on the plates of AGV at the entrance. The missing part of the analysis is the flow rate of the AH flowing through the flexible membranes, which will be calculated using CFD analysis in the next chapter.

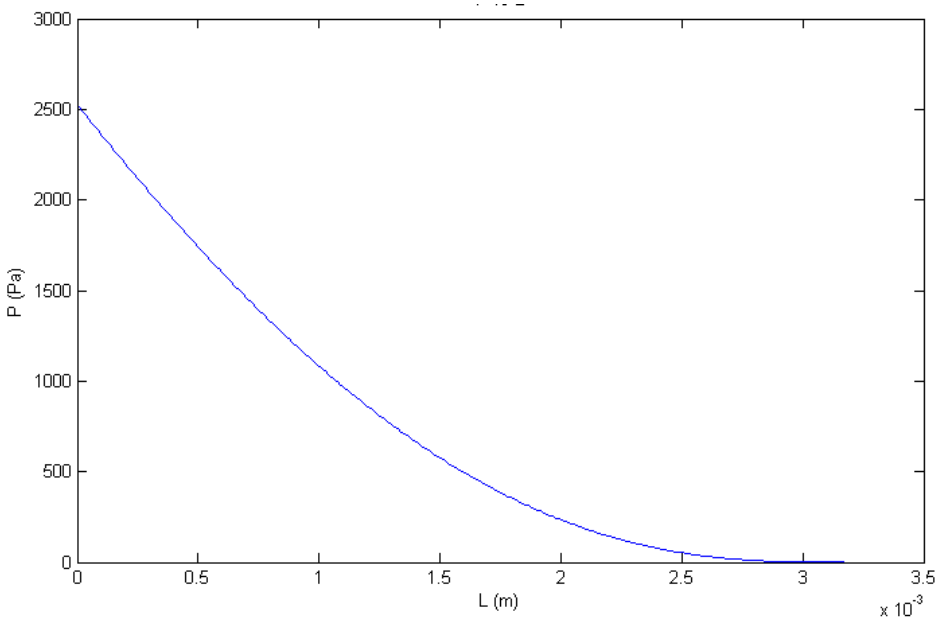

Figure 3.3: Change of the pressure difference through the AGV at no flow

3.4 NUMERICAL MODEL AND SIMULATION

Several techniques of numerical analysis exist in CFD. Among them, the most famous ones are finite difference, finite volume, finite element, spectral and pseudo-spectral methods [52]. The finite volume technique is employed in the present simulations for its simplicity and accuracy. In this study, the pressure drop across the valve is calculated using finite volume technique. In numerical simulations, a simplification is made since it is proven that the flow is fully developed and laminar in the pipe flow model. In the first part, the AGV model is modeled, solved and analyzed. In the second part, alternative valves are briefly explained and the most appropriate one is selected as the valve to be used in the new construction. Then, this valve is modeled, solved numerically and analyzed.

3.5 AHMED GLAUCOMA VALVE

3.5.1 Software features and usage

Computational Fluid Dynamics is basically a tool in the form of a software package which treats the flow field as being broken up into small volumes, and applies a suitable algorithm to solve the Navier-Stokes equations of flow motion under prescribed boundary condition and fluid properties [53]. In the content of the thesis, CFD simulation can be divided into three stages: Pre-processing (modeling), analysis (solving Navier-Stokes equations) and post-processing (results, output). All

simulations are performed on Windows XP with Intel Core Dual 6420 2.13 GHz CPU and 1.24 GB RAM. The maximum number of mesh elements (cells) used in the models is 129649.

The commercial package FLUENT is used to solve the flow and energy equations associated with the AGV model. This code is based on a control volume approach where the computational domain is divided into a number of cells, and the governing equations are discretized into algebraic equations in each cell. The control-volume approach leads to a discretized set of equations which satisfies the integral conservation of the mass and the momentum over each control volume.

The present chapter starts with emphasizing the principal features of each of the software packages used for carrying out the CFD analysis. First, the geometry modeler and grid generation software, GAMBIT, is explained. Then, the key features used in CFD solver, FLUENT, are presented.

3.5.2 GAMBIT

GAMBIT is a part of the FLUENT CFD software group. It is FLUENT's geometry and mesh generation software. For the purpose of modeling and meshing the AGV model and the domain, version 2.4.6 of GAMBIT was used. The sequence of steps followed in forming the flow field model is as follows [50]:

i. Geometry Construction
   - Vertices→Edges→Faces→Volumes(3D)

ii. Geometry Meshing
   - Volume Mesh→Validation of the Mesh

iii. Specify Zone Type
   - Boundary Type
   - Continuum Type
   - Exporting Mesh

3.5.2.1 Geometry construction

In the initial 3D analysis, the eye is drawn at the exact dimensions and the pipe of the glaucoma valve is placed following the instructions obtained from the Ahmed glaucoma surgery notes [45]. The pipe model used is constructed using

CATIA 3D drawing program. First, a hollow eyeball, the iris and the lens are drawn and, finally, the pipe of AGV with the appropriate dimensions is carefully inserted to the assembly, Figure 3.4.

To solve the flow through the pipe, the eye part of the drawing is deleted and the pipe drawing is imported to the GAMBIT software, Figure 3.5. Since the fluid flows inside the pipe, the interior of the pipe is preserved and the pipe material is deleted.

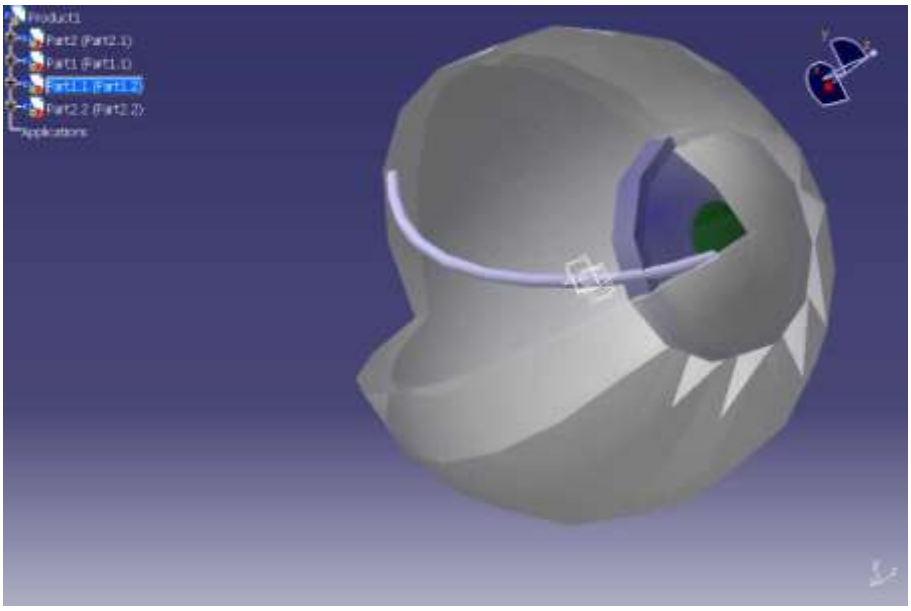

Figure 3.4: 3D drawing of the eye (lens, iris, eyeball) and AGV pipe

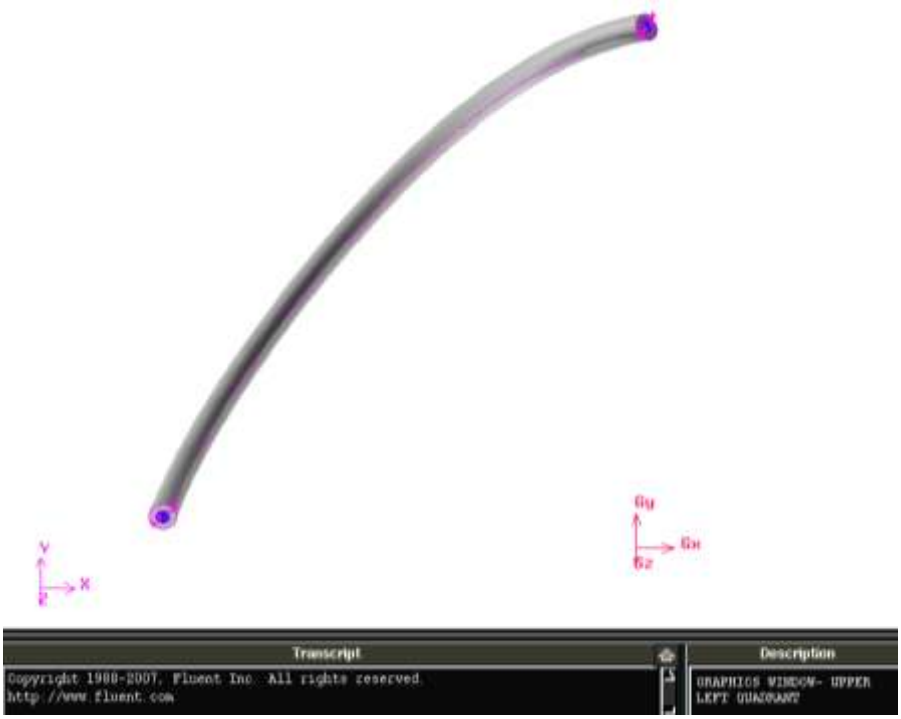

Figure 3.5: The AGV pipe in GAMBIT

The Ahmed implant consists of a silicone pipe connected to a silicone Venturi valve and the valve is connected to an oblong-shaped end plate. Since the end plate has no effect on the valve design, that part is not drawn. So the model has two parts, first one is the silicone pipe for which the flow inside can be computed easily. Second one is the AGV which is more complicated, but it can be created in GAMBIT having the dimensions given in the brochure of the device [24]. The AGV model drawn is shown in Figure 3.6.

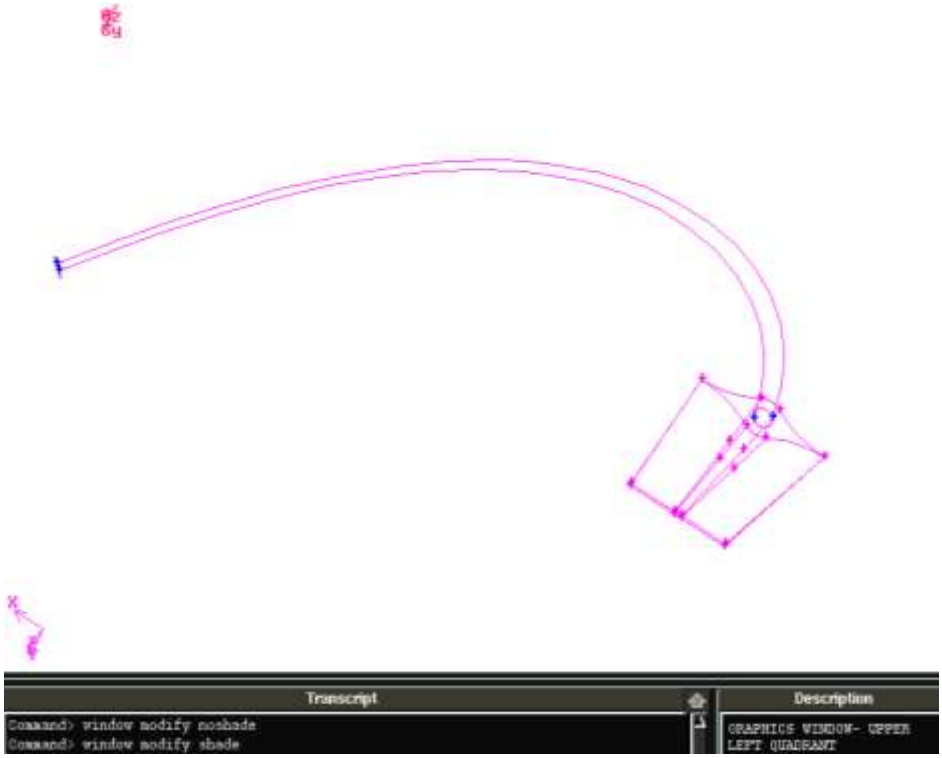

Figure 3.6: AGV model in GAMBIT

3.5.2.2 Geometry meshing

After the flow geometry is constructed, it has to be meshed. Meshing is the process of dividing the entire domain into a number of small and non-overlapping sub domains. When the domain is meshed, mesh is named as a grid. There are two main grid types, namely, structured and unstructured grids. GAMBIT automatically selects hexahedral type of structured grid for the AGV geometry and the 3D mesh is generated.

The degree of the refinement of the grid affects the accuracy of the solution directly. Refinement implies the use of large number of cells. But that is not the case everytime, since the mesh requires refinement only in needed areas. For the AGV

model, if the pressure control in the valve is being analyzed, the small area in clamped sides of valve leaflets needs to be made denser. The refinement is accessed by the "Size Function" command in GAMBIT [51].

GAMBIT also provides an option to smooth the generated meshes. This is particularly useful while generating a hexahedral volume mesh from an unstructured volume mesh. Sometimes during the process of volume meshing, GAMBIT can not mesh the volume if there are highly skewed elements present on the faces. That problem is the main issue for this study, since the areas to be meshed are too small to hold grids in it. These highly skewed elements are tried to be smoothed by increasing the number of rows or by decreasing first-row height. Problem is resolved by increasing the number of rows from 100,000 to 130,000 and using "Size Function" command for much denser meshing for the small volumes (Figure 3.7).

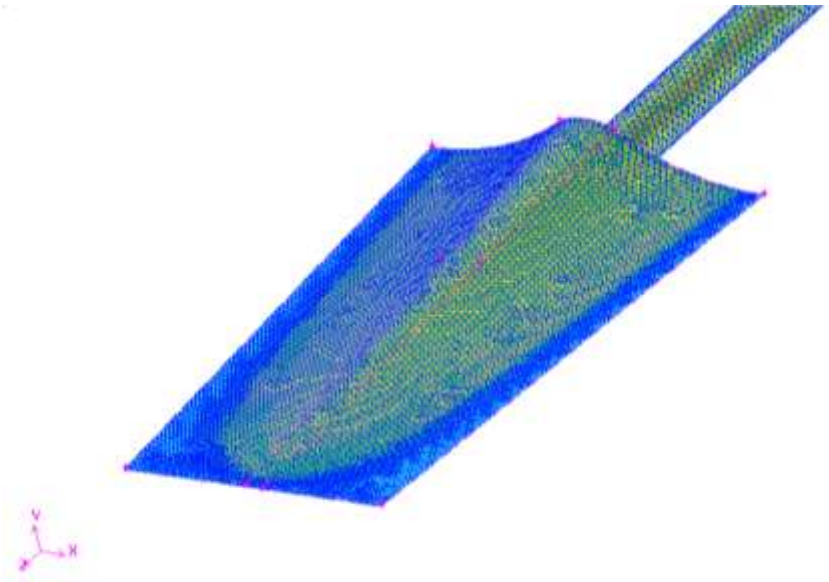

Figure 3.7: Unstructured mesh of AGV model (normally closed)

3.5.2.3 Specification of zone types

The specifications define physical and operational characteristics of the model at its boundaries. They can be classified as two types: Boundary and continuum type specifications.

Boundary type specifications are the characteristics of the model at its internal and external boundaries. For the AGV model simulation, the boundary types

that are used are wall (to define valve), mass_flow_inlet (to define an inlet based on mass flow as its parameter), and pressure_outlet (to define an outlet specified by pressure).

Continuum type specifications are the physical characteristics of the model within specific regions of its domain. FLUID continuum type specification is assigned for the simulations that are carried out, so that the model is defined by the equations of momentum, continuity, and transport at mesh nodes and/or cells that exist within the volume.

After the boundary and continuum types are specified in GAMBIT, the Export command is used to export the mesh into a *.msh file that is readable in format by FLUENT; the CFD solver.

3.5.3 FLUENT

FLUENT is the main CFD solver. The solvers, convergence criteria and other monitoring specifications and iterations to be made should be specified to run the program.

When a mesh is completed after solving its grid density and other complications, computations can be started. As for the GAMBIT software, a series of steps has to be performed for FLUENT to start computations [52]:

i. Grid Modifications
   - Checking

ii. Solution Parameters
   - Solver Selection
   - Specification of Boundary Conditions
   - Material Selection

iii. Solution
   - Defining the Convergence Criteria
   - Setting up Monitors
   - Initializing the Solution
   - Running the Iteration

3.5.3.1 Grid modifications

When the mesh is imported into FLUENT 6.3.26 from GAMBIT as a *.msh file, all the coordinates have to be approximately defined. The default units used for coordinates are SI units in FLUENT.

Grid Check command enables us to check the grid for various specifications such as skewness, inverted volumes etc. The sample grid check output is as shown below:

```
Grid Check

 Domain Extents:
   x-coordinate:  min  (m)  =  -1.211714e-002,  max  (m)  =
2.293865e-004
   y-coordinate:  min  (m)  =  1.916404e-004,  max  (m)  =
9.997773e-003
   z-coordinate:  min  (m)  =  -1.025517e-002,  max  (m)  =
2.680000e-003
 Volume statistics:
   minimum volume (m3): 2.109839e-015
   maximum volume (m3): 1.955037e-013
     total volume (m3): 2.641459e-009
 Face area statistics:
   minimum face area (m2): 9.972931e-011
   maximum face area (m2): 7.725860e-009
 Checking number of nodes per cell.
 Checking number of faces per cell.
 Checking thread pointers.
 Checking number of cells per face.
 Checking face cells.
 Checking bridge faces.
 Checking right-handed cells.
 Checking face handedness.
 Checking face node order.
 Checking element type consistency.
 Checking boundary types:
 Checking face pairs.
 Checking periodic boundaries.
 Checking node count.
 Checking nosolve cell count.
 Checking nosolve face count.
 Checking face children.
 Checking cell children.
 Checking storage.
Done.
```

Since the minimum volume value is not smaller than zero, there happens no inverted element in the domain. Also other aspects such as handedness, face pairs etc. have no failure effect on the flow.

3.5.3.2 Solution parameters

Aqueous humor is a Newtonian and an incompressible fluid. The solution parameters for this particular study are selected as isothermal, incompressible flow with steady state conditions. Temperature and velocity are assumed to be constant for this limited and small volume. For this particular study, the default version of laminar model is used.

The boundary conditions for each of the boundary types are defined. First, Mass_Flow_Inlet is defined as the inlet parameter in GAMBIT. Mass flow inlet boundary condition is used to define the flow rate along with the scalar properties of the fluid, at the flow inlet.

The outlet of the domain is defined as pressure_outlet in GAMBIT. Pressure_outlet boundary condition requires the specification of a gauge pressure at the outlet boundary.

The fluid is AH eye fluid in this study. Material properties (the properties taken from Table 2.1) are loaded to the FLUENT's User Defined Material Database [53]. The user defined code (UDC) is prepared as follows:

```
(test fluid
      (chemical-formula . aq)
      (density (constant . 1000))
      (viscosity (constant . 0.001))
      (specific-heat (constant . 4200))
      (thermal-conductivity (constant . 0.58))
      (formation-entropy (constant . 100000))
)
```

The parameters for this analysis are summarized in the table given below:

Table 3.1. Parameters for 3D analysis

Parameters in GAMBIT	
Type of Analysis	3ddp (Three-dimensional & double precision)
Total Mesh Size	129649 Elements
Mesh Density (Interval Size)	0.03 Units (mm)
Parameters in FLUENT	
Solver	Pressure Based
Time Dependence	Steady
Velocity Formulation	Absolute
Viscous Model	Laminar
Material	Aqueous Humor
Operating Pressure	0 Pa (Gauge pressure)
Boundary Condition	m_in = 4.16e-08 kg/s
Convergence Criteria	
Judging Convergence Method	Monitoring Residuals
Convergence Criteria	1e-05
Gauge Pressure	1200 Pa
Number of Iterations	200
Post Processor	FLUENT 6.3.26

3.5.3.3 Convergence

Convergence is the property of a numerical method to produce an acceptable solution, which approaches the exact solution as the grid spacing; control volume size or element size is reduced to zero. For this study, residuals of continuity and velocities are monitored and plotted. The residual checking for convergence is 10^{-3} by default. This value is reduced to 10^{-5}, since this would lead to a more refined solution, but the counter effect is that the solution convergence time is increased.

The convergence can be monitored during the solution process graphically, which is a useful method to see how and when each parameter is converging to an acceptable value during runtime. The parameter used for monitoring the solution is the residuals of the continuity equation. The use of an iterative solution method necessitates the definition of a convergence and stopping criteria to terminate the iteration process. The measure of convergence is a norm on the change in the solution vector between successive iterations. The iterative algorithm is terminated after a fixed number of iterations if the convergence has not been achieved. This criteria is used in slowly convergent or divergent problems to prevent waste of computation time. Convergence algorithm is given in Figure 3.8.

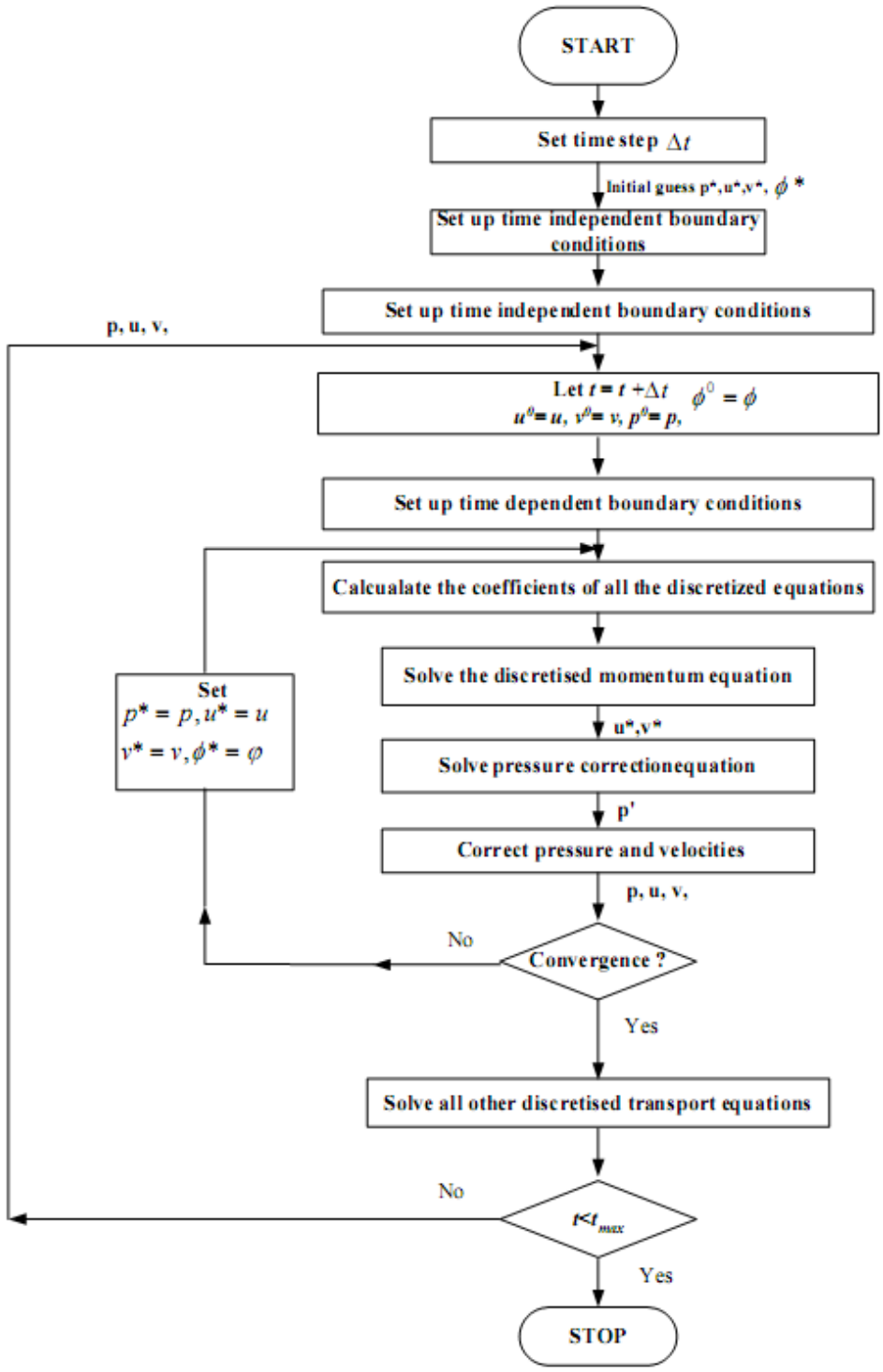

Figure 3.8. Convergence algorithm [52]

3.5.3.4 Solution

The entire flow field is initialized. First, for the incompressible flow the gauge pressure inlet is set to 1200 Pa. The operating pressure is set to 0, since the gauge pressures are used. Then the solution is ready to start. The maximum number of iterations is specified as 200 and the solution is started. The solution converges after 94 iterations for the convergence tolerance value of 10^{-5}. FLUENT automatically stops iterating and displays a message indicating that the solution has converged (Figure 3.9).

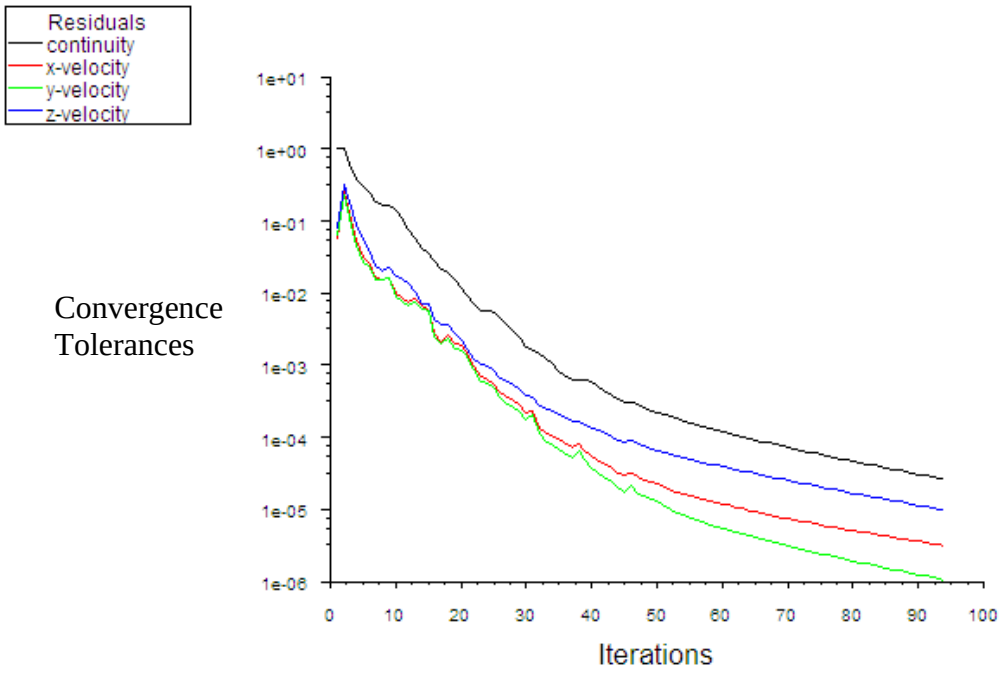

Figure 3.9: Convergence results

3.5.4 Analysis of the results

Once the equations are solved for the flow variables, the results are needed to be analyzed to see if they meet the requirements of the process such as uniform pressure or velocity profiles. There are several graphical options in FLUENT, the graphs that are presented in Appendix A and C are listed below:

- XY Plot: An XY plot can be used to see the variation of one variable with respect to an independent variable. These plots are easier to read as they are very simple and the relation between any two variables can be easily understood.

- Contour Plot: Contour plots represent the global nature of the variables and can be used for both vector and scalar quantities. A contour line represents a constant value of a particular variable. These figures are presented in such a way that the difference between adjacent contour lines is always constant.

- Vector Plot: A vector plot gives both the direction and magnitude of the variables. The direction is pointed by an arrow and the magnitude by color. As the name suggests, these types of plots can be used to view vector quantities.

The aqueous humor flow through the AGV model is simulated and analyzed at 6 different flow rate and corresponding pressure drops are given in the Table 3.2:

Table 3.2: Pressure drop vs flow rate (AGV, CFD)

Flow Rate (µl/min)	Pressure Drop (Pa)
1.6	716.77
2.5	1032.42
5	1135.60
10	1238.26
20	1505.06
25	1575.94

Example plots and figures are given in Appendix A.

3.6 ALTERNATIVE DESIGNS

The ideal GDD has not been developed yet. When today's technology and practical issues are taken into account, the AGV seems to be the closest device to the ideal GDD. However, the AGV design referred to as a valved design, behaves as a flow restrictor, and it does not employ a true valve which opens and closes at specific pressures. As mentioned before, the valve must close before the pressure drops below 1200 Pa, where the desired IOP is approximately 2000 Pa. The valve must be optimized to drain at a flow rate equal to the production of AH at elevated IOPs. It must open at IOP > 1200 Pa and close when IOP < 2933 Pa to prevent hypotony. AGV offers post-operative flow resistance. This may be a major progress over non-restrictive flow devices, but the problem of post-operative IOP control remains

unaddressed. AGV has not performed as advertised and is unable to perform the shut-off function required after desired IOP levels are met. Once the valve opens, it never closes and possibly is responsible for some of the observed complications.

A valve is a device within a fluidic system in which flow is allowed in one direction but suppressed in the opposite direction, thus introducing directionality into the flow. Valves are often classified by whether they work by themselves (i.e. by utilizing energy from flow) or they need external energy to function. The former are called passive or check valves, whereas the latter are called active valves [54].

Wishlist of ideal characteristics that a valve should have includes:

- Zero leakage
- Zero power consumption: Obviously not true for active valves.
- Zero dead volume: Extra volume should not be introduced which negatively affect the performance.
- Infinite differential pressure capability: A small amount of extra pressure from one side should open it, and a small amount of extra pressure from the other side should close it.
- Zero response time
- Ability to operate in the surrounding fluid

These criteria for the optimum design of a valve can be adapted to microsystems, specifically GDDs. The adapted and specific criteria are:

- Zero leakage: The valve should have definite opening and closing pressures in order to precisely control IOP. Active valves have the best response to pressure changes.
- Zero power consumption: Non-active valves do not require external energy.
- Zero dead volume: The end plates can be reduced in size.
- Infinite differential pressure capability: Active valves have the best response to initial pressure fluctuations.
- Zero response time: Passive valves have fairly fast response.

- Ability to operate with the present fluid: The valve material must be inert to AH.

Additional criteria are:

- Bleb encapsulation: It can be reduced if biocompatible materials are used for the implant design. The drainage plate can be reduced in size or eliminated altogether since it no longer needs to provide the basis for a bleb.
- Valve resistance: Passively-valved devices do not function correctly in vivo. They act as small restrictors but not act as cut-off valves. A pressure-controlled valve should be preferred for improved functioning.
- Ergonomics: The largest part of a GDD is its end plate. A pressure-controlled valve removes the requirement for a large end plate.
- Simplicity: The valve should not contain electronic components and must be durable.

For the sake of simplicity, a mechanical check valve could be selected as the drainage control. Mechanical check valves have mechanical moving parts, and there are three types of mechanical check valves [54]:

- Flap
- Membrane
- Ball

The three types of check valves are exemplificated and the most appropriate one is selected as the suggested valve. The check valves may lead to leakage but they are relatively simple to make, do not require external energy for operation, and have a fairly fast response. Many different valve designs are available. There is no optimum valve but instead, valves have to be chosen carefully depending on the intended use of microsystem. In the next part of the chapter, some of the mechanical micro check valves will be introduced and a new check valve model will be proposed for the novel and unique GDD.

3.6.1 Passive dynamic check valve

The passive dynamic check valve is a membrane type check valve. As controlling elements for liquid transportation, microvalves are essential in microfluidics. The valves offered by Bartels Mikro-Technik [55] function as passive dynamic check valves, normally closed, and are designed as a three layer system built up by two plastic materials. The Micro-Electro-Mechanical Systems (MEMS) are utilized for the fabrication of the microvalve. A flexible membrane fixed between the bottom and top layers seals the valve depending on the differential pressure of the fluid, Figure 3.10. General information for the valve is tabulated in Table 3.3.

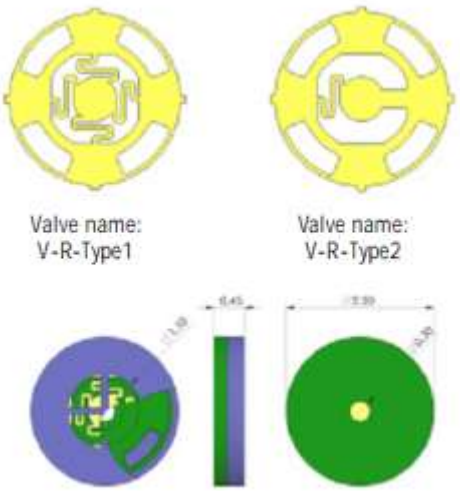

Figure 3.10: Bartels Mikro-Technik micro check valve [55]

The passive dynamic micro check valve is made out of plastic, the device is small and lightweight, consumes no energy, has a low dead volume, has good reaction for small pressure ranges. The device is used for micro surgery applications, so the valve is very large for glaucoma application. Besides that the pressure depending flow rate has a very high base limit, so it can not be used for the AH volumetric flow rate range of 2-3 µl/min. The valve is not fully feasible for the use in glaucoma therapy because of flow rate limitation.

Table 3.3: Technical data of Bartels Mikro-Technik micro check valve [55]

Classification	Normally Closed
Dimensions	Ø 2,2 mm x 0,5 mm
Mass	2 mg
Dead Volume	~2 nl
Material	Polyphenylenesulphone (PPSU) Polyimide (PI) Epoxy Resin (EP)
Max. Pressure	10 bar
Max. Temperature	100 °C
Power Consumption	-
Media	Liquids
Flow Rate	Pressure Dependent (min 6 ml/s)

3.6.2 Active parylene bowed type valve

Microvalves do not close or open until certain volumetric amount (the dead volume) of working fluid has been pumped into or out of the controlled actuators. This failure introduces a delay time of valves and lowers the working range of fluid actuators. In order to get rid of this time delay, Wang et al, [56] designed and fabricated a parylene valve that effectively blocks the working fluid in both rectangular and circular cross section channels. The dimensions are 0.305 mm for both diagonal of the rectangular one and diameter of the circular one, Figure 3.11. The valve is named bowed-type valve as the valve is bowed at desired pressure limits.

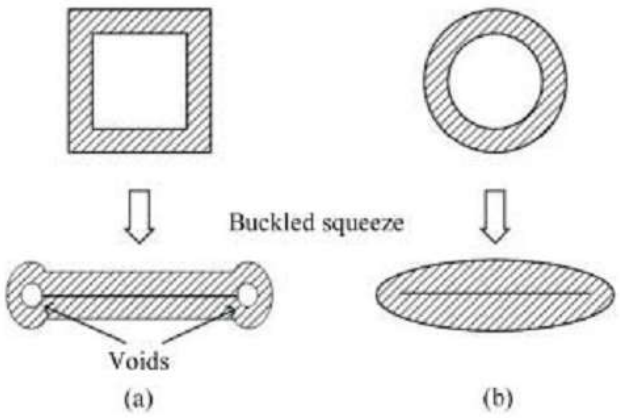

Figure 3.11: Operation of the bowed-type valves with different cross sections of channels: (a) rectangular; (b) circular [56]

The operation principle of the parylene bowed-type valve is similar to that of the AGV. The difference is that the parylene bowed-type valve needs an actuator to buckle and squeeze. The advantages of the valve are zero leakage, zero dead volume, infinite differential pressure capability, and small size. However, the design needs an actuator and a pressure limiter to work effectively. The response time can be higher for this type of active valve designs; differential pressure changes sent from the actuator to the valve may result in cracks on the corners of the squeezed channels after a while. The design is said to be feasible as Wang et al. [56] discuss after the experimental results, but the detailed design of buckling force and the following integration of actuating mechanism into the whole microfluidic system are not mentioned in the paper. So, the device is not fully reliable at this time.

3.6.3 Starr-Edwards valve

Starr-Edwards valve is a spherical ball valve. The popular application of ball valves is for heart valve prostheses. This valve is designed for implantation in a human body that has valvular disorders [57]. It has a silicone rubber ball with a diameter of 1.2 mm inside a cage with thick struts and a machined ring orifice with a diameter of 0.5 mm. The valve is inserted between two chambers of the heart. The valve is required to open with a flow rate of 20 ml/min at 10 kPa. If blood flow is regurgitated, the ball moves toward the ring orifice and stops blood flow. In a similar manner, these ball-type valves were miniaturized as passive check valves in micropump structures. The problem for this type of valve is that the device needs an actuator to move the spherical ball back and forth. Furthermore, the valve dimensions and flow rates are designed for milimetric sensitivities [57].

3.6.4 Proposed valve

In the cure of glaucoma disease, the most popular valve currently in use is the Ahmed Valve. However, as mentioned before, this device has several problems such as:

- having big dimensions relative to the eye geometry as a result of the covered area of external plate,
- inability to prevent undesired reversed flow.

An alternative valve, Fermat type spring mounted check valve, Figure 3.12, is suggested in this paper to solve these problems. The dimensions are in micron scale.

The depth of the springs and flappers are 25 μm and length of flappers is 3 μm. This valve has several advantages over the valves which have been used in glaucoma disease treatment. The advantages are summarized as follows:

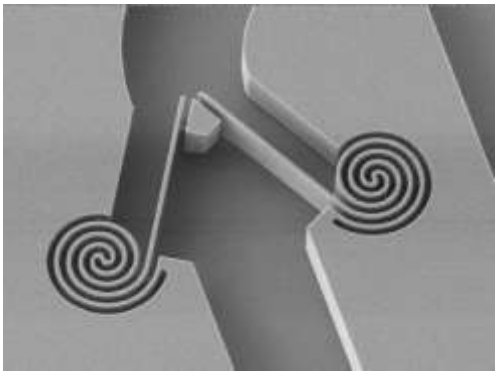

Figure 3.12: Fabricated spring mounted check valve [58]

- Reverse flow is automatically prevented with the help of the prismatic support assembled in the middle of the spring mounted check valve, as the flappers on the opposite side stand inclined. When a reverse flow, which is not desired, is about to start, flappers automatically lock the flow path by getting strongly in touch with the prismatic support.

- Spring is used as an auxiliary element of the valve. Spring is selected for its no energy dissipation and the mechanical properties such as stiffness are benefited to prevent the reverse flow as mentioned above.

- External plate is expected to be automatically reduced to a smaller volume by using this alternative valve. So the patient uses the device less problematically and more comfortably.

According to the researches held, spring mounted check valve is manufactured and experimented with the help of nanotechnology at Microfluidic Research at UC Berkeley [58] as seen in Figure 3.13. If this device can be manufactured by nanotechnology, then one can end up with a conclusion that it can also be used in microstructural valve design which is concerned in glaucoma treatment.

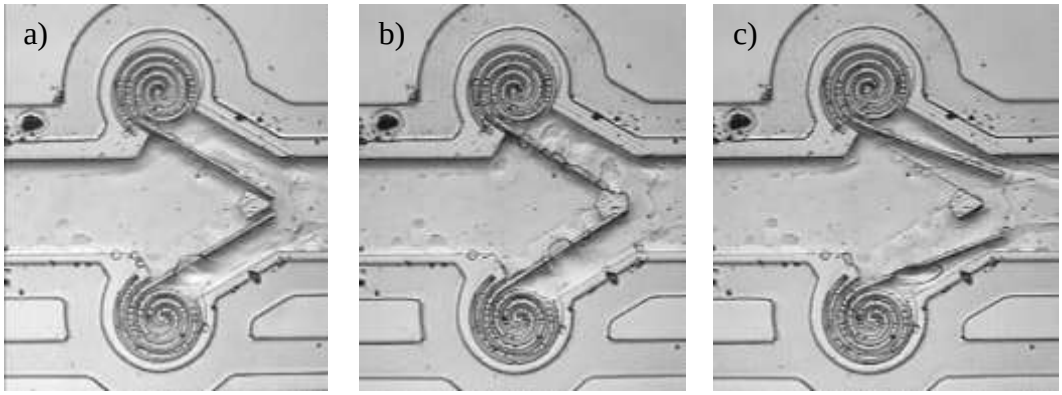

Figure 3.13: Operation of the spring mounted check valve; a) relaxed, b) closed, c) opened valve [57]

The new valve is desired to start operation between the pressure range of 2250-3500 Pa. Actually, 3500 Pa is the upper limit of opening process. However, at higher values than 3500 Pa, the valve is desired to open much slower than it does over the specified interval to prevent hypotony. The CFD analysis of the proposed model is presented in the last section of this chapter.

3.6.4.1 Software features and usage

In the present work the time-dependent flow through the valve with moving flappers was numerically simulated. The dynamic mesh modeling is used to simulate the movement of the flappers attached to the Fermat type springs. The model is solved as 2.5D geometry [52], since the geometry does not change in the +z direction (perpendicular to the flow direction). That makes the FLUENT solver more effective without spending the extra time for redundant calculations.

The shape of the domain changes with the time due to the rotational motion at the domain boundaries of the flappers. Updating the mesh is handled automatically by FLUENT at each time step based on the new positions of the boundaries. The rotational motion of the flappers is prescribed by user-defined functions (UDFs). Since FLUENT expects the description of the rotational motion to be specified on the face zones, both the moving and non-moving regions are identified and hooked into separate UDF codes. The source code of this C program implemented and coupled with FLUENT software is listed in the Appendix B. Furthermore, deforming regions due to rotational motion on their adjacent regions are grouped into separate zones in the starting mesh and hooked into a separate UDF code.

Two mesh motion methods are used in FLUENT to update the face mesh in the deforming regions subject to rotational motion:

- Spring-based smoothing method: The method is used to update the face zones whose boundary is moving or deforming. In the present case, the flappers are the moving parts and the interior of the boundaries and the springs are the deforming parts of the mesh [52].
- Local remeshing method: Since the geometry of the valve does not change in the direction perpendicular to the flow, the local face remeshing in two dimensions on the triangular (tetrahedral) surface mesh is applied. The mesh is locally updated with the new cells at each time step [52].

The maximum number of mesh elements (cells) used in the models is 4808. Since the basic steps of GAMBIT and FLUENT are described in previous chapter, here only the description of the model-specific steps will be explained.

3.6.5 GAMBIT

For the purpose of modeling and meshing the proposed model and the domain, version 2.4.6 of GAMBIT was used. The sequence of the jobs performed is as follows [50]:

i. Geometry Construction
   - Vertices→Edges→Faces(2D)

ii. Geometry Meshing
   - Face Mesh→Validation of the Mesh

iii. Specify Zone Type
   - Boundary Type
   - Continuum Type
   - Exporting Mesh

3.6.5.1 Geometry construction

Since the basic design consideration is the valve, the 2.5D model of valve is enough to solve in FLUENT. Therefore, the valve model must be drawn and meshed

in 2D and then swept into 2.5D model, Figure 3.14. The Fermat type spring mounted check valve, built in GAMBIT, consists of two flappers (valve) connected to two Fermat type springs, Figure 3.15.

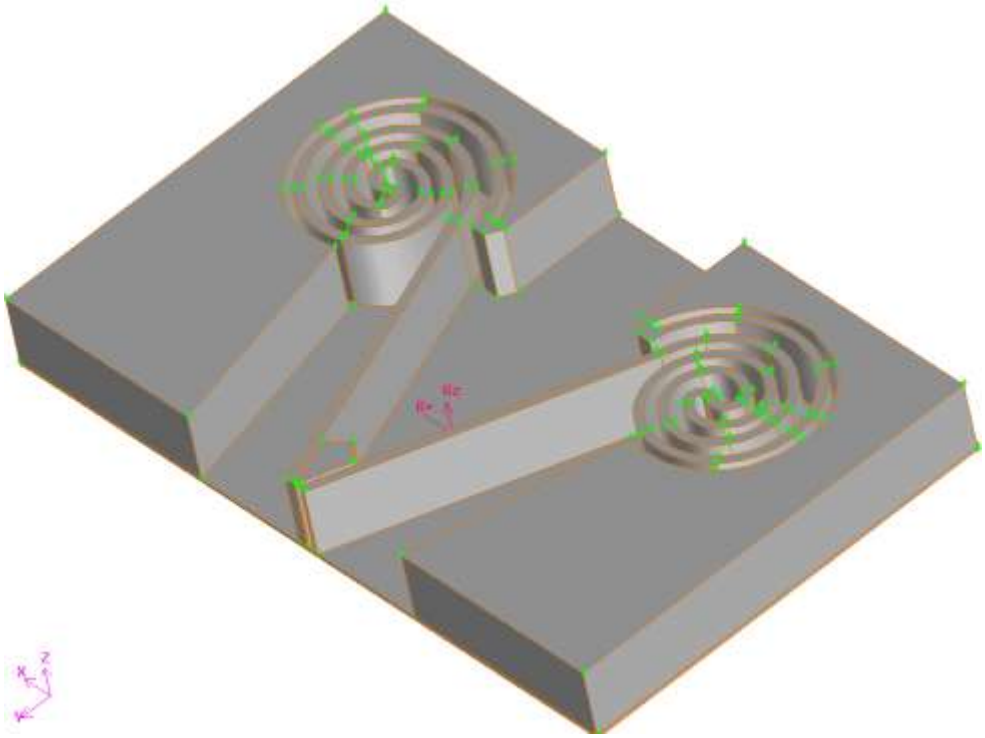

Figure 3.14: Proposed model drawn in CATIA

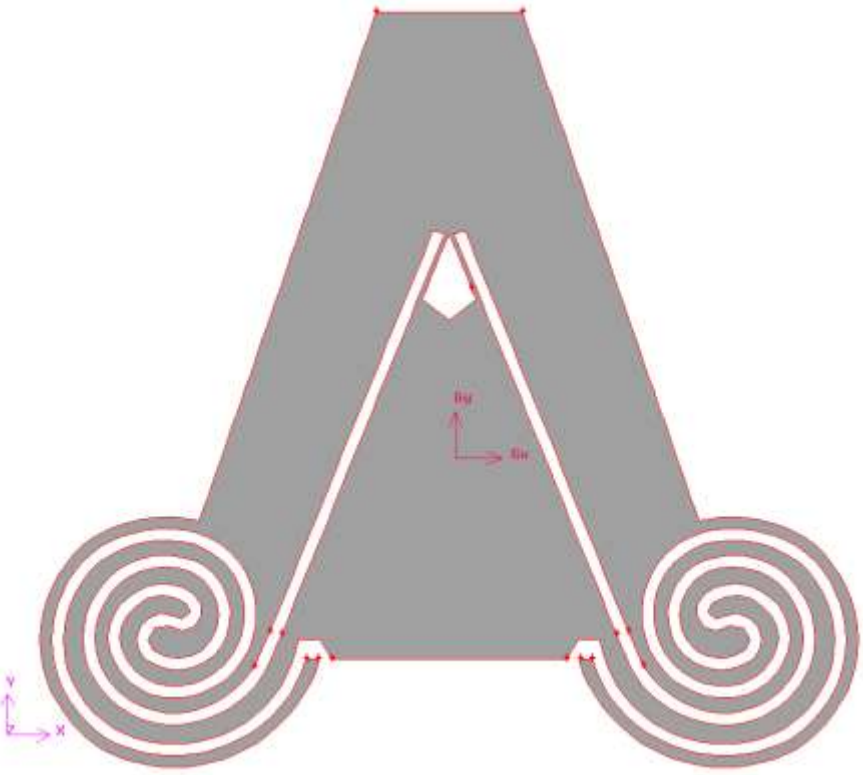

Figure 3.15: Spring mounted check valve in GAMBIT

3.6.5.2 Geometry meshing

After the geometry is built, it has to be meshed. GAMBIT automatically select triangular type of structured grid for the geometry and the 2D mesh is generated, Figure 3.16. Since the mesh is 2D with fine mesh sizes, there is no need to refine the constructed mesh. So the Size_Function command is not used for this model.

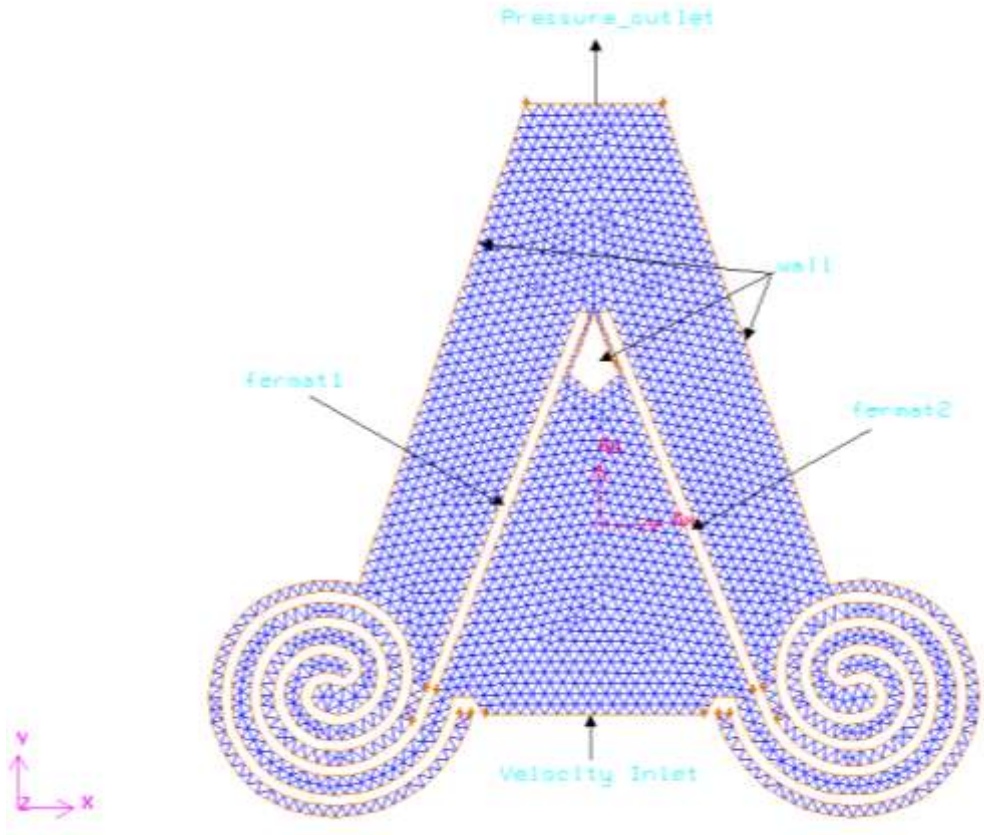

Figure 3.16: Tetrahedral mesh of the model (relaxed position)

3.6.5.3 Specification of zone types

For the valve model simulation, the boundary types that are used are wall (to define the boundaries), fermat1 (to define the first moving flapper), fermat2 (to define second moving flapper), velocity_inlet (to define an inlet based on mass flow as its parameter), and pressure_outlet (to define an outlet specified by pressure).

Continuum type specifications are the physical characteristics of the model within specific regions of its domain. FLUID continuum type specification is assigned for the simulations that are carried out, so that the model is identified by the

equations of momentum, continuity, and transport at mesh nodes and/or cells that exist within the volume.

After the boundary and continuum types are specified in GAMBIT, the Export command is used to export the mesh into a *.msh file that is readable by the CFD solver, FLUENT.

3.6.6 FLUENT

The solver, convergence criteria and other monitoring specifications are designated and the number of iterations are selected to run the mesh in FLUENT. When the mesh is completed with its grid density and other complications (e.g. highly skewed elements, inverted elements) are cleaned up, the actual computational part of CFD can be started. The completed geometry can be imported into FLUENT solver and the CFD simulation is ready to start. A series of preliminary steps are to be performed including the dynamic mesh module before start up [52]:

i. Grid Modifications
   - Checking
   - Scaling

ii. Solution Parameters
   - Solver Selection
   - Specification of Boundary Conditions
   - Material Selection
   - UDF Hooking
   - Dynamic Mesh Module

iii. Solution
   - Setting up Monitors
   - Setting up Animations
   - Initializing the Solution
   - Running the Iteration

3.6.6.1 Grid modifications

When the mesh is imported into FLUENT 6.3.26 from GAMBIT as a *.msh file, all the coordinates have to be approximately defined. The default units used for coordinates are SI units in FLUENT.

Grid is checked and, since the minimum volume value is not smaller than zero, there happens no inverted element in the domain. Also other aspects such as handedness, face pairs etc. have no failure effect on the flow are controlled. For sake of ease of design, the geometry of the mesh was created at 5 times the original dimensions in GAMBIT and then scaled down in FLUENT.

3.6.6.2 Solution parameters

The same parameters of AGV model are used during the solution, except that the flow condition is set to be unsteady, since this time, the flow is time-dependent. Dynamic mesh simulations currently work only with the first order time advancement [52]. So, the default unsteady formulation of 1st-Order Implicit is selected as the solver. The standard laminar model is also enabled from the viscous model section in FLUENT.

The boundary condition for each of the boundary type is defined. First, Mass_Flow_Inlet is defined as the inlet parameter in GAMBIT. But for the dynamic mesh modeling and unsteady conditions Mass_Flow_Inlet and Pressure_Outlet can not work together, resulting in a floating point error. So, Mass_Flow_Inlet is changed into Velocity_Inlet in FLUENT. Velocity inlet boundary condition is used to define the flow rate along with the scalar properties of the flow, at flow inlet. The outlet wall of the domain is again defined as Pressure_Outlet as in GAMBIT. Also, the same UDC code used in AGV model is used in the present model.

The *DEFINE_CG_MOTION UDF* is used to prescribe the rotational motion of the flappers. The required source files are written in C code and built into a library named *library-fermatspring*. FLUENT automatically set up the directory structure and compile the code. If there are any errors in the source code, FLUENT reports the errata. The UDF source code is presented in Appendix B.

Under the mesh motion setup, the dynamic mesh motion is enabled and the associated parameters are specified as shown in Figure 3.17a. The rotational motion of the model is specified in the dynamic mesh zones panel in FLUENT, Figure 3.17b. The zones of rotational motion are also described in Figure 3.18.

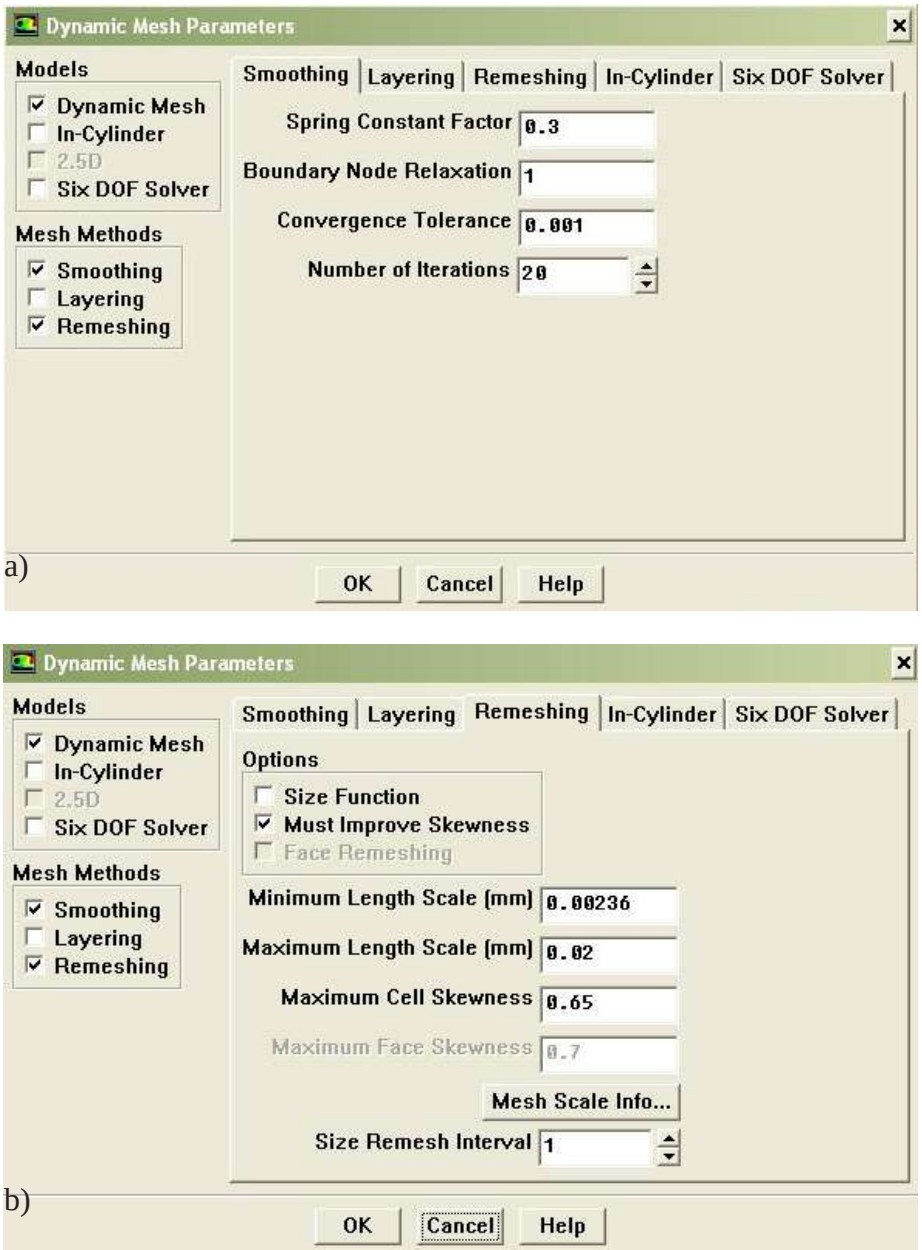

Figure 3.17: Dynamic mesh parameters a) smoothing, b) remeshing

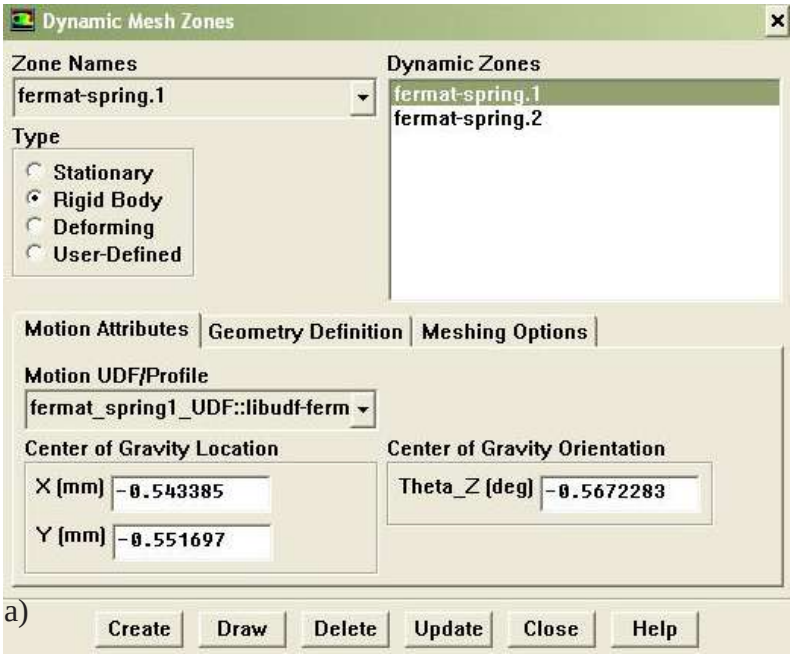

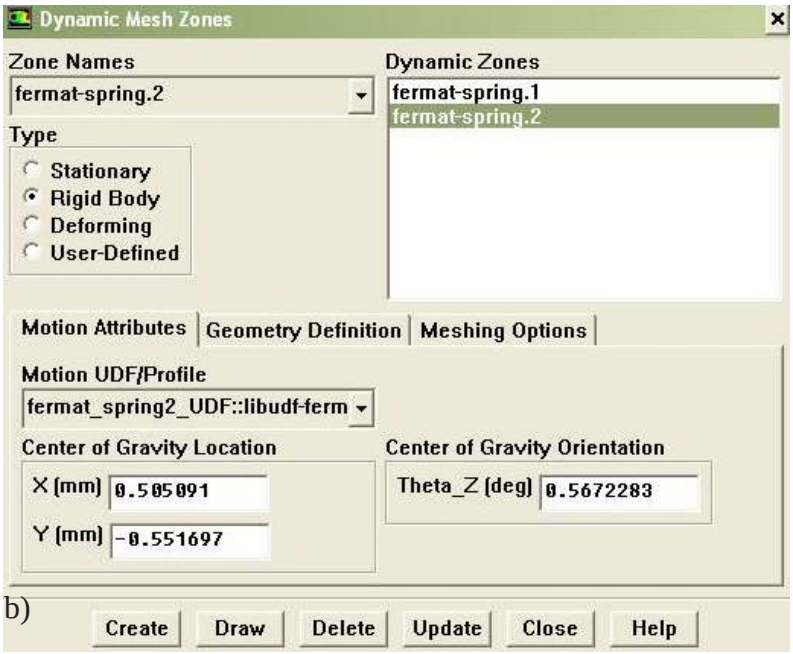

Figure 3.18: Dynamic mesh zones a) first flapper, b) second flapper

Spring based smoothing is applied on the mesh using Text User Interface (TUI) in FLUENT command window:

```
> define/models/dynamic-mesh-controls <Enter>
> define/models/dynamic-mesh-controls > sp <Enter>
> define/models/dynamic-mesh-controls/smoothing-
  parameter > soas <Enter>
```

```
> spring-based smoothing for all cell types [no] yes
  <Enter>
```

The parameters used in this analysis are summarized in the table given below:

Table 3.4. Parameters for 2.5D analysis

Parameters in GAMBIT	
Type of Analysis	2ddp (Two-dimensional & double precision)
Total Mesh Size	4808 Cells
Mesh Density (Interval Size)	0.03 Units (mm)
Parameters in FLUENT	
Solver	Pressure Based
Time Dependence	Unsteady
Velocity Formulation	Absolute
Viscous Model	Laminar
Material	Aqueous Humor (aq)
Operating Pressure	0 Pa (Gauge pressure is used)
Boundary Condition	v_in: Changes with the mass flow rate
Convergence Criteria	
Judging Convergence Method	Monitoring Residuals
Convergence Criteria	Changes with Time Step Size
Gauge Pressure	1200
Number of Iterations	Changes with Different Velocity Inlet Values
Post Processor	FLUENT 6.3.26

3.6.6.3 Solution

It is important to monitor convergence of the solution and it is approaching to the pre-specified residual limit. For example, when the mass flow rate is selected as 2.5 μl/min, the time step size is selected as 0.002 s and maximum iteration number per time step retains as the default value, 20 iterations. The entire flow field is

initialized, and the iterative solution process is ready to start. The time step is specified as 123 for the maximum opening of the flappers and the solution is started. The solution is seen to converge after some iterations at each time step. FLUENT automatically stops iterating and displays a message indicating that the solution has converged. Figure 3.19 shows the convergence of the residuals with the mass flow rate of 2.5 µl/min.

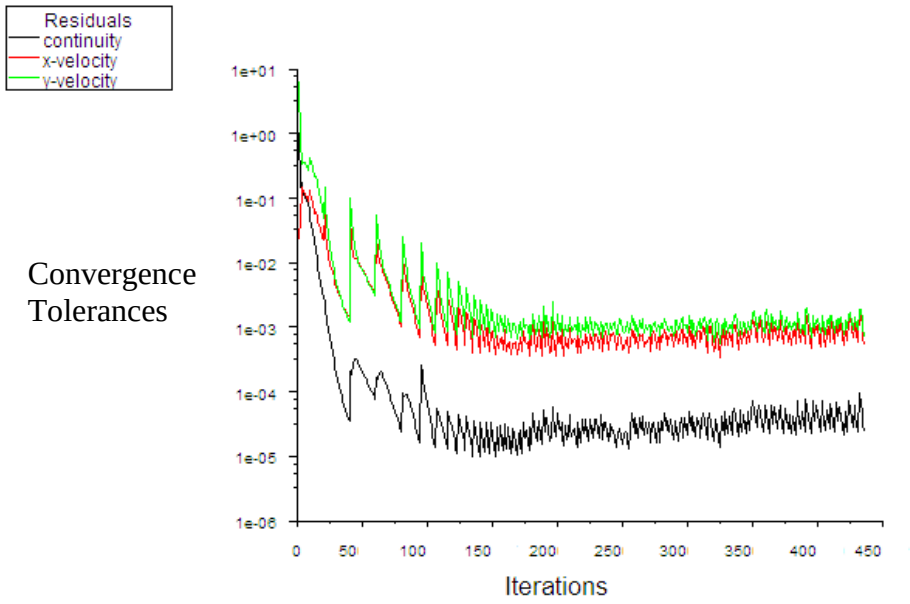

Figure 3.19: Convergence results

3.6.7 Analysis of the results

The aqueous humor flow through the proposed model is simulated and analyzed at 6 different flow rates of 1.6 µl/min, 2.5 µl/min, 5 µl/min, 10 µl/min, 20 µl/min, and 25 µl/min. Example plots and figures are given in Appendix A. The numerically calculated pressure drops are given in the table below:

Table 3.5: Pressure drop vs flow rate (Fermat, CFD)

Flow Rate (µl/min)	Pressure Drop (Pa)
1.6	800.60
2.5	1054.58
5	1645.41
10	1862.87
20	2207.56
25	2379.61

CHAPTER 4

COMPARISON OF THE RESULTS

In this chapter, the comparison of designed AGV with experimental results of AGV available in literature and the comparison of designed AGV and the proposed GDD are given.

4.1 EXPERIMENTAL STUDIES ON AGV

Experimental studies on AGV are needed to be investigated to validate the model. No matter how influential the CFD solver is, if the numerical model is not correctly defined, the simulation result will not reflect the reality. In this aspect, experiments are necessary to verify the numerical model. Five experimental studies are found [4, 5, 35, 36, 43], the measurement were given explicitly [45].

Prata et al. [35] were the first to analyze and characterize the performance of GDDs in vitro. They built an experimental setup to supply steady-state flow of saline through GDDs (Molteno, Baerveldt, Krupin and Ahmed). All devices, with the exception of AGV, have shown a linear relation between flow rate (in the range from 2 to 100 μl/min) and pressure drop. Francis et al. [36] confirmed results of Prata for GDDs.

In vitro studies of Stay et al. [45], the AGV exhibited a sublinear pressure drop to increased flow rate, due to the flexibility of the valve material and the complicated geometry of the valve. The study revealed that the pressure drop/flow rate curve for the AGV is nonlinear because of the valve leaflets continue to deform in increased flow rates. Studies of both Prata [35] and Stay [45] exhibits a range of 666-2666 Pa in vitro pressure drop across the AGV. The dimensions of the glaucoma valve in both studies are the same as the data obtained from the Ahmed glaucoma surgery notes [24].

The experimental setup used by Stay [45] to test the performance of the AGV is shown in Figure 4.1. The setup consists of a syringe pump, a pipe stand column, AGV mounted in a sealed glass tube, a plastic outlet tube, and a three-way stopcock. The setup starts to work, when the syringe pump feeds a steady flow of saline through the three-way stopcock to AGV. After working its way through AGV, AH exits through a 21 gauge needle into the outlet tube. Taking the outlet pressure equal to ambient pressure, the measured inlet pressure to the outlet tube is equal to the pressure drop across the valve [45].

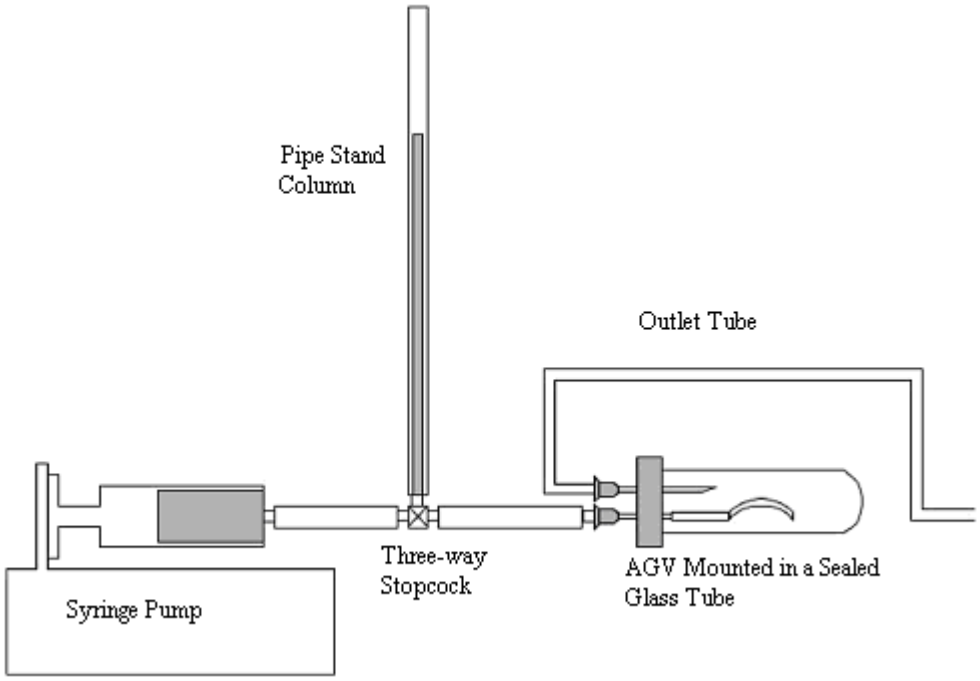

Figure 4.1: In vitro experimental setup of AGV

The CFD results of AGV that are solved in FLUENT, are compared with these experimental and theoretical data [43], in Tables 4.1 and 4.2, respectively:

Table 4.1: Pressure drop vs flow rate (experimental) [45]

Flow Rate (μl/min)	Pressure Drop (Pa)
1.6	693.27
2.5	999.92
5	1133.24
10	1279.89
20	1386.55
25	1439.88

Table 4.2: Pressure drop vs flow rate (theory) [45]

Flow Rate (µl/min)	Pressure Drop (Pa)
1.6	773.27
2.5	893.26
5	1039.91
10	1226.57
20	1466.55
25	1533.21

Figure 4.2 shows the comparison between the predicted and measured pressure drop/flow rate curves and the CFD simulation results (Table 3.2). The experimental and CFD curves get along well with each other for the normal physiological flow rates, i.e. between 2.5 and 3 µl/min and even for slightly higher values, i.e. 5-15 µl/min. The CFD model overpredicts the experimental pressure drops for the flow rate in the range of 15-25 µl/min. Thus, the qualitative assessment of the experimental curve was predicted well by the CFD simulations.

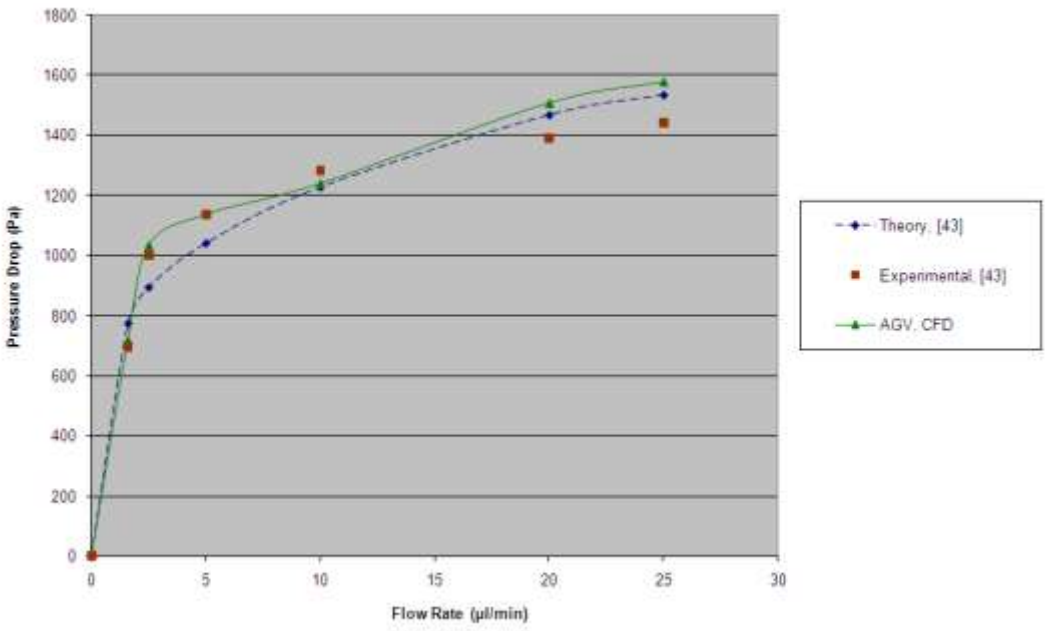

Figure 4.2: Comparison of pressure drop in AGV

4.2 COMPARISON OF CFD RESULTS OF AGV WITH CFD RESULTS OF PROPOSED MODEL

Since the CFD results of AGV matches well with the experimental results of AGV, the comparison of AGV CFD simulation and Fermat (proposed model) CFD simulation can give us a better and qualitative support as shown in Figure 4.3. The simulation results of AGV were compared with published experimental data in Figure 4.2, and now they are used to clarify the performance of the proposed model.

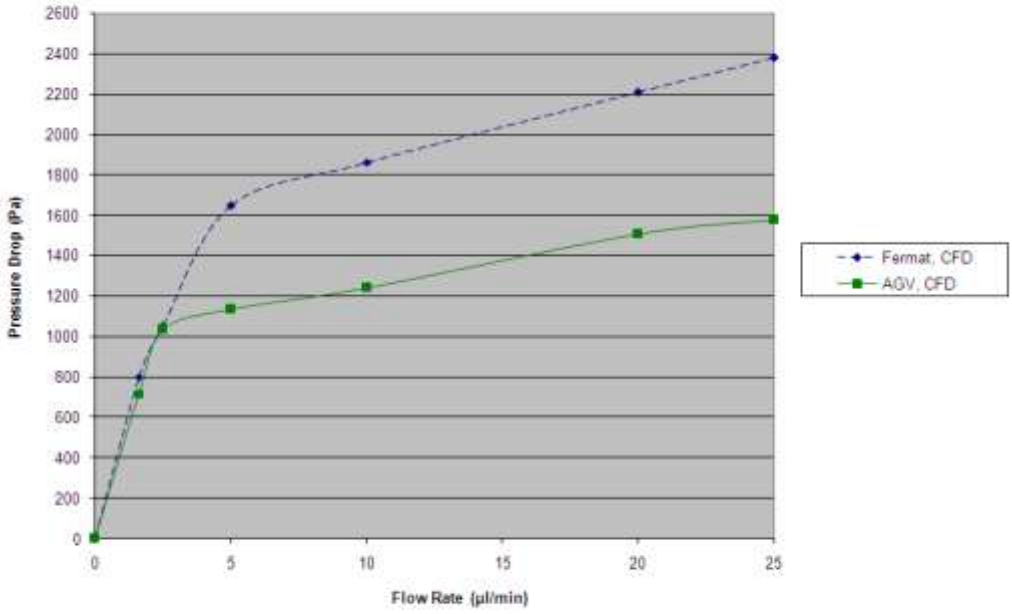

Figure 4.3: Comparison of AGV & Fermat CFD Results

The Fermat curve gives a lower pressure drop at a range of 1.6-2.5 µl/min, but at the upper limit of physiological flow rate, 3 µl/min, the pressure drop increases. At the higher values of flow rate, proposed model gives higher pressure drop. This result is an encouraging result for this study, since at higher values than the normal physiological flow rate, IOP can decrease to normal ranges easily and effectively.

CHAPTER 5

DISCUSSIONS AND CONCLUSIONS

In the last chapter of the thesis, the discussions are presented from the point of view of practical problems GDD involved in and CFD analysis. The problems faced and likely to be faced in future are also be pointed out. Conclusions reached on the basis of the results obtained are given in details. Also, the possible future work related with this subject is proposed.

5.1 MAIN PROBLEMS OF GLAUCOMA DRAINAGE DEVICES AND SOLUTIONS APPROACHED

The general problems involved in GDDs, and specifically, the main problems in AGV design were discussed in Chapter 2. In the light of these factors, a new design is suggested and analyzed by using CFD solvers. The problems resolved are:

- Ergonomics: The proposed model has a very low profile (0.023 mm height). As mentioned before, after the device is implanted, the body reacts to the GDD and begins to encapsulate it with fibrous tissue, forming a bleb. The bleb must grow to a lower profile than AGV has, to regulate the pressure acceptably. The low profile bleb also results in patient comfort, and less micromotion.

- Valve Function: In AGV system, the most important failure was the valve malfunctioning. The valve in Ahmed Implant acts as a flow-restriction device or regulator rather than as a true valve that open and close in response to pressure changes after implantation. In the proposed model, the spring mounted check valve exhibits the real valve function. The desired pressure range of the valve can be achieved by regulating the spring constant, or by changing the material, the length of the flappers, etc.

- Reversed Flow: Another problem with AGV is the reverse flow. Once the valve opens, it never closes and possibly experiences a reverse flow at low IOP cases (hypertensive phase). In the proposed model, the prismatic support assembled in the upper-middle of the valve prevents the reverse flow by locking the flow path.

- Pressure Control: The post-operative IOP control of AGV remains unaddressed. The proposed model performs a shut-off function when a reversed flow occurs and the flappers should open and close as the springs relax and squeeze, respectively.

Besides the problems achieved, it was deduced from the CFD study that the proposed model, Fermat type spring mounted micro check valve, shows a nonlinear pressure drop response, which is quite similar to that of AGV. Based on the range of flow rates and pressure drops used in this study, the optimum combination would be 2.5 μl/min and 1054.58 Pa for the proposed model.

5.2 CFD AND ITS ACCURACY

Computational Fluid Dynamics is a powerful tool for many types of fluid flow problems. It results in large savings of cost and time. But, as mentioned in Chapter 4, the CFD results must be validated by experimentally. Other than that, the accuracy of the FLUENT is principally governed by the past experience of the individuals who operate it. Hence, the appropriate usage of software is vital in achieving acceptable results. Reasons for numerically modeling the AH flow in Fermat type spring mounted check valve with moving flappers are:

- Once the proper valve model has been set up and validated, carrying out simulations can be both less time consuming and cheaper than conducting the corresponding experiments.

- Numerically solved designs can be very helpful in understanding the physical phenomena that occur in AH flow because it can estimate very small changes in parameters that might be very difficult to measure during experiments.

5.3 PROBLEMS FACED

The problem most frequently faced is the meshing of the geometry. Meshing primarily influences the accuracy of the FLUENT solver. The main parameters of a good mesh are the mesh type and the mesh refinement. The unstructured mesh with "Size Function" refinement command is used for AGV design. Owing to the fact that structured mesh gives better accuracy for simple 2D geometries, the proposed model is solved with a tetrahedral structured mesh. The 2D mesh is then sufficiently refined without overconsuming the computational resources. Temporarily, there was a problem that was encountered during the uniting the pipe and the valve of AGV model. The problem is solved by smoothing the face and meshing it, before the volume meshing.

In the FLUENT solver, a time wasting was faced while UDF hooking. The UDF was written in C, but can not be linked to the FLUENT solver directly. The problem is then solved by using older version of Visual Basic, i.e. Visual Studio.NET 2003 instead of Visual Basic 2008.

There were various problems encountered during meshing. These problems are sometimes not easy to explain and solve directly. For example, the meshing process in GAMBIT suddenly crashed many times. Occasionally the volume mesh would not continue because the face meshes contained somewhat highly skewed elements. This was surprising since all faces were checked in advance for highly skewed elements and inverted volumes. Also, while dynamic mesh module was used in FLUENT, introducing mass flow inlet and pressure outlet boundary types simultaneously gave floating point error, again and again, causing the solver to crash.

5.4 CONCLUSIONS AND FUTURE WORK

The aim of this thesis was to analyze the AH flow through the existing GDDs, and to develop a new model to overcome some existing problems in these devices. As a result, it is believed that the most of the problems are successfully solved. Also, computational results had lead to some new useful ideas in forming real-life models.

From an educational viewpoint, lots of experience and knowledge was gained in using CFD analysis tools. The problems associated with the solvers are noted and overcome during the analysis.

Computational Fluids Dynamics is an excellent tool to determine flow characteristics of a fluid in varying set of operational conditions. Although, there are some difficulties that can be encountered during the analysis, in the near future, CFD design approach can be the most reliable design tool, before the production of a prototype.

The analysis carried out during this thesis has shown the importance of the valve mechanism of a GDD. Without a pressure regulator, the pressure drop is about 5 Pa. The use of a valved design results in 100 to 500 times higher pressure changes at varying flow rates. Hence, as the starting point of CFD analysis, it is seen that the selection of the valve as the design issue was the right choice.

As the first future work suggestion, the all eyeball may be analyzed directly using CFD solvers. The AH path can be selected from the ciliary body to the valve. The problem can be made more realistic by involving temperature changes of the AC and cornea in the CFD solution.

Experiments may be devised to explore the fluid flow behavior and then be compared with results obtained from the CFD solver.

Finally, the proposed model can be produced in a nanotechnology laboratory. Then, an experimental setup can be constructed which is similar to the experimental setup used for AGV. The experimental results can be compared with results obtained from the CFD solver.

APPENDIX A

POSTPROCESSING OF AGV MODEL

1.6 µl/min

FLUENT Summary Report File:

```
FLUENT
Version: 3d, dp, pbns, lam (3d, double precision, pressure-based,
laminar)
Release: 6.3.26
Title:

Models
------

   Model                         Settings
   ------------------------------------
   Space                         3D
   Time                          Steady
   Viscous                       Laminar
   Heat Transfer                 Disabled
   Solidification and Melting    Disabled
   Species Transport             Disabled
   Coupled Dispersed Phase       Disabled
   Pollutants                    Disabled
   Pollutants                    Disabled
   Soot                          Disabled

Boundary Conditions
-------------------

   Zones

      name               id   type
      ---------------------------------------
      new_fluid          2    fluid
      m_in               5    mass-flow-inlet
      moving_wall        7    wall
      deforming_walls    6    wall
      wall               3    wall
      p_out              4    pressure-outlet
      default-interior   9    interior


Boundary Conditions                                        aq_humor

Condition                                                    Value
-------------------------------------------------------------------
Material Name                                                test
Specify source terms?                                        no
Source Terms                                                 ((mass)
                                                            (x-momentum)
                                                            (y-momentum)
                                                            (z-momentum))
Specify fixed values?                                        no
Local Coordinate System for Fixed Velocities                 no
Fixed Values                                          (x-velocity
                                                     (inactive . #f)
                                                     (constant . 0)
                                                          profile  )) (y-
                                                     velocity (inactive .
                                                     #f) (constant . 0)
                                                     (profile  )) (z-
```

	velocity (inactive . #f) (constant . 0) (profile)))
Motion Type	0
X-Velocity Of Zone (m/s)	0
Y-Velocity Of Zone (m/s)	0
Z-Velocity Of Zone (m/s)	0
Rotation speed (rad/s)	0
X-Origin of Rotation-Axis (mm)	0
Y-Origin of Rotation-Axis (mm)	0
Z-Origin of Rotation-Axis (mm)	0
X-Component of Rotation-Axis	0
Y-Component of Rotation-Axis	0
Z-Component of Rotation-Axis	1
Deactivated Thread	no
Porous zone?	no
Conical porous zone?	no
X-Component of Direction-1 Vector	1
Y-Component of Direction-1 Vector	0
Z-Component of Direction-1 Vector	0
X-Component of Direction-2 Vector	0
Y-Component of Direction-2 Vector	1
Z-Component of Direction-2 Vector	0
X-Component of Cone Axis Vector	1
Y-Component of Cone Axis Vector	0
Z-Component of Cone Axis Vector	0
X-Coordinate of Point on Cone Axis (mm)	1
Y-Coordinate of Point on Cone Axis (mm)	0
Z-Coordinate of Point on Cone Axis (mm)	0
Half Angle of Cone Relative to its Axis (deg)	0
Relative Velocity Resistance Formulation?	yes
Direction-1 Viscous Resistance (1/m2)	0
Direction-2 Viscous Resistance (1/m2)	0
Direction-3 Viscous Resistance (1/m2)	0
Choose alternative formulation for inertial resistance?	no
Direction-1 Inertial Resistance (1/m)	0
Direction-2 Inertial Resistance (1/m)	0
Direction-3 Inertial Resistance (1/m)	0
C0 Coefficient for Power-Law	0
C1 Coefficient for Power-Law	0
Porosity	1

m_in

Condition	Value
Mass Flow Specification Method	0
Mass Flow-Rate (kg/s)	2.66e-08
Mass Flux (kg/m2-s)	1
Average Mass Flux (kg/m2-s)	1
Upstream Torque Integral (n-m)	1
Upstream Total Enthalpy Integral (w/m2)	1
Supersonic/Initial Gauge Pressure (pascal)	0
Direction Specification Method	1
Reference Frame	0
Coordinate System	0
X-Component of Flow Direction	1
Y-Component of Flow Direction	0
Z-Component of Flow Direction	0

X-Component of Axis Direction	1
Y-Component of Axis Direction	0
Z-Component of Axis Direction	0
X-Coordinate of Axis Origin (mm)	0
Y-Coordinate of Axis Origin (mm)	0
Z-Coordinate of Axis Origin (mm)	0
is zone used in mixing-plane model?	no

moving_wall

Condition	Value
Enable shell conduction?	no
Wall Motion	0
Shear Boundary Condition	0
Define wall motion relative to adjacent cell zone?	yes
Apply a rotational velocity to this wall?	no
Velocity Magnitude (m/s)	0
X-Component of Wall Translation	1
Y-Component of Wall Translation	0
Z-Component of Wall Translation	0
Define wall velocity components?	no
X-Component of Wall Translation (m/s)	0
Y-Component of Wall Translation (m/s)	0
Z-Component of Wall Translation (m/s)	0
Rotation Speed (rad/s)	0
X-Position of Rotation-Axis Origin (mm)	0
Y-Position of Rotation-Axis Origin (mm)	0
Z-Position of Rotation-Axis Origin (mm)	0
X-Component of Rotation-Axis Direction	0
Y-Component of Rotation-Axis Direction	0
Z-Component of Rotation-Axis Direction	1
X-component of shear stress (pascal)	0
Y-component of shear stress (pascal)	0
Z-component of shear stress (pascal)	0
Specularity Coefficient	0

deforming_walls

Condition	Value
Enable shell conduction?	no
Wall Motion	0
Shear Boundary Condition	0
Define wall motion relative to adjacent cell zone?	yes
Apply a rotational velocity to this wall?	no
Velocity Magnitude (m/s)	0
X-Component of Wall Translation	1
Y-Component of Wall Translation	0
Z-Component of Wall Translation	0
Define wall velocity components?	no
X-Component of Wall Translation (m/s)	0
Y-Component of Wall Translation (m/s)	0
Z-Component of Wall Translation (m/s)	0
Rotation Speed (rad/s)	0
X-Position of Rotation-Axis Origin (mm)	0
Y-Position of Rotation-Axis Origin (mm)	0
Z-Position of Rotation-Axis Origin (mm)	0
X-Component of Rotation-Axis Direction	0
Y-Component of Rotation-Axis Direction	0
Z-Component of Rotation-Axis Direction	1

X-component of shear stress (pascal)	0
Y-component of shear stress (pascal)	0
Z-component of shear stress (pascal)	0
Specularity Coefficient	0

wall

Condition	Value
Enable shell conduction?	no
Wall Motion	0
Shear Boundary Condition	0
Define wall motion relative to adjacent cell zone?	yes
Apply a rotational velocity to this wall?	no
Velocity Magnitude (m/s)	0
X-Component of Wall Translation	1
Y-Component of Wall Translation	0
Z-Component of Wall Translation	0
Define wall velocity components?	no
X-Component of Wall Translation (m/s)	0
Y-Component of Wall Translation (m/s)	0
Z-Component of Wall Translation (m/s)	0
Rotation Speed (rad/s)	0
X-Position of Rotation-Axis Origin (mm)	0
Y-Position of Rotation-Axis Origin (mm)	0
Z-Position of Rotation-Axis Origin (mm)	0
X-Component of Rotation-Axis Direction	0
Y-Component of Rotation-Axis Direction	0
Z-Component of Rotation-Axis Direction	1
X-component of shear stress (pascal)	0
Y-component of shear stress (pascal)	0
Z-component of shear stress (pascal)	0
Specularity Coefficient	0

p_out

Condition	Value
Gauge Pressure (pascal)	1200
Backflow Direction Specification Method	1
Coordinate System	0
X-Component of Flow Direction	1
Y-Component of Flow Direction	0
Z-Component of Flow Direction	0
X-Component of Axis Direction	1
Y-Component of Axis Direction	0
Z-Component of Axis Direction	0
X-Coordinate of Axis Origin (mm)	0
Y-Coordinate of Axis Origin (mm)	0
Z-Coordinate of Axis Origin (mm)	0
is zone used in mixing-plane model?	no
Radial Equilibrium Pressure Distribution	no
Specify targeted mass flow rate	no
Targeted mass flow (kg/s)	1

default-interior

Condition	Value

Solver Controls

Equations

Equation	Solved
Flow	yes

Numerics

Numeric	Enabled
Absolute Velocity Formulation	yes

Relaxation

Variable	Relaxation Factor
Pressure	0.3
Density	1
Body Forces	1
Momentum	0.7

Linear Solver

Variable	Solver Type	Termination Criterion	Residual Reduction Tolerance
Pressure	V-Cycle	0.1	
X-Momentum	Flexible	0.1	0.7
Y-Momentum	Flexible	0.1	0.7
Z-Momentum	Flexible	0.1	0.7

Pressure-Velocity Coupling

Parameter	Value
Type	SIMPLE

Discretization Scheme

Variable	Scheme
Pressure	Standard
Momentum	First Order Upwind

Solution Limits

Quantity	Limit
Minimum Absolute Pressure	1
Maximum Absolute Pressure	5e+10
Minimum Temperature	1
Maximum Temperature	5000

Material Properties

Material: test (fluid)

Property	Units	Method	Value(s)
Density	kg/m3	constant	1000
Cp (Specific Heat)	j/kg-k	constant	4200
Thermal Conductivity	w/m-k	constant	0.58

Viscosity	kg/m-s	constant	0.001
Molecular Weight	kg/kgmol	constant	28
L-J Characteristic Length	angstrom	constant	0
L-J Energy Parameter	k	constant	0
Thermal Expansion Coefficient	1/k	constant	0
Degrees of Freedom		constant	0
Speed of Sound	m/s	none	#f

Material: air (fluid)

Property	Units	Method	Value(s)
Density	kg/m3	constant	1.225
Cp (Specific Heat)	j/kg-k	constant	1006.43
Thermal Conductivity	w/m-k	constant	0.0242
Viscosity	kg/m-s	constant	1.7894e-05
Molecular Weight	kg/kgmol	constant	28.966
L-J Characteristic Length	angstrom	constant	3.711
L-J Energy Parameter	k	constant	78.6
Thermal Expansion Coefficient	1/k	constant	0
Degrees of Freedom		constant	0
Speed of Sound	m/s	none	#f

Material: aluminum (solid)

Property	Units	Method	Value(s)
Density	kg/m3	constant	2719
Cp (Specific Heat)	j/kg-k	constant	871
Thermal Conductivity	w/m-k	constant	202.4

"Volume Integral Report"

	Min Static Pressure (pascal)
new_fluid	1199.0335

	Max Static Pressure (pascal)
new_fluid	1915.8024

"Flux Report"

	Mass Flow Rate (kg/s)
default-interior	-3.7030289e-07
deforming_walls	0
m_in	2.66e-08
moving_wall	0
p_out	-2.6600057e-08
wall	0
Net	-5.6574937e-14

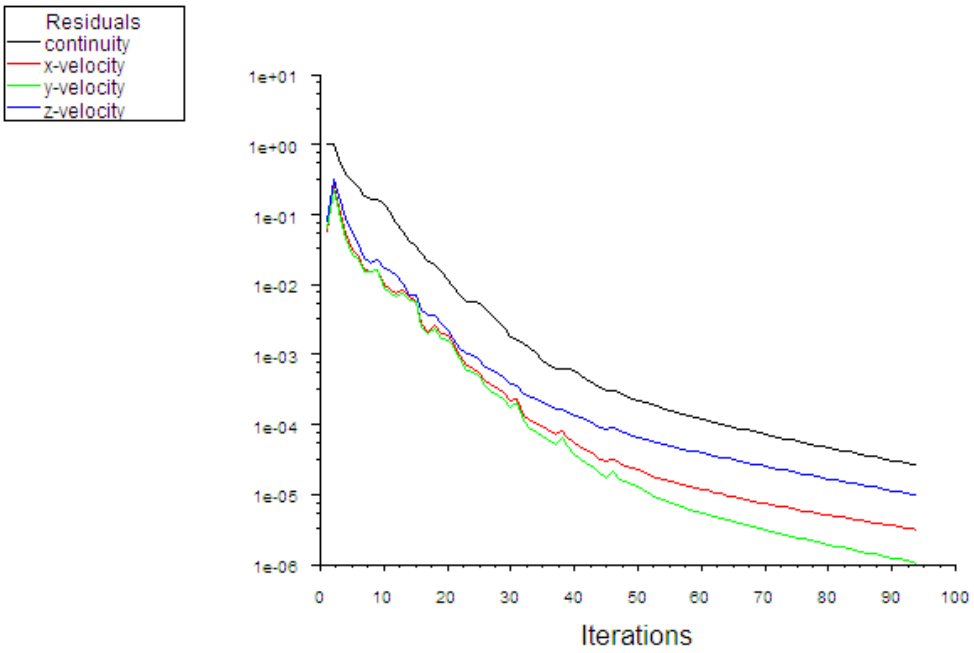

Figure A.1: Convergence results of Ahmed implant (1.6 µl/min)

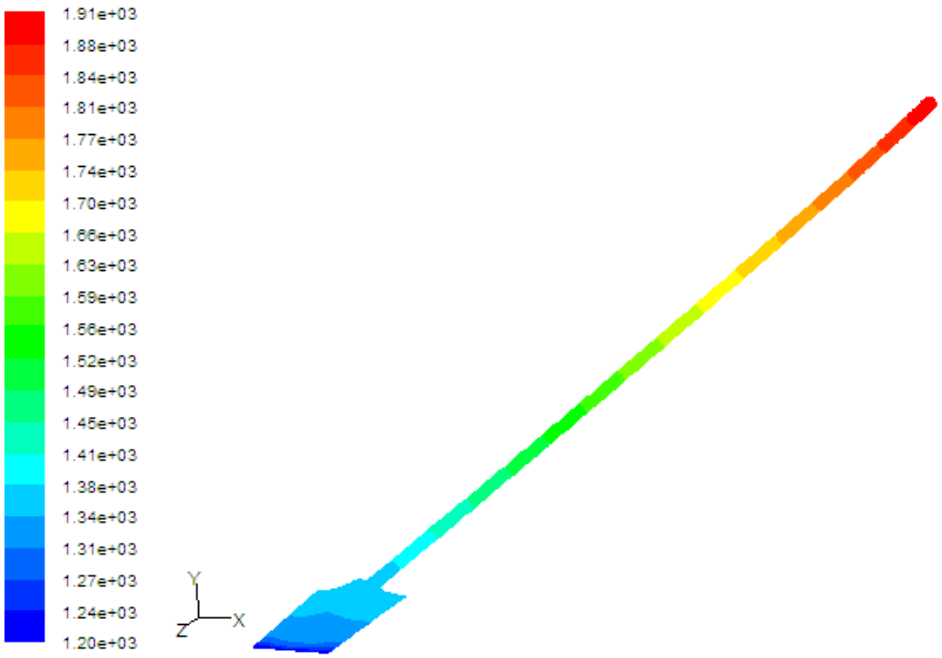

Figure A.2: Contours of static pressure on Ahmed implant (1.6 µl/min)

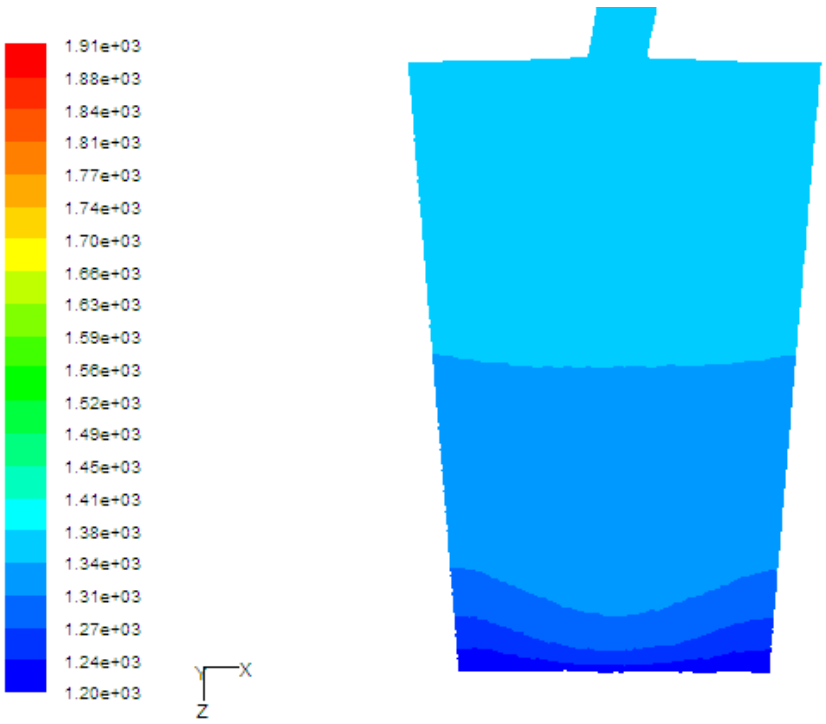

Figure A.3: Contours of static pressure on AGV (1.6 µl/min)

2.5 µl/min

FLUENT Summary Report File:

```
FLUENT
Version: 3d, dp, pbns, lam (3d, double precision, pressure-based,
laminar)
Release: 6.3.26
Title:

Models
------

   Model                         Settings
   ------------------------------------
   Space                         3D
   Time                          Steady
   Viscous                       Laminar
   Heat Transfer                 Disabled
   Solidification and Melting    Disabled
   Species Transport             Disabled
   Coupled Dispersed Phase       Disabled
   Pollutants                    Disabled
   Pollutants                    Disabled
   Soot                          Disabled

Boundary Conditions
-------------------

   Zones

      name               id   type
      ------------------------------------
      new_fluid          2    fluid
      m_in               5    mass-flow-inlet
      moving_wall        7    wall
      deforming_walls    6    wall
      wall               3    wall
      p_out              4    pressure-outlet
      default-interior   9    interior


Boundary Conditions                                    aq_humor

Condition                                                Value
-----------------------------------------------------------------
Material Name                                             test
Specify source terms?                                     no
Source Terms                                              ((mass)
                                                        (x-momentum)
                                                        (y-momentum)
                                                       (z-momentum))
Specify fixed values?                                     no
Local Coordinate System for Fixed Velocities              no
Fixed Values                                       (x-velocity
                                                   (inactive . #f)
                                                   (constant . 0)
                                                       profile  )) (y-
                                                   velocity (inactive .
                                                   #f) (constant . 0)
                                                   (profile  )) (z-
```

	velocity (inactive . #f) (constant . 0) (profile)))
Motion Type	0
X-Velocity Of Zone (m/s)	0
Y-Velocity Of Zone (m/s)	0
Z-Velocity Of Zone (m/s)	0
Rotation speed (rad/s)	0
X-Origin of Rotation-Axis (mm)	0
Y-Origin of Rotation-Axis (mm)	0
Z-Origin of Rotation-Axis (mm)	0
X-Component of Rotation-Axis	0
Y-Component of Rotation-Axis	0
Z-Component of Rotation-Axis	1
Deactivated Thread	no
Porous zone?	no
Conical porous zone?	no
X-Component of Direction-1 Vector	1
Y-Component of Direction-1 Vector	0
Z-Component of Direction-1 Vector	0
X-Component of Direction-2 Vector	0
Y-Component of Direction-2 Vector	1
Z-Component of Direction-2 Vector	0
X-Component of Cone Axis Vector	1
Y-Component of Cone Axis Vector	0
Z-Component of Cone Axis Vector	0
X-Coordinate of Point on Cone Axis (mm)	1
Y-Coordinate of Point on Cone Axis (mm)	0
Z-Coordinate of Point on Cone Axis (mm)	0
Half Angle of Cone Relative to its Axis (deg)	0
Relative Velocity Resistance Formulation?	yes
Direction-1 Viscous Resistance (1/m2)	0
Direction-2 Viscous Resistance (1/m2)	0
Direction-3 Viscous Resistance (1/m2)	0
Choose alternative formulation for inertial resistance?	no
Direction-1 Inertial Resistance (1/m)	0
Direction-2 Inertial Resistance (1/m)	0
Direction-3 Inertial Resistance (1/m)	0
C0 Coefficient for Power-Law	0
C1 Coefficient for Power-Law	0
Porosity	1

m_in

Condition	Value
Mass Flow Specification Method	0
Mass Flow-Rate (kg/s)	4.16e-08
Mass Flux (kg/m2-s)	1
Average Mass Flux (kg/m2-s)	1
Upstream Torque Integral (n-m)	1
Upstream Total Enthalpy Integral (w/m2)	1
Supersonic/Initial Gauge Pressure (pascal)	0
Direction Specification Method	1
Reference Frame	0
Coordinate System	0
X-Component of Flow Direction	1
Y-Component of Flow Direction	0
Z-Component of Flow Direction	0
X-Component of Axis Direction	1
Y-Component of Axis Direction	0
Z-Component of Axis Direction	0
X-Coordinate of Axis Origin (mm)	0

Y-Coordinate of Axis Origin (mm)	0
Z-Coordinate of Axis Origin (mm)	0
is zone used in mixing-plane model?	no

moving_wall

Condition	Value
Enable shell conduction?	no
Wall Motion	0
Shear Boundary Condition	0
Define wall motion relative to adjacent cell zone?	yes
Apply a rotational velocity to this wall?	no
Velocity Magnitude (m/s)	0
X-Component of Wall Translation	1
Y-Component of Wall Translation	0
Z-Component of Wall Translation	0
Define wall velocity components?	no
X-Component of Wall Translation (m/s)	0
Y-Component of Wall Translation (m/s)	0
Z-Component of Wall Translation (m/s)	0
Rotation Speed (rad/s)	0
X-Position of Rotation-Axis Origin (mm)	0
Y-Position of Rotation-Axis Origin (mm)	0
Z-Position of Rotation-Axis Origin (mm)	0
X-Component of Rotation-Axis Direction	0
Y-Component of Rotation-Axis Direction	0
Z-Component of Rotation-Axis Direction	1
X-component of shear stress (pascal)	0
Y-component of shear stress (pascal)	0
Z-component of shear stress (pascal)	0
Specularity Coefficient	0

deforming_walls

Condition	Value
Enable shell conduction?	no
Wall Motion	0
Shear Boundary Condition	0
Define wall motion relative to adjacent cell zone?	yes
Apply a rotational velocity to this wall?	no
Velocity Magnitude (m/s)	0
X-Component of Wall Translation	1
Y-Component of Wall Translation	0
Z-Component of Wall Translation	0
Define wall velocity components?	no
X-Component of Wall Translation (m/s)	0
Y-Component of Wall Translation (m/s)	0
Z-Component of Wall Translation (m/s)	0
Rotation Speed (rad/s)	0
X-Position of Rotation-Axis Origin (mm)	0
Y-Position of Rotation-Axis Origin (mm)	0
Z-Position of Rotation-Axis Origin (mm)	0
X-Component of Rotation-Axis Direction	0
Y-Component of Rotation-Axis Direction	0
Z-Component of Rotation-Axis Direction	1
X-component of shear stress (pascal)	0
Y-component of shear stress (pascal)	0
Z-component of shear stress (pascal)	0
Specularity Coefficient	0

wall

Condition	Value
Enable shell conduction?	no
Wall Motion	0
Shear Boundary Condition	0
Define wall motion relative to adjacent cell zone?	yes
Apply a rotational velocity to this wall?	no
Velocity Magnitude (m/s)	0
X-Component of Wall Translation	1
Y-Component of Wall Translation	0
Z-Component of Wall Translation	0
Define wall velocity components?	no
X-Component of Wall Translation (m/s)	0
Y-Component of Wall Translation (m/s)	0
Z-Component of Wall Translation (m/s)	0
Rotation Speed (rad/s)	0
X-Position of Rotation-Axis Origin (mm)	0
Y-Position of Rotation-Axis Origin (mm)	0
Z-Position of Rotation-Axis Origin (mm)	0
X-Component of Rotation-Axis Direction	0
Y-Component of Rotation-Axis Direction	0
Z-Component of Rotation-Axis Direction	1
X-component of shear stress (pascal)	0
Y-component of shear stress (pascal)	0
Z-component of shear stress (pascal)	0
Specularity Coefficient	0

p_out

Condition	Value
Gauge Pressure (pascal)	1200
Backflow Direction Specification Method	1
Coordinate System	0
X-Component of Flow Direction	1
Y-Component of Flow Direction	0
Z-Component of Flow Direction	0
X-Component of Axis Direction	1
Y-Component of Axis Direction	0
Z-Component of Axis Direction	0
X-Coordinate of Axis Origin (mm)	0
Y-Coordinate of Axis Origin (mm)	0
Z-Coordinate of Axis Origin (mm)	0
is zone used in mixing-plane model?	no
Radial Equilibrium Pressure Distribution	no
Specify targeted mass flow rate	no
Targeted mass flow (kg/s)	1

default-interior

Condition	Value

Solver Controls

Equations

Equation	Solved

Flow yes

Numerics

Numeric	Enabled
Absolute Velocity Formulation	yes

Relaxation

Variable	Relaxation Factor
Pressure	0.3
Density	1
Body Forces	1
Momentum	0.7

Linear Solver

Variable	Solver Type	Termination Criterion	Residual Reduction Tolerance
Pressure	V-Cycle	0.1	
X-Momentum	Flexible	0.1	0.7
Y-Momentum	Flexible	0.1	0.7
Z-Momentum	Flexible	0.1	0.7

Pressure-Velocity Coupling

Parameter	Value
Type	SIMPLE

Discretization Scheme

Variable	Scheme
Pressure	Standard
Momentum	First Order Upwind

Solution Limits

Quantity	Limit
Minimum Absolute Pressure	1
Maximum Absolute Pressure	5e+10
Minimum Temperature	1
Maximum Temperature	5000

Material Properties

Material: test (fluid)

Property	Units	Method	Value(s)
Density	kg/m3	constant	1000
Cp (Specific Heat)	j/kg-k	constant	4200
Thermal Conductivity	w/m-k	constant	0.58
Viscosity	kg/m-s	constant	0.001
Molecular Weight	kg/kgmol	constant	28
L-J Characteristic Length	angstrom	constant	0
L-J Energy Parameter	k	constant	0

Thermal Expansion Coefficient	1/k	constant	0
Degrees of Freedom		constant	0
Speed of Sound	m/s	none	#f

Material: air (fluid)

Property	Units	Method	Value(s)
Density	kg/m3	constant	1.225
Cp (Specific Heat)	j/kg-k	constant	1006.43
Thermal Conductivity	w/m-k	constant	0.0242
Viscosity	kg/m-s	constant	1.7894e-05
Molecular Weight	kg/kgmol	constant	28.966
L-J Characteristic Length	angstrom	constant	3.711
L-J Energy Parameter	k	constant	78.6
Thermal Expansion Coefficient	1/k	constant	0
Degrees of Freedom		constant	0
Speed of Sound	m/s	none	#f

Material: aluminum (solid)

Property	Units	Method	Value(s)
Density	kg/m3	constant	2719
Cp (Specific Heat)	j/kg-k	constant	871
Thermal Conductivity	w/m-k	constant	202.4

"Volume Integral Report"

Min Static Pressure	(pascal)
new_fluid	1198.6108

Max Static Pressure	(pascal)
new_fluid	2231.0333

"Flux Report"

Mass Flow Rate	(kg/s)
default-interior	-5.7999208e-07
deforming_walls	0
m_in	4.16e-08
moving_wall	0
p_out	-4.1600094e-08
wall	0
Net	-9.4471992e-14

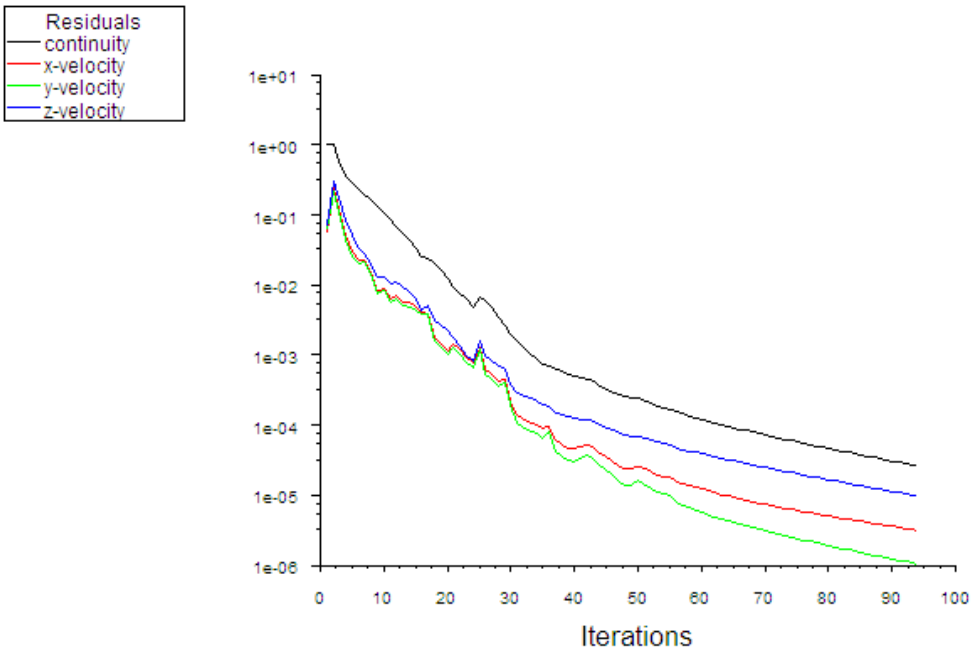

Figure A.4: Convergence results of Ahmed implant (2.5 µl/min)

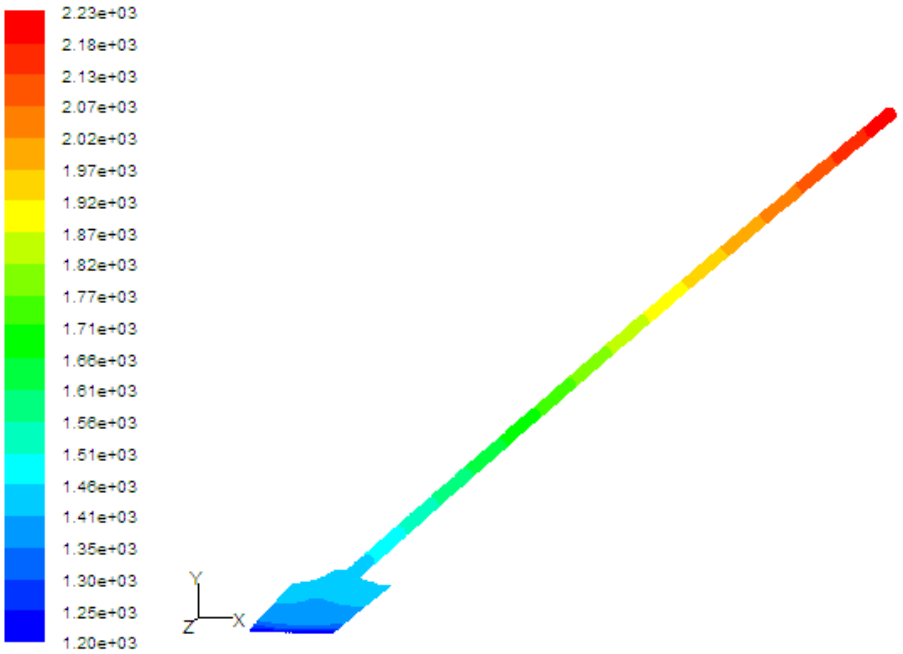

Figure A.5: Contours of static pressure on Ahmed implant (2.5 µl/min)

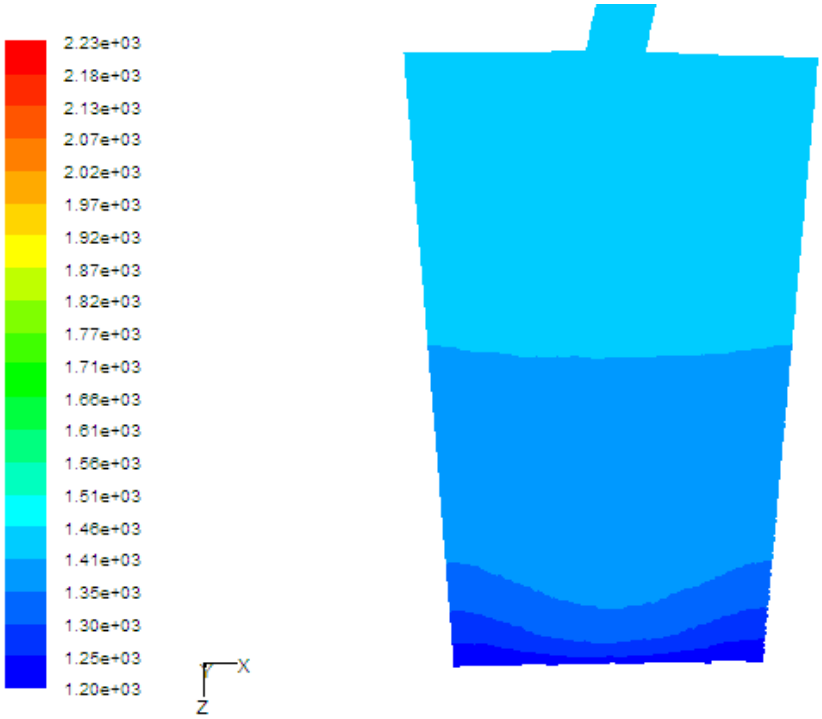

Figure A.6: Contours of static pressure on AGV (2.5 µl/min)

20 µl/min

FLUENT Summary Report File:

```
FLUENT
Version: 3d, dp, pbns, lam (3d, double precision, pressure-based,
laminar)
Release: 6.3.26
Title:

Models
------

   Model                         Settings
   ------------------------------------
   Space                         3D
   Time                          Steady
   Viscous                       Laminar
   Heat Transfer                 Disabled
   Solidification and Melting    Disabled
   Species Transport             Disabled
   Coupled Dispersed Phase       Disabled
   Pollutants                    Disabled
   Pollutants                    Disabled
   Soot                          Disabled

Boundary Conditions
-------------------

   Zones

      name               id   type
      ---------------------------------------
      new_fluid          2    fluid
      m_in               5    mass-flow-inlet
      moving_wall        7    wall
      deforming_walls    6    wall
      wall               3    wall
      p_out              4    pressure-outlet
      default-interior   9    interior

Boundary Conditions                                    aq_humor

Condition                                                Value
-------------------------------------------------------------------
Material Name                                              test
Specify source terms?                                      no
Source Terms                                               ((mass)
                                                          (x-momentum)
                                                          (y-momentum)
                                                          (z-momentum))
Specify fixed values?                                      no
Local Coordinate System for Fixed Velocities               no
Fixed Values                                          (x-velocity
                                                      (inactive . #f)
                                                      (constant . 0)
                                                           profile  )) (y-
                                                      velocity (inactive .
                                                      #f) (constant . 0)
                                                      (profile  )) (z-
                                                      velocity (inactive .
```

```
                                                #f) (constant . 0)
                                                (profile  )))
Motion Type                                              0
X-Velocity Of Zone (m/s)                                 0
Y-Velocity Of Zone (m/s)                                 0
Z-Velocity Of Zone (m/s)                                 0
Rotation speed (rad/s)                                   0
X-Origin of Rotation-Axis (mm)                           0
Y-Origin of Rotation-Axis (mm)                           0
Z-Origin of Rotation-Axis (mm)                           0
X-Component of Rotation-Axis                             0
Y-Component of Rotation-Axis                             0
Z-Component of Rotation-Axis                             1
Deactivated Thread                                       no
Porous zone?                                             no
Conical porous zone?                                     no
X-Component of Direction-1 Vector                        1
Y-Component of Direction-1 Vector                        0
Z-Component of Direction-1 Vector                        0
X-Component of Direction-2 Vector                        0
Y-Component of Direction-2 Vector                        1
Z-Component of Direction-2 Vector                        0
X-Component of Cone Axis Vector                          1
Y-Component of Cone Axis Vector                          0
Z-Component of Cone Axis Vector                          0
X-Coordinate of Point on Cone Axis (mm)                  1
Y-Coordinate of Point on Cone Axis (mm)                  0
Z-Coordinate of Point on Cone Axis (mm)                  0
Half Angle of Cone Relative to its Axis (deg)            0
Relative Velocity Resistance Formulation?                yes
Direction-1 Viscous Resistance (1/m2)                    0
Direction-2 Viscous Resistance (1/m2)                    0
Direction-3 Viscous Resistance (1/m2)                    0
Choose alternative formulation for inertial resistance?  no
Direction-1 Inertial Resistance (1/m)                    0
Direction-2 Inertial Resistance (1/m)                    0
Direction-3 Inertial Resistance (1/m)                    0
C0 Coefficient for Power-Law                             0
C1 Coefficient for Power-Law                             0
Porosity                                                 1
```

m_in

Condition	Value
Mass Flow Specification Method	0
Mass Flow-Rate (kg/s)	3.32e-07
Mass Flux (kg/m2-s)	1
Average Mass Flux (kg/m2-s)	1
Upstream Torque Integral (n-m)	1
Upstream Total Enthalpy Integral (w/m2)	1
Supersonic/Initial Gauge Pressure (pascal)	0
Direction Specification Method	1
Reference Frame	0
Coordinate System	0
X-Component of Flow Direction	1
Y-Component of Flow Direction	0
Z-Component of Flow Direction	0
X-Component of Axis Direction	1
Y-Component of Axis Direction	0
Z-Component of Axis Direction	0
X-Coordinate of Axis Origin (mm)	0
Y-Coordinate of Axis Origin (mm)	0

Z-Coordinate of Axis Origin (mm)	0
is zone used in mixing-plane model?	no

moving_wall

Condition	Value
Enable shell conduction?	no
Wall Motion	0
Shear Boundary Condition	0
Define wall motion relative to adjacent cell zone?	yes
Apply a rotational velocity to this wall?	no
Velocity Magnitude (m/s)	0
X-Component of Wall Translation	1
Y-Component of Wall Translation	0
Z-Component of Wall Translation	0
Define wall velocity components?	no
X-Component of Wall Translation (m/s)	0
Y-Component of Wall Translation (m/s)	0
Z-Component of Wall Translation (m/s)	0
Rotation Speed (rad/s)	0
X-Position of Rotation-Axis Origin (mm)	0
Y-Position of Rotation-Axis Origin (mm)	0
Z-Position of Rotation-Axis Origin (mm)	0
X-Component of Rotation-Axis Direction	0
Y-Component of Rotation-Axis Direction	0
Z-Component of Rotation-Axis Direction	1
X-component of shear stress (pascal)	0
Y-component of shear stress (pascal)	0
Z-component of shear stress (pascal)	0
Specularity Coefficient	0

deforming_walls

Condition	Value
Enable shell conduction?	no
Wall Motion	0
Shear Boundary Condition	0
Define wall motion relative to adjacent cell zone?	yes
Apply a rotational velocity to this wall?	no
Velocity Magnitude (m/s)	0
X-Component of Wall Translation	1
Y-Component of Wall Translation	0
Z-Component of Wall Translation	0
Define wall velocity components?	no
X-Component of Wall Translation (m/s)	0
Y-Component of Wall Translation (m/s)	0
Z-Component of Wall Translation (m/s)	0
Rotation Speed (rad/s)	0
X-Position of Rotation-Axis Origin (mm)	0
Y-Position of Rotation-Axis Origin (mm)	0
Z-Position of Rotation-Axis Origin (mm)	0
X-Component of Rotation-Axis Direction	0
Y-Component of Rotation-Axis Direction	0
Z-Component of Rotation-Axis Direction	1
X-component of shear stress (pascal)	0
Y-component of shear stress (pascal)	0
Z-component of shear stress (pascal)	0
Specularity Coefficient	0

wall

Condition	Value
Enable shell conduction?	no
Wall Motion	0
Shear Boundary Condition	0
Define wall motion relative to adjacent cell zone?	yes
Apply a rotational velocity to this wall?	no
Velocity Magnitude (m/s)	0
X-Component of Wall Translation	1
Y-Component of Wall Translation	0
Z-Component of Wall Translation	0
Define wall velocity components?	no
X-Component of Wall Translation (m/s)	0
Y-Component of Wall Translation (m/s)	0
Z-Component of Wall Translation (m/s)	0
Rotation Speed (rad/s)	0
X-Position of Rotation-Axis Origin (mm)	0
Y-Position of Rotation-Axis Origin (mm)	0
Z-Position of Rotation-Axis Origin (mm)	0
X-Component of Rotation-Axis Direction	0
Y-Component of Rotation-Axis Direction	0
Z-Component of Rotation-Axis Direction	1
X-component of shear stress (pascal)	0
Y-component of shear stress (pascal)	0
Z-component of shear stress (pascal)	0
Specularity Coefficient	0

p_out

Condition	Value
Gauge Pressure (pascal)	1200
Backflow Direction Specification Method	1
Coordinate System	0
X-Component of Flow Direction	1
Y-Component of Flow Direction	0
Z-Component of Flow Direction	0
X-Component of Axis Direction	1
Y-Component of Axis Direction	0
Z-Component of Axis Direction	0
X-Coordinate of Axis Origin (mm)	0
Y-Coordinate of Axis Origin (mm)	0
Z-Coordinate of Axis Origin (mm)	0
is zone used in mixing-plane model?	no
Radial Equilibrium Pressure Distribution	no
Specify targeted mass flow rate	no
Targeted mass flow (kg/s)	1

default-interior

Condition	Value

Solver Controls

Equations

Equation	Solved
Flow	yes

Numerics

Numeric	Enabled
Absolute Velocity Formulation	yes

Relaxation

Variable	Relaxation Factor
Pressure	0.3
Density	1
Body Forces	1
Momentum	0.7

Linear Solver

Variable	Solver Type	Termination Criterion	Residual Reduction Tolerance
Pressure	V-Cycle	0.1	
X-Momentum	Flexible	0.1	0.7
Y-Momentum	Flexible	0.1	0.7
Z-Momentum	Flexible	0.1	0.7

Pressure-Velocity Coupling

Parameter	Value
Type	SIMPLE

Discretization Scheme

Variable	Scheme
Pressure	Standard
Momentum	First Order Upwind

Solution Limits

Quantity	Limit
Minimum Absolute Pressure	1
Maximum Absolute Pressure	5e+10
Minimum Temperature	1
Maximum Temperature	5000

Material Properties

Material: test (fluid)

Property	Units	Method	Value(s)
Density	kg/m3	constant	1000
Cp (Specific Heat)	j/kg-k	constant	4200
Thermal Conductivity	w/m-k	constant	0.58
Viscosity	kg/m-s	constant	0.001
Molecular Weight	kg/kgmol	constant	28
L-J Characteristic Length	angstrom	constant	0
L-J Energy Parameter	k	constant	0
Thermal Expansion Coefficient	1/k	constant	0

Degrees of Freedom		constant	0
Speed of Sound	m/s	none	#f

Material: air (fluid)

Property	Units	Method	Value(s)
Density	kg/m3	constant	1.225
Cp (Specific Heat)	j/kg-k	constant	1006.43
Thermal Conductivity	w/m-k	constant	0.0242
Viscosity	kg/m-s	constant	1.7894e-05
Molecular Weight	kg/kgmol	constant	28.966
L-J Characteristic Length	angstrom	constant	3.711
L-J Energy Parameter	k	constant	78.6
Thermal Expansion Coefficient	1/k	constant	0
Degrees of Freedom		constant	0
Speed of Sound	m/s	none	#f

Material: aluminum (solid)

Property	Units	Method	Value(s)
Density	kg/m3	constant	2719
Cp (Specific Heat)	j/kg-k	constant	871
Thermal Conductivity	w/m-k	constant	202.4

"Volume Integral Report"

Min Static Pressure	(pascal)
new_fluid	1198.0136

Max Static Pressure	(pascal)
new_fluid	2333.076

"Flux Report"

Mass Flow Rate	(kg/s)
default-interior	-4.7158852e-06
deforming_walls	0
m_in	3.3329999e-07
moving_wall	0
p_out	-3.333007e-07
wall	0
Net	-7.0742251e-13

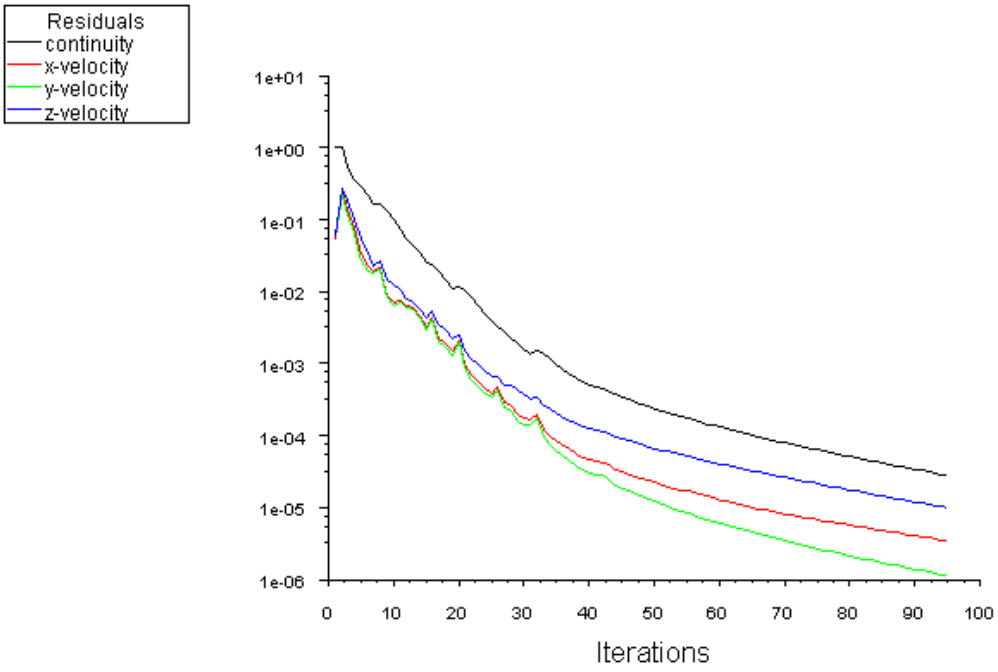

Figure A.7: Convergence results of Ahmed implant (20 µl/min)

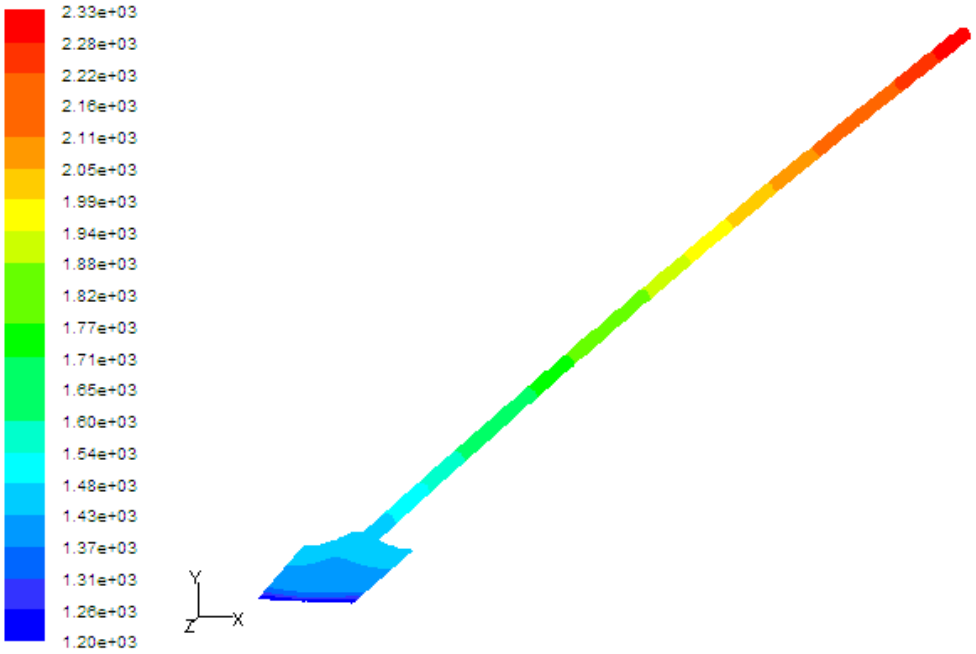

Figure A.8: Contours of static pressure on Ahmed implant (20 µl/min)

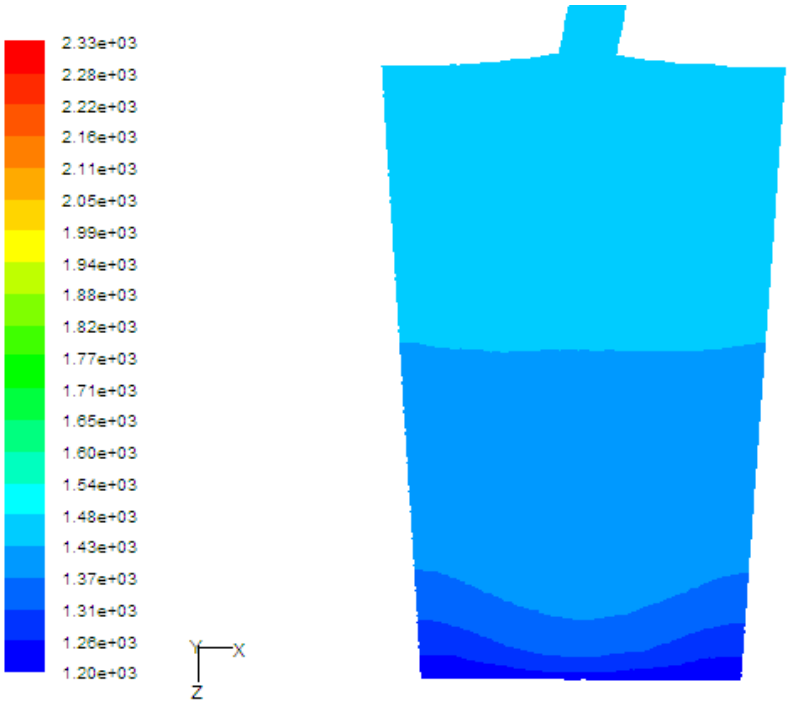

Figure A.9: Contours of static pressure on AGV (20 µl/min)

APPENDIX B

UDF FOR ROTATIONAL MOTION

```
//*********************************************************************
Microsoft (R) 32-bit C/C++ Optimizing Compiler Version 13.10.3077 for 80x86
Copyright (C) Microsoft Corporation 1984-2002. All rights reserved.
**/

/*

      fermat_spring_UDF  = name shown in FLUENT GUI
                   dt  = thread
                cg_vel  = cg velocity (global)
              cg_omega  = angular velocity (global)
                 time  = current time
                dtime  = time step
                                                */
/*********************************************************************
**/

/* This file generated automatically. */
/* Do not modify. */
#include "udf.h"
#include "prop.h"
#include "dpm.h"
extern DEFINE_CG_MOTION(fermat_spring1_UDF, dt, cg_vel, cg_omega, time,
dtime);
extern DEFINE_CG_MOTION(fermat_spring2_UDF, dt, cg_vel, cg_omega, time,
dtime);
__declspec(dllexport) UDF_Data udf_data[] = {
{"fermat_spring1_UDF",              (void              (*)())fermat_spring1_UDF,
UDF_TYPE_CG_MOTION},
{"fermat_spring2_UDF",              (void              (*)())fermat_spring2_UDF,
UDF_TYPE_CG_MOTION},
};
__declspec(dllexport) int n_udf_data = sizeof(udf_data)/sizeof(UDF_Data);
#include "version.h"
```

```
__declspec(dllexport) void UDF_Inquire_Release(int *major, int *minor, int *revision)
{
*major = RampantReleaseMajor;
*minor = RampantReleaseMinor;
*revision = RampantReleaseRevision;
}

/* Main UDF Code        */

#include "udf.h"

#define  omega      1.0          /* rotational speed, rad/sec        */

DEFINE_CG_MOTION(fermat_spring1_UDF, dt, cg_vel, cg_omega, time, dtime)
{
  cg_vel[0] = 0.0;
  cg_vel[1] = 0.0;
  cg_vel[2] = 0.0;

  cg_omega[0] = 0.0;
  cg_omega[1] = 0.0;
  cg_omega[2] = omega;
}

DEFINE_CG_MOTION(fermat_spring2_UDF, dt, cg_vel, cg_omega, time, dtime)
{
  cg_vel[0] = 0.0;
  cg_vel[1] = 0.0;
  cg_vel[2] = 0.0;

  cg_omega[0] = 0.0;
  cg_omega[1] = 0.0;
  cg_omega[2] = -omega;
}
```

```
/*****************************************************************
**/
/*                                                               */
/*       End of the UDF.                                         */
/*                                                               */
/*****************************************************************
**/
```

APPENDIX C

POSTPROCESSING OF PROPOSED MODEL

2.5 µl/min

```
FLUENT
Version: 2d, dp, pbns, dynamesh, lam, unsteady (2d, double
precision, pressure-based, dynamic mesh, laminar, unsteady)
Release: 6.3.26
Title:

Models
------

   Model                         Settings
   ------------------------------------------------------------
   Space                         2D
   Time                          Unsteady, 1st-Order Implicit
   Viscous                       Laminar
   Heat Transfer                 Disabled
   Solidification and Melting    Disabled
   Species Transport             Disabled
   Coupled Dispersed Phase       Disabled
   Pollutants                    Disabled
   Pollutants                    Disabled
   Soot                          Disabled

Boundary Conditions
-------------------

   Zones

      name                 id   type
      ---------------------------------------
      aq_humor             2    fluid
      wall                 3    wall
      wall.5               4    wall
      fermat-spring.2      5    wall
      fermat-spring.1      6    wall
      velocity_inlet.2     7    velocity-inlet
      pressure_outlet.1    8    pressure-outlet
      default-interior     10   interior


Boundary Conditions                                    aq_humor


Condition                                                 Value
------------------------------------------------------------------
Material Name                                               test
Specify source terms?                                       no
Source Terms                                                ((mass)
                                                          (x-momentum)
                                                          (y-momentum)
)
Specify fixed values?                                       no
Local Coordinate System for Fixed Velocities                no
Fixed Values                                         (x-velocity
                                                    (inactive . #f)
                                                    (constant . 0)
                                                         profile  )) (y-
                                                   velocity (inactive .
```

	#f) (constant . 0) (profile))
Motion Type	0
X-Velocity Of Zone (m/s)	0
Y-Velocity Of Zone (m/s)	0
Rotation speed (rad/s)	0
X-Origin of Rotation-Axis (mm)	0
Y-Origin of Rotation-Axis (mm)	0
X-Component of Rotation-Axis	0
Y-Component of Rotation-Axis	0
Deactivated Thread	no
Porous zone?	no
Conical porous zone?	no
X-Component of Direction-1 Vector	1
Y-Component of Direction-1 Vector	0
X-Component of Direction-2 Vector	0
Y-Component of Direction-2 Vector	1
X-Component of Cone Axis Vector	1
Y-Component of Cone Axis Vector	0
X-Coordinate of Point on Cone Axis (mm)	1
Y-Coordinate of Point on Cone Axis (mm)	0
Half Angle of Cone Relative to its Axis (deg)	0
Relative Velocity Resistance Formulation?	yes
Direction-1 Viscous Resistance (1/m2)	0
Direction-2 Viscous Resistance (1/m2)	0
Choose alternative formulation for inertial resistance?	no
Direction-1 Inertial Resistance (1/m)	0
Direction-2 Inertial Resistance (1/m)	0
C0 Coefficient for Power-Law	0
C1 Coefficient for Power-Law	0
Porosity	1

wall

Condition	Value
Wall Motion	0
Shear Boundary Condition	0
Define wall motion relative to adjacent cell zone?	yes
Apply a rotational velocity to this wall?	no
Velocity Magnitude (mm/s)	0
X-Component of Wall Translation	1
Y-Component of Wall Translation	0
Define wall velocity components?	no
X-Component of Wall Translation (mm/s)	0
Y-Component of Wall Translation (mm/s)	0
Rotation Speed (rad/s)	0
X-Position of Rotation-Axis Origin (mm)	0
Y-Position of Rotation-Axis Origin (mm)	0
X-component of shear stress (pascal)	0
Y-component of shear stress (pascal)	0
Specularity Coefficient	0

wall.5

Condition	Value
Wall Motion	0
Shear Boundary Condition	0
Define wall motion relative to adjacent cell zone?	yes
Apply a rotational velocity to this wall?	no

Velocity Magnitude (mm/s)	0
X-Component of Wall Translation	1
Y-Component of Wall Translation	0
Define wall velocity components?	no
X-Component of Wall Translation (mm/s)	0
Y-Component of Wall Translation (mm/s)	0
Rotation Speed (rad/s)	0
X-Position of Rotation-Axis Origin (mm)	0
Y-Position of Rotation-Axis Origin (mm)	0
X-component of shear stress (pascal)	0
Y-component of shear stress (pascal)	0
Specularity Coefficient	0

fermat-spring.2

Condition	Value
Wall Motion	0
Shear Boundary Condition	0
Define wall motion relative to adjacent cell zone?	yes
Apply a rotational velocity to this wall?	no
Velocity Magnitude (mm/s)	0
X-Component of Wall Translation	1
Y-Component of Wall Translation	0
Define wall velocity components?	no
X-Component of Wall Translation (mm/s)	0
Y-Component of Wall Translation (mm/s)	0
Rotation Speed (rad/s)	0
X-Position of Rotation-Axis Origin (mm)	0
Y-Position of Rotation-Axis Origin (mm)	0
X-component of shear stress (pascal)	0
Y-component of shear stress (pascal)	0
Specularity Coefficient	0

fermat-spring.1

Condition	Value
Wall Motion	0
Shear Boundary Condition	0
Define wall motion relative to adjacent cell zone?	yes
Apply a rotational velocity to this wall?	no
Velocity Magnitude (mm/s)	0
X-Component of Wall Translation	1
Y-Component of Wall Translation	0
Define wall velocity components?	no
X-Component of Wall Translation (mm/s)	0
Y-Component of Wall Translation (mm/s)	0
Rotation Speed (rad/s)	0
X-Position of Rotation-Axis Origin (mm)	0
Y-Position of Rotation-Axis Origin (mm)	0
X-component of shear stress (pascal)	0
Y-component of shear stress (pascal)	0
Specularity Coefficient	0

velocity_inlet.2

Condition	Value
Velocity Specification Method	2
Reference Frame	0
Velocity Magnitude (mm/s)	0.0025000002

X-Velocity (mm/s)	0
Y-Velocity (mm/s)	0
X-Component of Flow Direction	1
Y-Component of Flow Direction	0
X-Component of Axis Direction	1
Y-Component of Axis Direction	0
Z-Component of Axis Direction	0
X-Coordinate of Axis Origin (mm)	0
Y-Coordinate of Axis Origin (mm)	0
Z-Coordinate of Axis Origin (mm)	0
Angular velocity (rad/s)	0
is zone used in mixing-plane model?	no

pressure_outlet.1

Condition	Value
Gauge Pressure (pascal)	1200
Backflow Direction Specification Method	1
X-Component of Flow Direction	1
Y-Component of Flow Direction	0
X-Component of Axis Direction	1
Y-Component of Axis Direction	0
Z-Component of Axis Direction	0
X-Coordinate of Axis Origin (mm)	0
Y-Coordinate of Axis Origin (mm)	0
Z-Coordinate of Axis Origin (mm)	0
is zone used in mixing-plane model?	no
Specify targeted mass flow rate	no
Targeted mass flow (kg/s)	1

default-interior

Condition	Value

Solver Controls

Equations

Equation	Solved
Flow	yes

Numerics

Numeric	Enabled
Absolute Velocity Formulation	yes

Unsteady Calculation Parameters

Time Step (s)	0.0018
Max. Iterations Per Time Step	20

Relaxation

Variable	Relaxation Factor
Pressure	0.3
Density	1
Body Forces	1
Momentum	0.7

Linear Solver

Variable	Solver Type	Termination Criterion	Residual Reduction Tolerance
Pressure	V-Cycle	0.1	
X-Momentum	Flexible	0.1	0.7
Y-Momentum	Flexible	0.1	0.7

Pressure-Velocity Coupling

Parameter	Value
Type	SIMPLE

Discretization Scheme

Variable	Scheme
Pressure	Standard
Momentum	First Order Upwind

Solution Limits

Quantity	Limit
Minimum Absolute Pressure	1
Maximum Absolute Pressure	5e+10
Minimum Temperature	1
Maximum Temperature	5000

Material Properties

Material: test (fluid)

Property	Units	Method	Value(s)
Density	kg/m3	constant	1000
Cp (Specific Heat)	j/kg-k	constant	4200
Thermal Conductivity	w/m-k	constant	0.58
Viscosity	kg/m-s	constant	0.001
Molecular Weight	kg/kgmol	constant	28
L-J Characteristic Length	angstrom	constant	0
L-J Energy Parameter	k	constant	0
Thermal Expansion Coefficient	1/k	constant	0
Degrees of Freedom		constant	0
Speed of Sound	mm/s	none	#f

Material: air (fluid)

Property	Units	Method	Value(s)
Density	kg/m3	constant	1.225
Cp (Specific Heat)	j/kg-k	constant	1006.43
Thermal Conductivity	w/m-k	constant	0.0242
Viscosity	kg/m-s	constant	1.78e-05
Molecular Weight	kg/kgmol	constant	28.966
L-J Characteristic Length	angstrom	constant	3.711
L-J Energy Parameter	k	constant	78.6
Thermal Expansion Coefficient	1/k	constant	0
Degrees of Freedom		constant	0
Speed of Sound	mm/s	none	#f

Material: aluminum (solid)

Property	Units	Method	Value(s)
Density	kg/m3	constant	2719
Cp (Specific Heat)	j/kg-k	constant	871
Thermal Conductivity	w/m-k	constant	202.4

"Volume Integral Report"

Min Static Pressure	(pascal)
aq_humor	1199.7339

Max Static Pressure	(pascal)
new_fluid	2335.7620

"Flux Report"

Mass Flow Rate	(kg/s)
default-interior	0.00055987832
fermat-spring.1	0
fermat-spring.2	0
pressure_outlet.1	-4.2016861e-05
velocity_inlet.2	4.2098778e-05
wall	0
wall.5	0
Net	8.1916838e-08

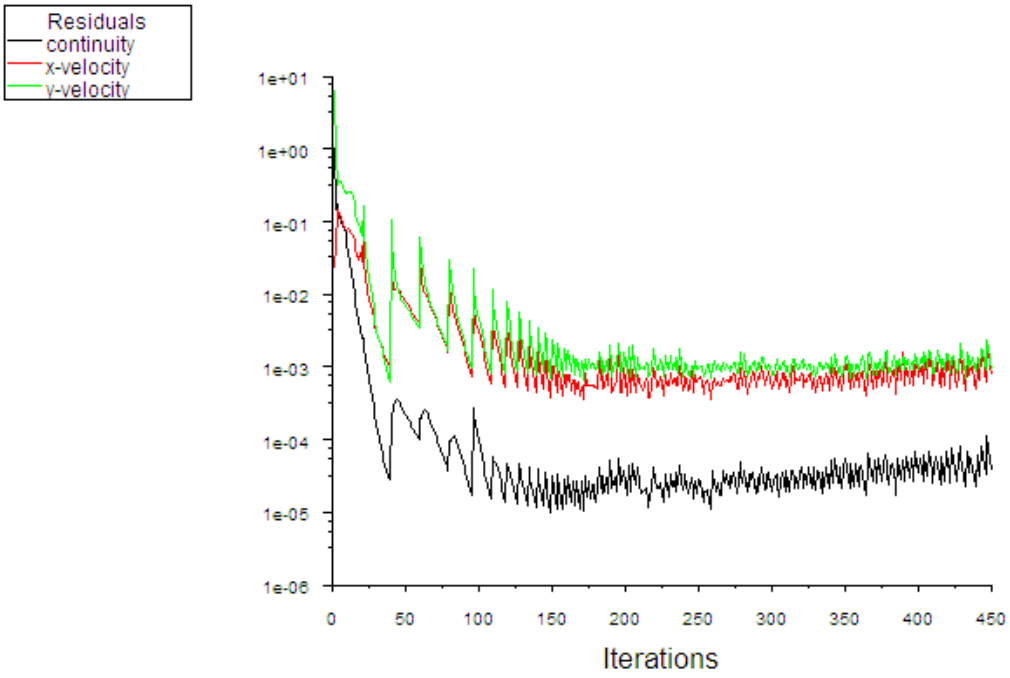

Figure C.1: Convergence results of the proposed model (2.5 µl/min)

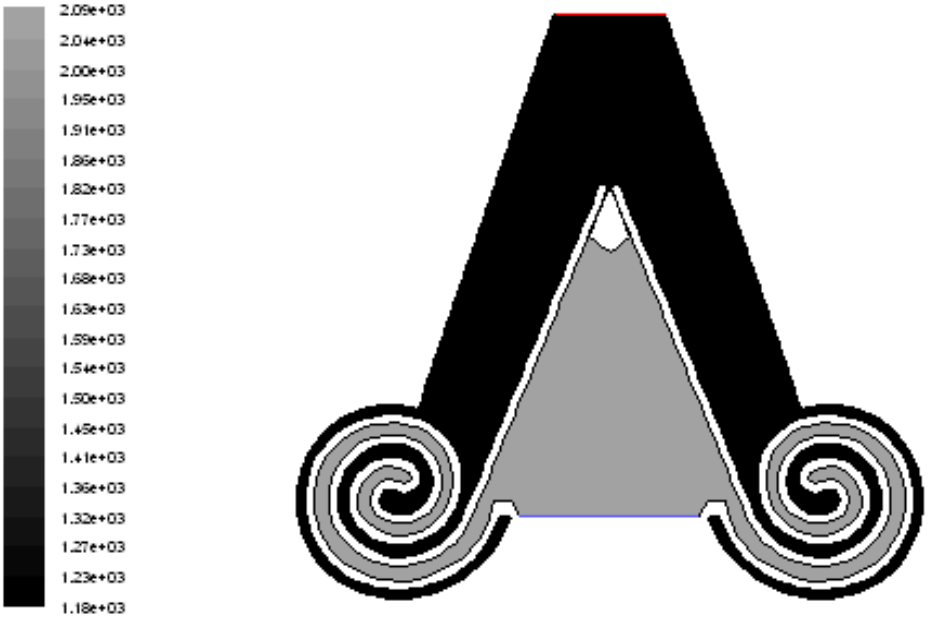

Figure C.2: Contours of static pressure on the proposed model (2.5 µl/min) - 2 ms

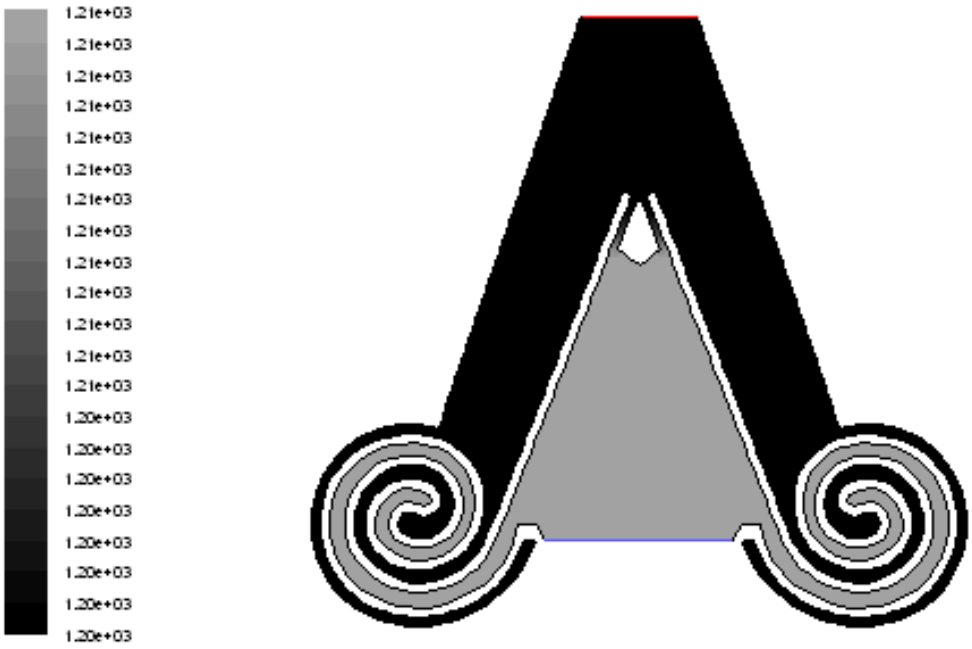

Figure C.3: Contours of static pressure on the proposed model (2.5 µl/min) - 20 ms

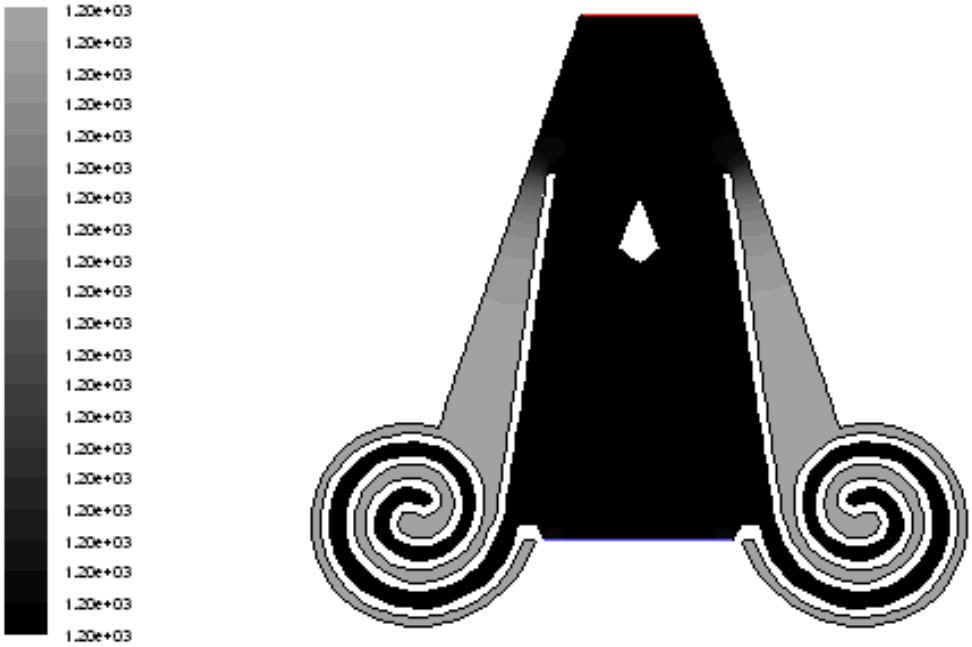

Figure C.4: Contours of static pressure on the proposed model (2.5 µl/min) – 246 ms

,

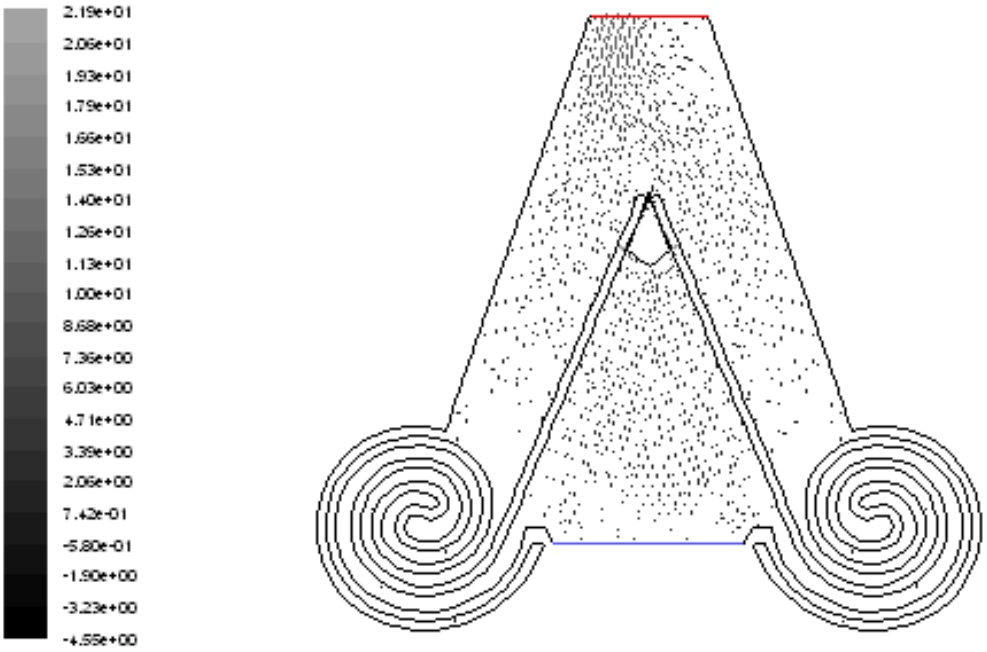

Figure C.5: Y velocity vectors on the proposed model (2.5 µl/min) - 2 ms

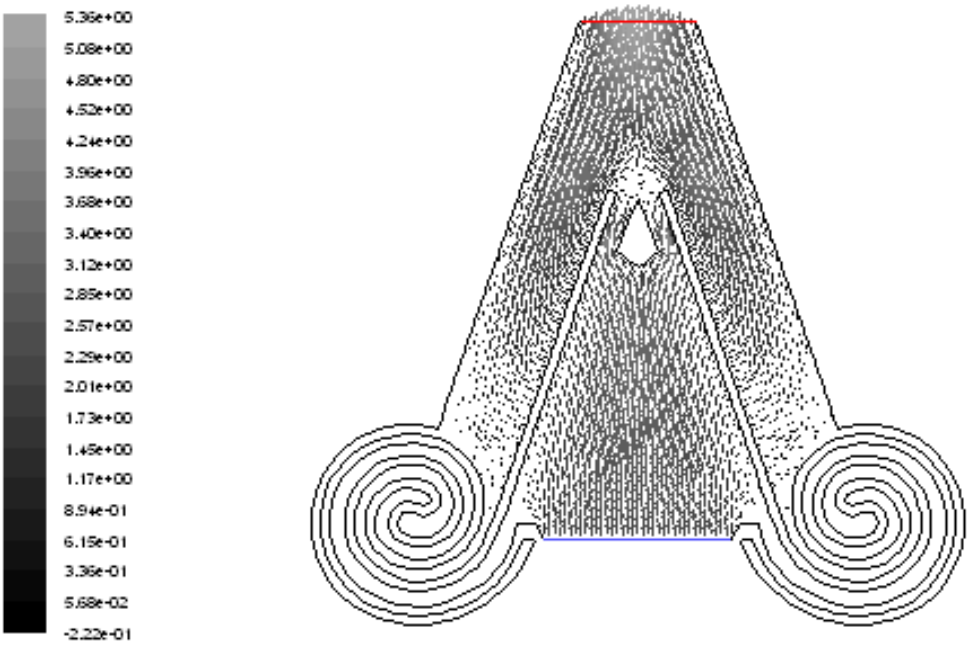

Figure C.6: Y velocity vectors on the proposed model (2.5 µl/min) - 64 ms

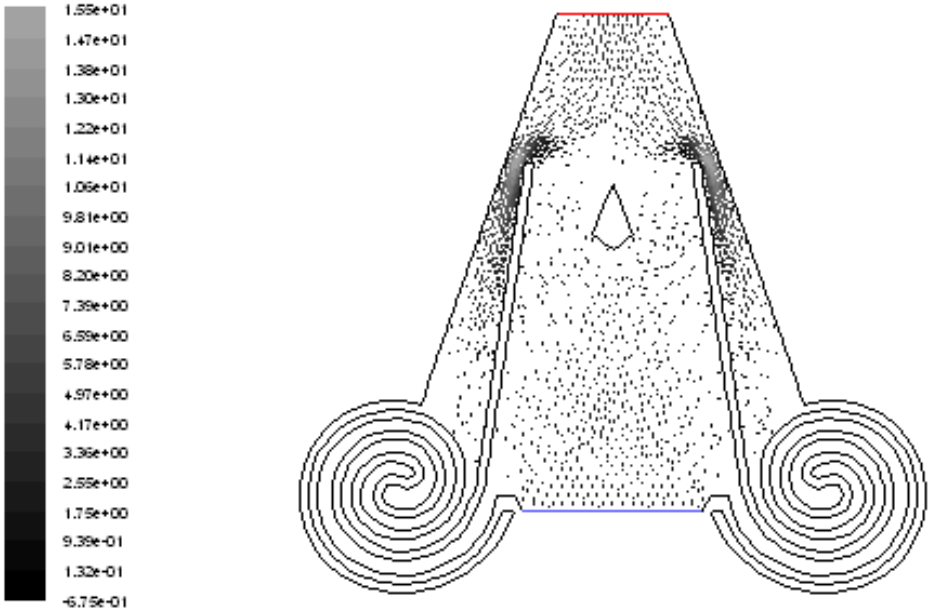

Figure C.7: Y velocity vectors on the proposed model (2.5 µl/min) - 246 ms

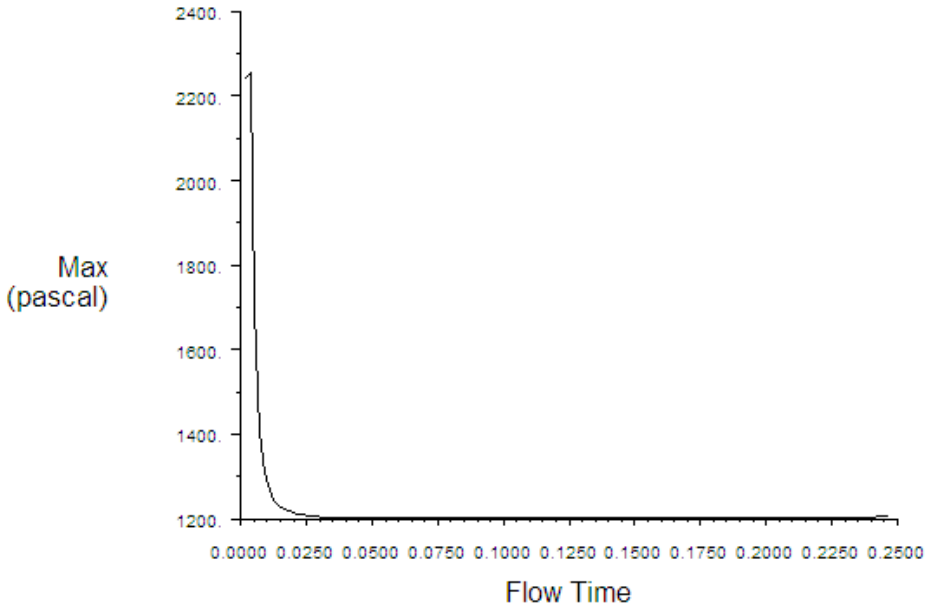

Figure C.8: Maximum pressure convergence on the proposed model (2.5 µl/min)

5 µl/min

FLUENT Summary Report File:

```
FLUENT
Version: 2d, dp, pbns, dynamesh, lam, unsteady (2d, double
precision, pressure-based, dynamic mesh, laminar, unsteady)
Release: 6.3.26
Title:

Models
------

   Model                         Settings
   ------------------------------------------------------------
   Space                         2D
   Time                          Unsteady, 1st-Order Implicit
   Viscous                       Laminar
   Heat Transfer                 Disabled
   Solidification and Melting    Disabled
   Species Transport             Disabled
   Coupled Dispersed Phase       Disabled
   Pollutants                    Disabled
   Pollutants                    Disabled
   Soot                          Disabled

Boundary Conditions
-------------------

   Zones

      name                id   type
      ---------------------------------------
      aq_humor            2    fluid
      wall                3    wall
      wall.5              4    wall
      fermat-spring.2     5    wall
      fermat-spring.1     6    wall
      velocity_inlet.2    7    velocity-inlet
      pressure_outlet.1   8    pressure-outlet
      default-interior    10   interior


Boundary Conditions                                    aq_humor


Condition                                                 Value
------------------------------------------------------------------------
Material Name                                             test
Specify source terms?                                     no
Source Terms                                              ((mass)
                                                         (x-momentum)
                                                         (y-momentum)
)
Specify fixed values?                                     no
Local Coordinate System for Fixed Velocities              no
Fixed Values                                          (x-velocity
                                                     (inactive . #f)
                                                     (constant . 0)
                                                          profile  )) (y-
                                                     velocity (inactive .
                                                     #f) (constant . 0)
                                                     (profile  ))
```

Motion Type	0
X-Velocity Of Zone (m/s)	0
Y-Velocity Of Zone (m/s)	0
Rotation speed (rad/s)	0
X-Origin of Rotation-Axis (mm)	0
Y-Origin of Rotation-Axis (mm)	0
X-Component of Rotation-Axis	0
Y-Component of Rotation-Axis	0
Deactivated Thread	no
Porous zone?	no
Conical porous zone?	no
X-Component of Direction-1 Vector	1
Y-Component of Direction-1 Vector	0
X-Component of Direction-2 Vector	0
Y-Component of Direction-2 Vector	1
X-Component of Cone Axis Vector	1
Y-Component of Cone Axis Vector	0
X-Coordinate of Point on Cone Axis (mm)	1
Y-Coordinate of Point on Cone Axis (mm)	0
Half Angle of Cone Relative to its Axis (deg)	0
Relative Velocity Resistance Formulation?	yes
Direction-1 Viscous Resistance (1/m2)	0
Direction-2 Viscous Resistance (1/m2)	0
Choose alternative formulation for inertial resistance?	no
Direction-1 Inertial Resistance (1/m)	0
Direction-2 Inertial Resistance (1/m)	0
C0 Coefficient for Power-Law	0
C1 Coefficient for Power-Law	0
Porosity	1

wall

Condition	Value
Wall Motion	0
Shear Boundary Condition	0
Define wall motion relative to adjacent cell zone?	yes
Apply a rotational velocity to this wall?	no
Velocity Magnitude (mm/s)	0
X-Component of Wall Translation	1
Y-Component of Wall Translation	0
Define wall velocity components?	no
X-Component of Wall Translation (mm/s)	0
Y-Component of Wall Translation (mm/s)	0
Rotation Speed (rad/s)	0
X-Position of Rotation-Axis Origin (mm)	0
Y-Position of Rotation-Axis Origin (mm)	0
X-component of shear stress (pascal)	0
Y-component of shear stress (pascal)	0
Specularity Coefficient	0

wall.5

Condition	Value
Wall Motion	0
Shear Boundary Condition	0
Define wall motion relative to adjacent cell zone?	yes
Apply a rotational velocity to this wall?	no
Velocity Magnitude (mm/s)	0
X-Component of Wall Translation	1

Y-Component of Wall Translation	0
Define wall velocity components?	no
X-Component of Wall Translation (mm/s)	0
Y-Component of Wall Translation (mm/s)	0
Rotation Speed (rad/s)	0
X-Position of Rotation-Axis Origin (mm)	0
Y-Position of Rotation-Axis Origin (mm)	0
X-component of shear stress (pascal)	0
Y-component of shear stress (pascal)	0
Specularity Coefficient	0

fermat-spring.2

Condition	Value
Wall Motion	0
Shear Boundary Condition	0
Define wall motion relative to adjacent cell zone?	yes
Apply a rotational velocity to this wall?	no
Velocity Magnitude (mm/s)	0
X-Component of Wall Translation	1
Y-Component of Wall Translation	0
Define wall velocity components?	no
X-Component of Wall Translation (mm/s)	0
Y-Component of Wall Translation (mm/s)	0
Rotation Speed (rad/s)	0
X-Position of Rotation-Axis Origin (mm)	0
Y-Position of Rotation-Axis Origin (mm)	0
X-component of shear stress (pascal)	0
Y-component of shear stress (pascal)	0
Specularity Coefficient	0

fermat-spring.1

Condition	Value
Wall Motion	0
Shear Boundary Condition	0
Define wall motion relative to adjacent cell zone?	yes
Apply a rotational velocity to this wall?	no
Velocity Magnitude (mm/s)	0
X-Component of Wall Translation	1
Y-Component of Wall Translation	0
Define wall velocity components?	no
X-Component of Wall Translation (mm/s)	0
Y-Component of Wall Translation (mm/s)	0
Rotation Speed (rad/s)	0
X-Position of Rotation-Axis Origin (mm)	0
Y-Position of Rotation-Axis Origin (mm)	0
X-component of shear stress (pascal)	0
Y-component of shear stress (pascal)	0
Specularity Coefficient	0

velocity_inlet.2

Condition	Value
Velocity Specification Method	2
Reference Frame	0
Velocity Magnitude (mm/s)	0.0050000004
X-Velocity (mm/s)	0
Y-Velocity (mm/s)	0
X-Component of Flow Direction	1

Y-Component of Flow Direction	0
X-Component of Axis Direction	1
Y-Component of Axis Direction	0
Z-Component of Axis Direction	0
X-Coordinate of Axis Origin (mm)	0
Y-Coordinate of Axis Origin (mm)	0
Z-Coordinate of Axis Origin (mm)	0
Angular velocity (rad/s)	0
is zone used in mixing-plane model?	no

pressure_outlet.1

Condition	Value
Gauge Pressure (pascal)	1200
Backflow Direction Specification Method	1
X-Component of Flow Direction	1
Y-Component of Flow Direction	0
X-Component of Axis Direction	1
Y-Component of Axis Direction	0
Z-Component of Axis Direction	0
X-Coordinate of Axis Origin (mm)	0
Y-Coordinate of Axis Origin (mm)	0
Z-Coordinate of Axis Origin (mm)	0
is zone used in mixing-plane model?	no
Specify targeted mass flow rate	no
Targeted mass flow (kg/s)	1

default-interior

Condition	Value

Solver Controls

Equations

Equation	Solved
Flow	yes

Numerics

Numeric	Enabled
Absolute Velocity Formulation	yes

Unsteady Calculation Parameters

Time Step (s)	0.0065000001
Max. Iterations Per Time Step	20

Relaxation

Variable	Relaxation Factor
Pressure	0.3
Density	1
Body Forces	1
Momentum	0.7

Linear Solver

Variable	Solver Type	Termination Criterion	Residual Reduction Tolerance
Pressure	V-Cycle	0.1	
X-Momentum	Flexible	0.1	0.7
Y-Momentum	Flexible	0.1	0.7

Pressure-Velocity Coupling

Parameter	Value
Type	SIMPLE

Discretization Scheme

Variable	Scheme
Pressure	Standard
Momentum	First Order Upwind

Solution Limits

Quantity	Limit
Minimum Absolute Pressure	1
Maximum Absolute Pressure	5e+10
Minimum Temperature	1
Maximum Temperature	5000

Material Properties

Material: test (fluid)

Property	Units	Method	Value(s)
Density	kg/m3	constant	1000
Cp (Specific Heat)	j/kg-k	constant	4200
Thermal Conductivity	w/m-k	constant	0.58
Viscosity	kg/m-s	constant	0.001
Molecular Weight	kg/kgmol	constant	28
L-J Characteristic Length	angstrom	constant	0
L-J Energy Parameter	k	constant	0
Thermal Expansion Coefficient	1/k	constant	0
Degrees of Freedom		constant	0
Speed of Sound	mm/s	none	#f

Material: air (fluid)

Property	Units	Method	Value(s)
Density	kg/m3	constant	1.225
Cp (Specific Heat)	j/kg-k	constant	1006.43
Thermal Conductivity	w/m-k	constant	0.0242
Viscosity	kg/m-s	constant	1.78e-05
Molecular Weight	kg/kgmol	constant	28.966
L-J Characteristic Length	angstrom	constant	3.711
L-J Energy Parameter	k	constant	78.6
Thermal Expansion Coefficient	1/k	constant	0
Degrees of Freedom		constant	0

```
      Speed of Sound                    mm/s       none       #f

   Material: aluminum (solid)

      Property                Units     Method     Value(s)
      ------------------------------------------------------
      Density                 kg/m3     constant   2719
      Cp (Specific Heat)      j/kg-k    constant   871
      Thermal Conductivity    w/m-k     constant   202.4


                              "Volume Integral Report"
                              Min
                 Static Pressure                (pascal)
------------------------------- --------------------
                       new_fluid             1190.3550
                              Max
                 Static Pressure                (pascal)
------------------------------- --------------------
                       new_fluid             2835.7620

                          "Flux Report"

                  Mass Flow Rate                  (kg/s)
------------------------------- --------------------
                default-interior         0.00099261721
                 fermat-spring.1                     0
                 fermat-spring.2                     0
               pressure_outlet.1        -8.4169657e-08
                velocity_inlet.2         8.4197556e-08
                            wall                     0
                          wall.5                     0
               --------------- --------------------
                             Net         2.7898417e-11
```

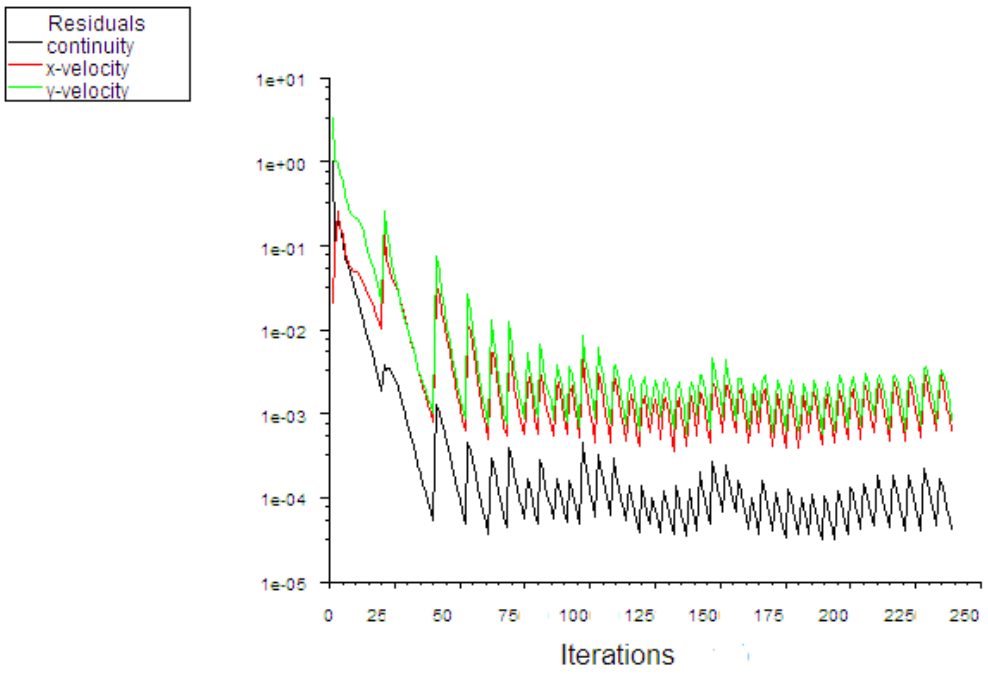

Figure C.9: Convergence results of the proposed model (5 µl/min)

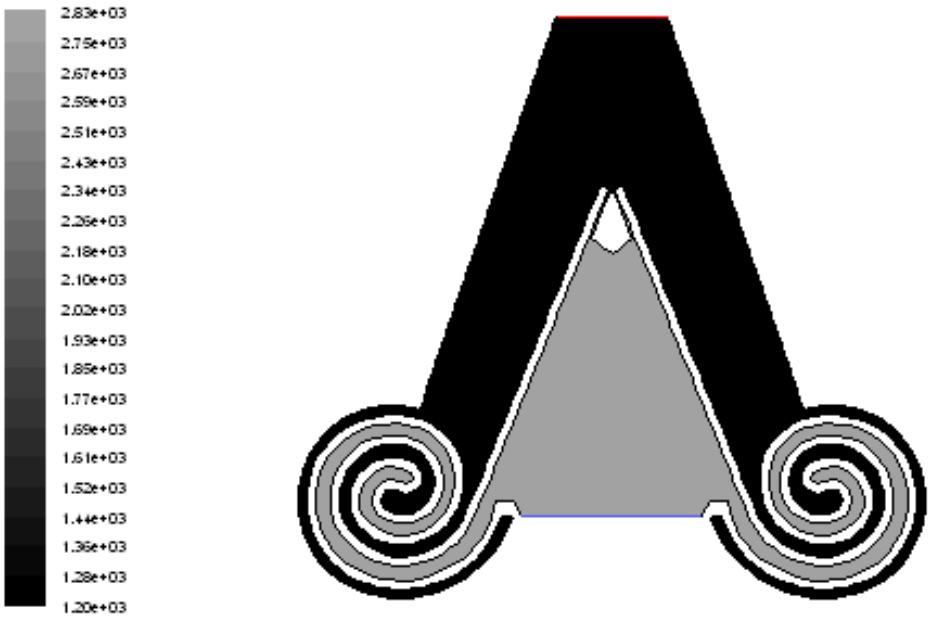

Figure C.10: Contours of static pressure on the proposed model (5 µl/min) – 6.5 ms

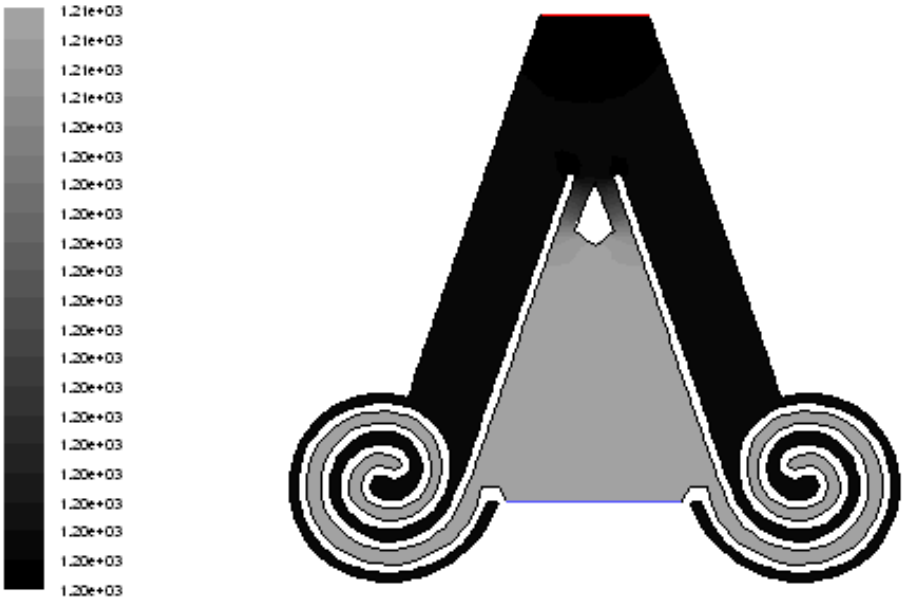

Figure C.11: Contours of static pressure on the proposed model (5 µl/min) -58.5 ms

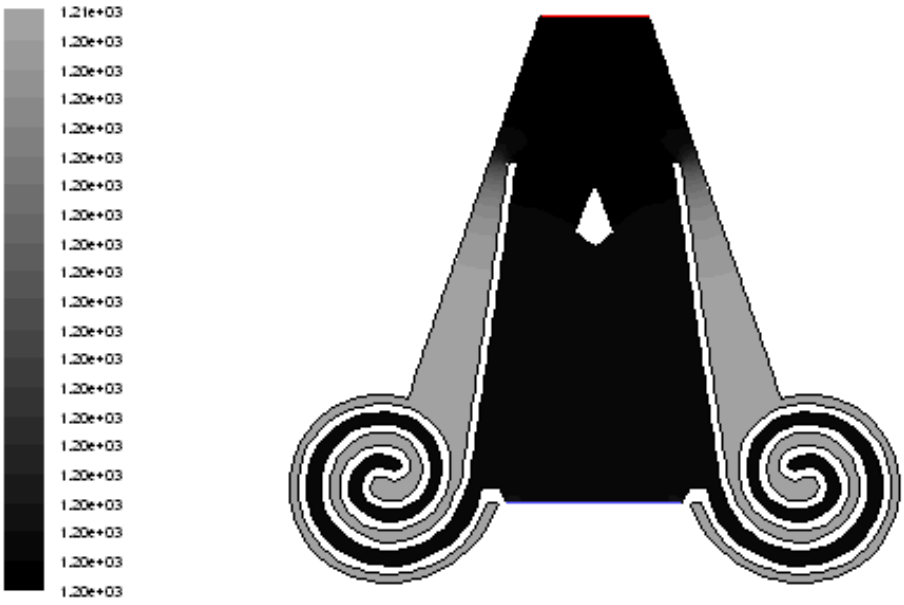

Figure C.12: Contours of static pressure on the proposed model (5 µl/min) - 247 ms

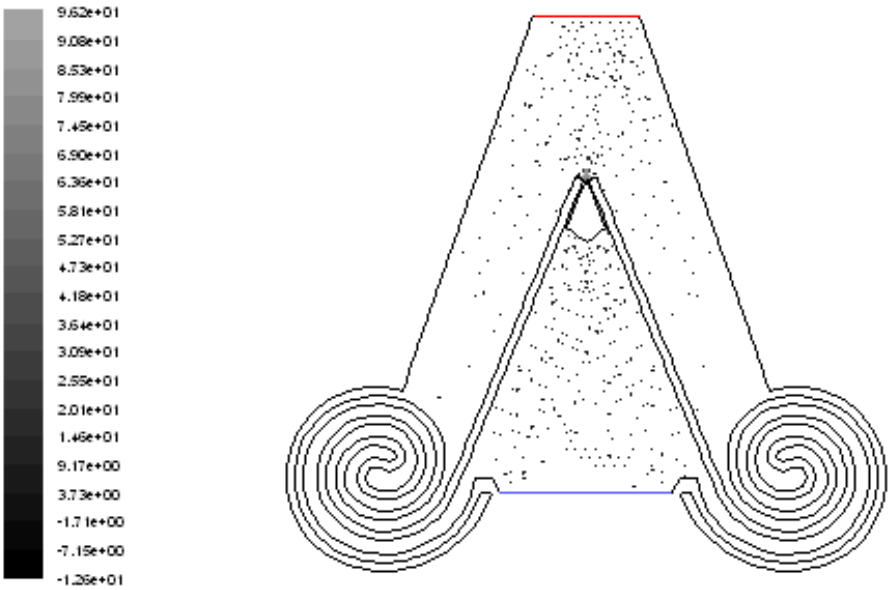

Figure C.13: Y velocity vectors on the proposed model (5 µl/min) – 6.5 ms

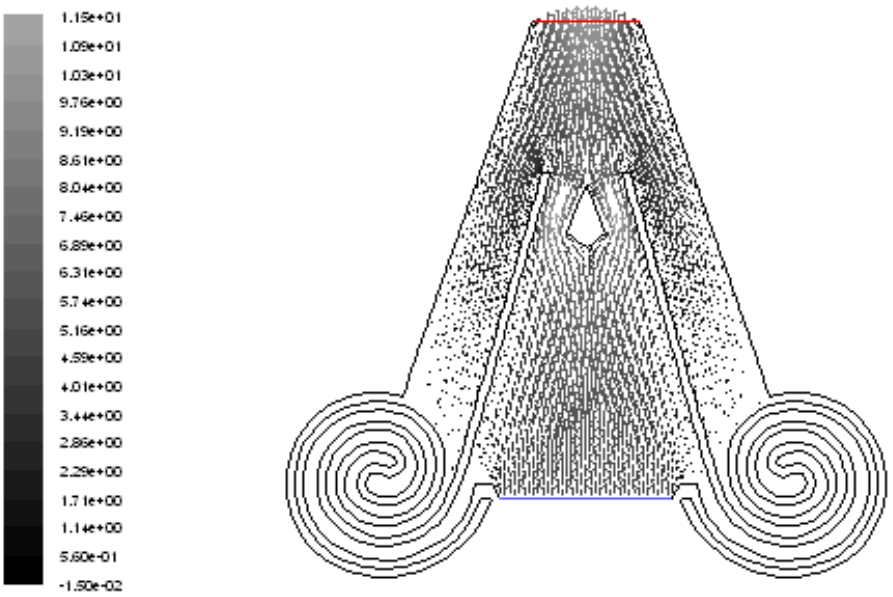

Figure C.14: Y velocity vectors on the proposed model (5 µl/min) - 117 ms

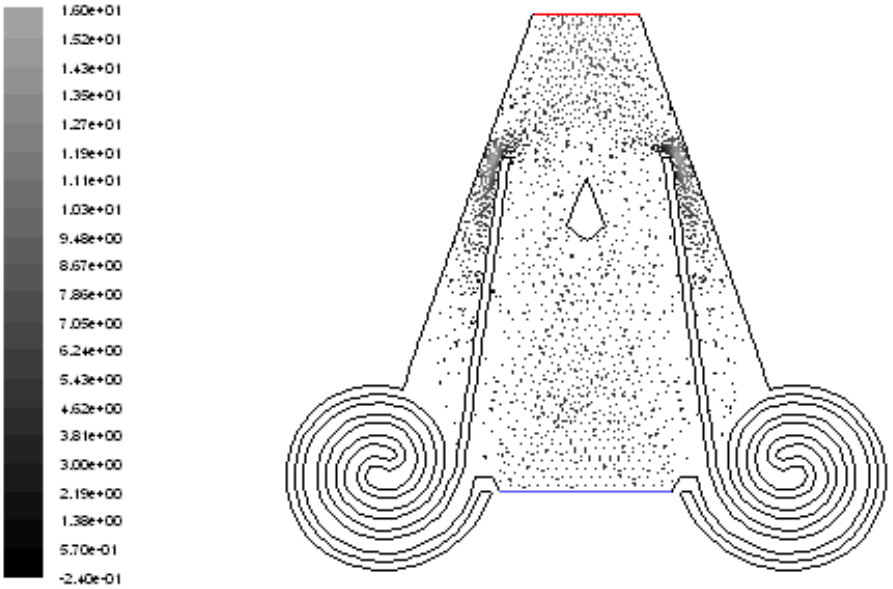

Figure C.15: Y velocity vectors on the proposed model (5 µl/min) - 247 ms

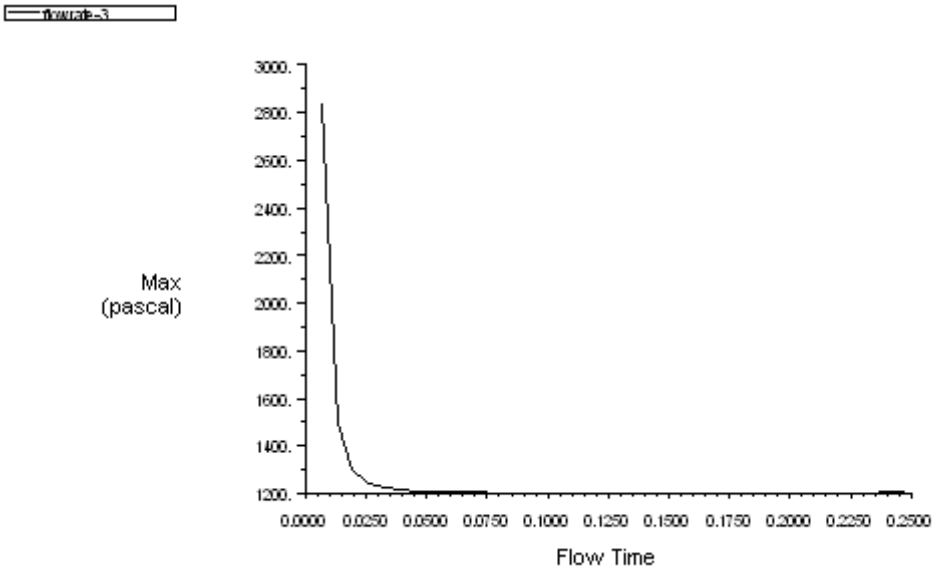

Figure C.16: Maximum pressure convergence on the proposed model (5 µl/min)

20 µl/min

FLUENT Summary Report File:

```
FLUENT
Version: 2d, dp, pbns, dynamesh, lam, unsteady (2d, double
precision, pressure-based, dynamic mesh, laminar, unsteady)
Release: 6.3.26
Title:

Models
------

   Model                         Settings
   ------------------------------------------------------------
   Space                         2D
   Time                          Unsteady, 1st-Order Implicit
   Viscous                       Laminar
   Heat Transfer                 Disabled
   Solidification and Melting    Disabled
   Species Transport             Disabled
   Coupled Dispersed Phase       Disabled
   Pollutants                    Disabled
   Pollutants                    Disabled
   Soot                          Disabled

Boundary Conditions
-------------------

   Zones

      name                id   type
      ---------------------------------------
      aq_humor            2    fluid
      wall                3    wall
      wall.5              4    wall
      fermat-spring.2     5    wall
      fermat-spring.1     6    wall
      velocity_inlet.2    7    velocity-inlet
      pressure_outlet.1   8    pressure-outlet
      default-interior    10   interior


Boundary Conditions                                    aq_humor


Condition                                                Value
------------------------------------------------------------------------
Material Name                                              test
Specify source terms?                                      no
Source Terms                                               ((mass)
                                                         (x-momentum)
                                                         (y-momentum)
)
Specify fixed values?                                      no
Local Coordinate System for Fixed Velocities               no
Fixed Values                                          (x-velocity
                                                     (inactive . #f)
                                                     (constant . 0)
                                                          profile  )) (y-
                                                    velocity (inactive .
```

	#f) (constant . 0) (profile))
Motion Type	0
X-Velocity Of Zone (m/s)	0
Y-Velocity Of Zone (m/s)	0
Rotation speed (rad/s)	0
X-Origin of Rotation-Axis (mm)	0
Y-Origin of Rotation-Axis (mm)	0
X-Component of Rotation-Axis	0
Y-Component of Rotation-Axis	0
Deactivated Thread	no
Porous zone?	no
Conical porous zone?	no
X-Component of Direction-1 Vector	1
Y-Component of Direction-1 Vector	0
X-Component of Direction-2 Vector	0
Y-Component of Direction-2 Vector	1
X-Component of Cone Axis Vector	1
Y-Component of Cone Axis Vector	0
X-Coordinate of Point on Cone Axis (mm)	1
Y-Coordinate of Point on Cone Axis (mm)	0
Half Angle of Cone Relative to its Axis (deg)	0
Relative Velocity Resistance Formulation?	yes
Direction-1 Viscous Resistance (1/m2)	0
Direction-2 Viscous Resistance (1/m2)	0
Choose alternative formulation for inertial resistance?	no
Direction-1 Inertial Resistance (1/m)	0
Direction-2 Inertial Resistance (1/m)	0
C0 Coefficient for Power-Law	0
C1 Coefficient for Power-Law	0
Porosity	1

wall

Condition	Value
Wall Motion	0
Shear Boundary Condition	0
Define wall motion relative to adjacent cell zone?	yes
Apply a rotational velocity to this wall?	no
Velocity Magnitude (mm/s)	0
X-Component of Wall Translation	1
Y-Component of Wall Translation	0
Define wall velocity components?	no
X-Component of Wall Translation (mm/s)	0
Y-Component of Wall Translation (mm/s)	0
Rotation Speed (rad/s)	0
X-Position of Rotation-Axis Origin (mm)	0
Y-Position of Rotation-Axis Origin (mm)	0
X-component of shear stress (pascal)	0
Y-component of shear stress (pascal)	0
Specularity Coefficient	0

wall.5

Condition	Value
Wall Motion	0
Shear Boundary Condition	0
Define wall motion relative to adjacent cell zone?	yes
Apply a rotational velocity to this wall?	no

Velocity Magnitude (mm/s)	0
X-Component of Wall Translation	1
Y-Component of Wall Translation	0
Define wall velocity components?	no
X-Component of Wall Translation (mm/s)	0
Y-Component of Wall Translation (mm/s)	0
Rotation Speed (rad/s)	0
X-Position of Rotation-Axis Origin (mm)	0
Y-Position of Rotation-Axis Origin (mm)	0
X-component of shear stress (pascal)	0
Y-component of shear stress (pascal)	0
Specularity Coefficient	0

fermat-spring.2

Condition	Value
Wall Motion	0
Shear Boundary Condition	0
Define wall motion relative to adjacent cell zone?	yes
Apply a rotational velocity to this wall?	no
Velocity Magnitude (mm/s)	0
X-Component of Wall Translation	1
Y-Component of Wall Translation	0
Define wall velocity components?	no
X-Component of Wall Translation (mm/s)	0
Y-Component of Wall Translation (mm/s)	0
Rotation Speed (rad/s)	0
X-Position of Rotation-Axis Origin (mm)	0
Y-Position of Rotation-Axis Origin (mm)	0
X-component of shear stress (pascal)	0
Y-component of shear stress (pascal)	0
Specularity Coefficient	0

fermat-spring.1

Condition	Value
Wall Motion	0
Shear Boundary Condition	0
Define wall motion relative to adjacent cell zone?	yes
Apply a rotational velocity to this wall?	no
Velocity Magnitude (mm/s)	0
X-Component of Wall Translation	1
Y-Component of Wall Translation	0
Define wall velocity components?	no
X-Component of Wall Translation (mm/s)	0
Y-Component of Wall Translation (mm/s)	0
Rotation Speed (rad/s)	0
X-Position of Rotation-Axis Origin (mm)	0
Y-Position of Rotation-Axis Origin (mm)	0
X-component of shear stress (pascal)	0
Y-component of shear stress (pascal)	0
Specularity Coefficient	0

velocity_inlet.2

Condition	Value
Velocity Specification Method	2
Reference Frame	0
Velocity Magnitude (mm/s)	0.020000001
X-Velocity (mm/s)	0

```
      Y-Velocity (mm/s)                     0
      X-Component of Flow Direction         1
      Y-Component of Flow Direction         0
      X-Component of Axis Direction         1
      Y-Component of Axis Direction         0
      Z-Component of Axis Direction         0
      X-Coordinate of Axis Origin (mm)      0
      Y-Coordinate of Axis Origin (mm)      0
      Z-Coordinate of Axis Origin (mm)      0
      Angular velocity (rad/s)              0
      is zone used in mixing-plane model?   no

   pressure_outlet.1

      Condition                                  Value
      -------------------------------------------------
      Gauge Pressure (pascal)                    1200
      Backflow Direction Specification Method    1
      X-Component of Flow Direction              1
      Y-Component of Flow Direction              0
      X-Component of Axis Direction              1
      Y-Component of Axis Direction              0
      Z-Component of Axis Direction              0
      X-Coordinate of Axis Origin (mm)           0
      Y-Coordinate of Axis Origin (mm)           0
      Z-Coordinate of Axis Origin (mm)           0
      is zone used in mixing-plane model?        no
      Specify targeted mass flow rate            no
      Targeted mass flow (kg/s)                  1

   default-interior

      Condition   Value
      -----------------

Solver Controls
---------------

   Equations

      Equation   Solved
      -----------------
      Flow       yes

   Numerics

      Numeric                            Enabled
      ---------------------------------------
      Absolute Velocity Formulation      yes

   Unsteady Calculation Parameters


      ---------------------------------------
      Time Step (s)                      0.0123
      Max. Iterations Per Time Step      20

   Relaxation

      Variable      Relaxation Factor
      --------------------------------
      Pressure      0.3
      Density       1
```

Body Forces 1
Momentum 0.7

Linear Solver

Variable	Solver Type	Termination Criterion	Residual Reduction Tolerance
Pressure	V-Cycle	0.1	
X-Momentum	Flexible	0.1	0.7
Y-Momentum	Flexible	0.1	0.7

Pressure-Velocity Coupling

Parameter	Value
Type	SIMPLE

Discretization Scheme

Variable	Scheme
Pressure	Standard
Momentum	First Order Upwind

Solution Limits

Quantity	Limit
Minimum Absolute Pressure	1
Maximum Absolute Pressure	5e+10
Minimum Temperature	1
Maximum Temperature	5000

Material Properties

Material: test (fluid)

Property	Units	Method	Value(s)
Density	kg/m3	constant	1000
Cp (Specific Heat)	j/kg-k	constant	4200
Thermal Conductivity	w/m-k	constant	0.58
Viscosity	kg/m-s	constant	0.001
Molecular Weight	kg/kgmol	constant	28
L-J Characteristic Length	angstrom	constant	0
L-J Energy Parameter	k	constant	0
Thermal Expansion Coefficient	1/k	constant	0
Degrees of Freedom		constant	0
Speed of Sound	mm/s	none	#f

Material: air (fluid)

Property	Units	Method	Value(s)
Density	kg/m3	constant	1.225
Cp (Specific Heat)	j/kg-k	constant	1006.43
Thermal Conductivity	w/m-k	constant	0.0242
Viscosity	kg/m-s	constant	1.78e-05
Molecular Weight	kg/kgmol	constant	28.966
L-J Characteristic Length	angstrom	constant	3.711
L-J Energy Parameter	k	constant	78.6

```
      Thermal Expansion Coefficient   1/k          constant   0
      Degrees of Freedom                           constant   0
      Speed of Sound                  mm/s         none       #f

   Material: aluminum (solid)

      Property                Units     Method     Value(s)
      ------------------------------------------------------
      Density                 kg/m3     constant   2719
      Cp (Specific Heat)      j/kg-k    constant   871
      Thermal Conductivity    w/m-k     constant   202.4

                              "Volume Integral Report"
                              Min
                  Static Pressure                (pascal)
-------------------------------- --------------------
                        new_fluid             1147.1800
                              Max
                  Static Pressure                (pascal)
-------------------------------- --------------------
                        new_fluid             3354.7420

                           "Flux Report"

                   Mass Flow Rate                   (kg/s)
-------------------------------- --------------------
                 default-interior           0.003563574
                  fermat-spring.1                     0
                  fermat-spring.2                     0
                pressure_outlet.1        -3.3682046e-08
                 velocity_inlet.2         3.3679022e-08
                             wall                     0
                           wall.5                     0
                ---------------- --------------------
                              Net        -3.0234278e-11
```

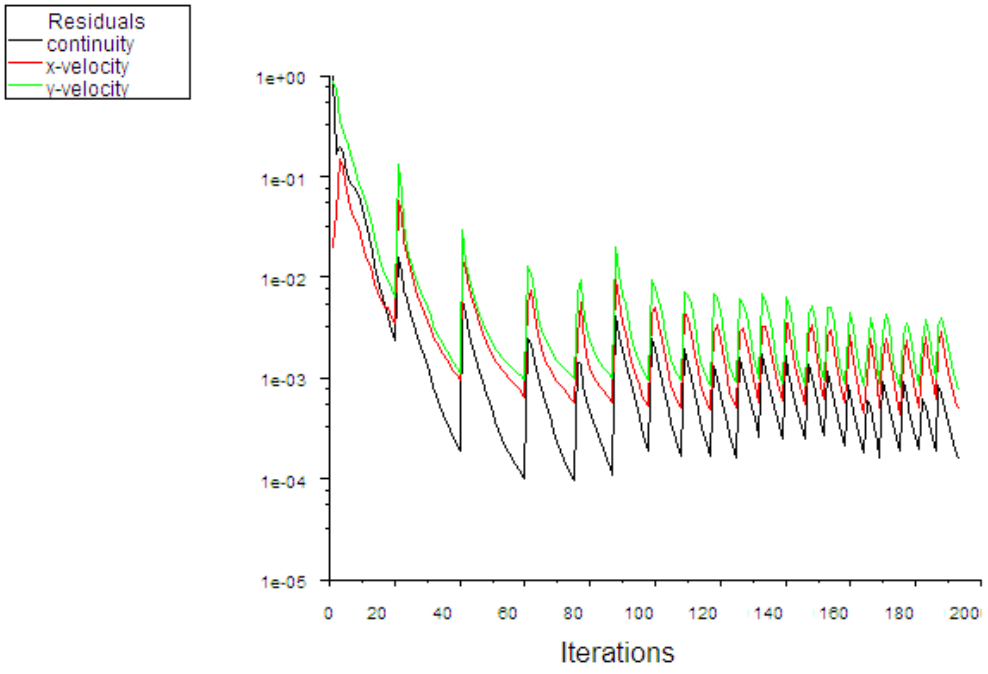

Figure C.17: Convergence results of the proposed model (20 µl/min)

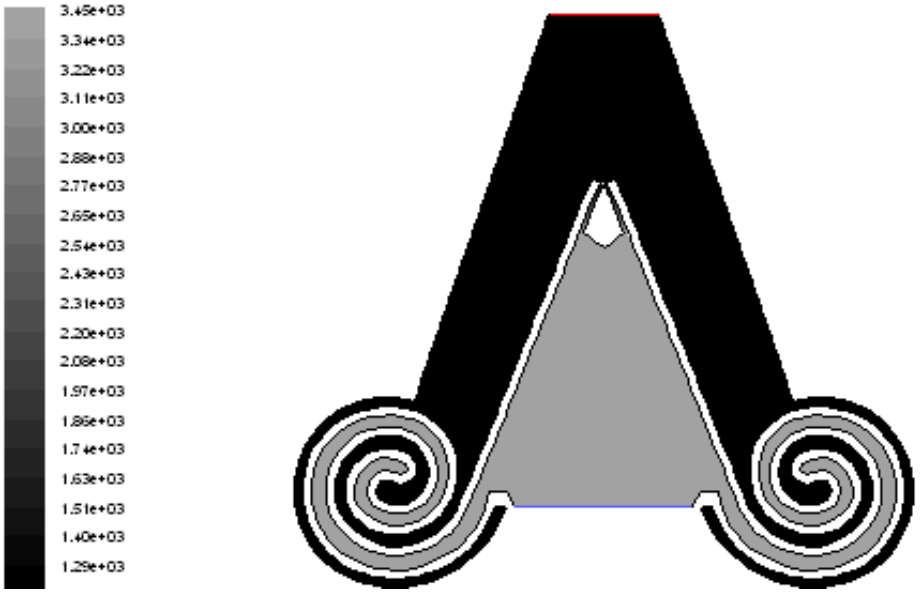

Figure C.18: Contours of static pressure on the proposed Model (20 µl/min)-12.3 ms

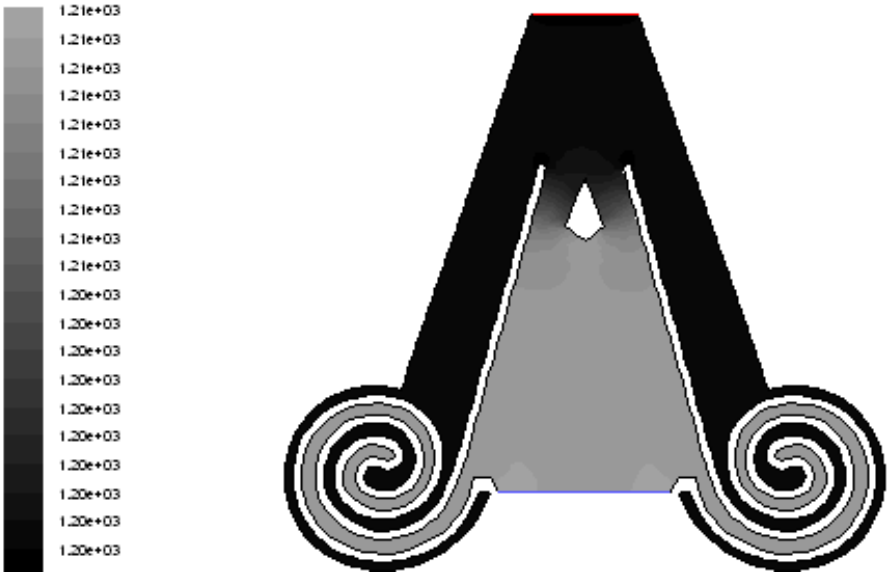

Figure C.19: Contours of static pressure on the proposed model (20 µl/min) - 123 ms

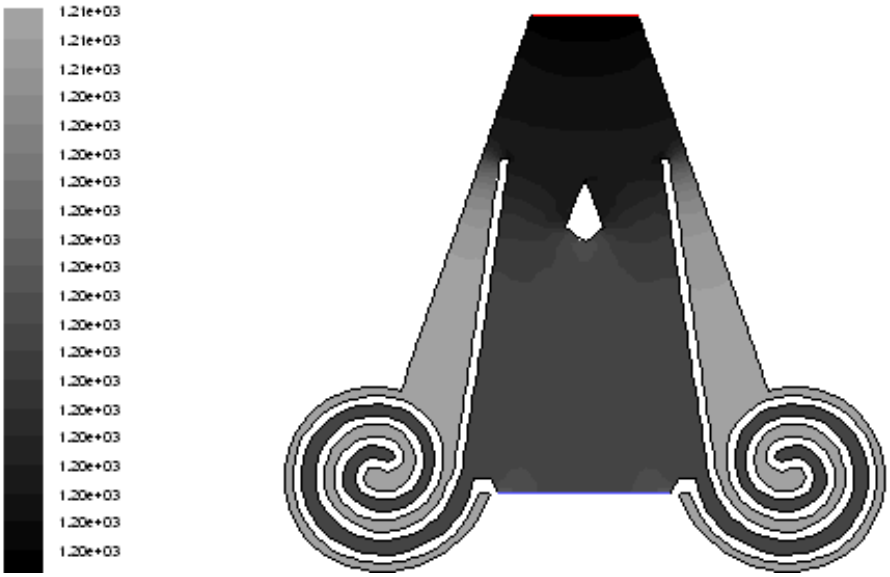

Figure C.20: Contours of static pressure on the proposed model (20 µl/min) - 246 ms

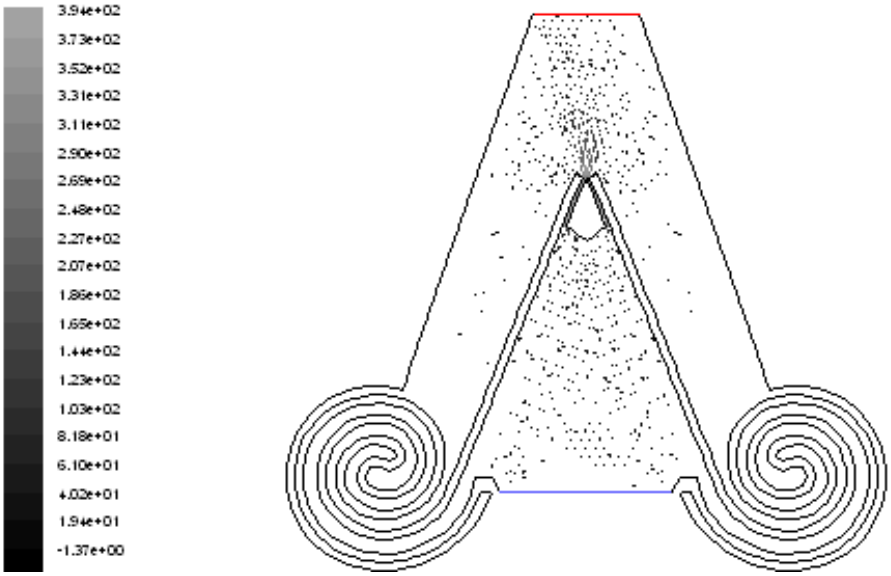

Figure C.21: Y velocity vectors on the proposed model (20 µl/min) -12.3 ms

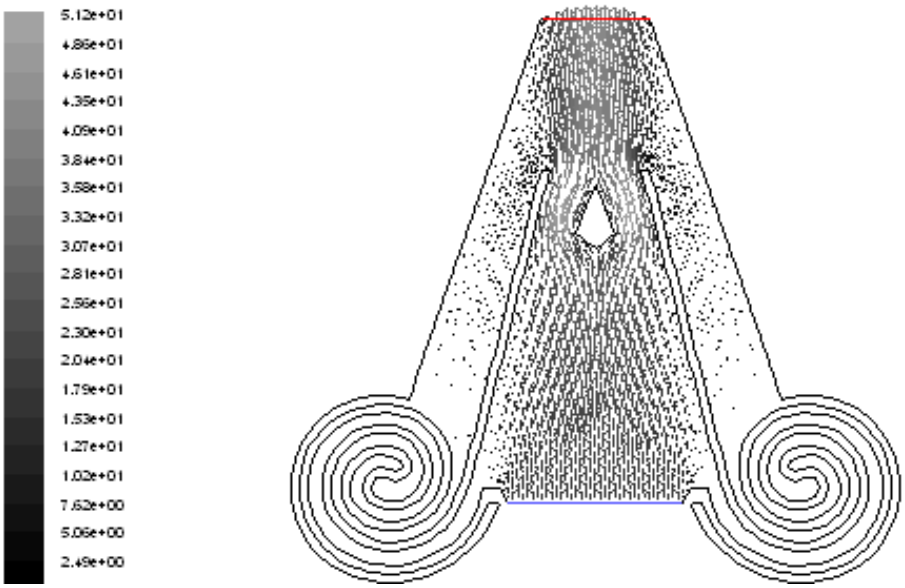

Figure C.22: Y velocity vectors on the proposed model (20 µl/min) – 147.6 ms

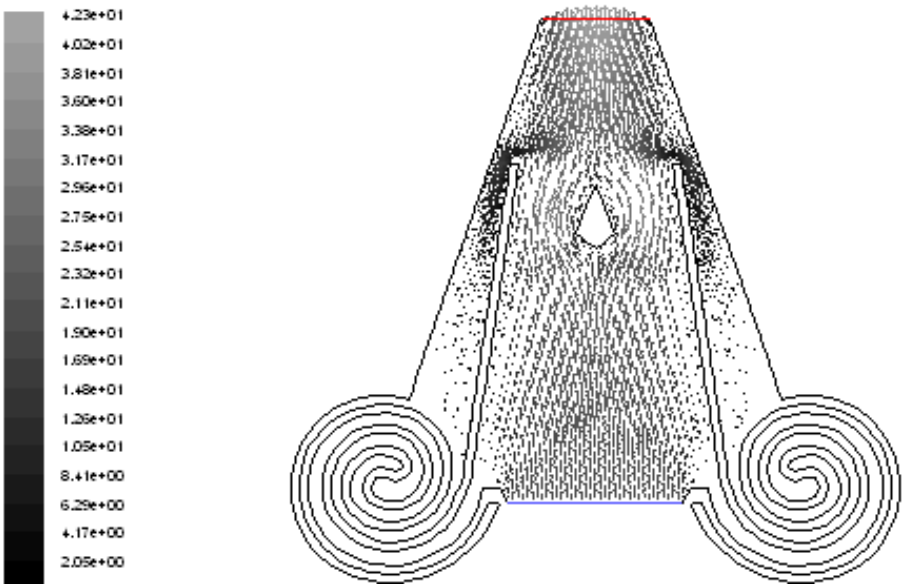

Figure C.23: Y velocity vectors on the proposed model (20 µl/min) - 246 ms

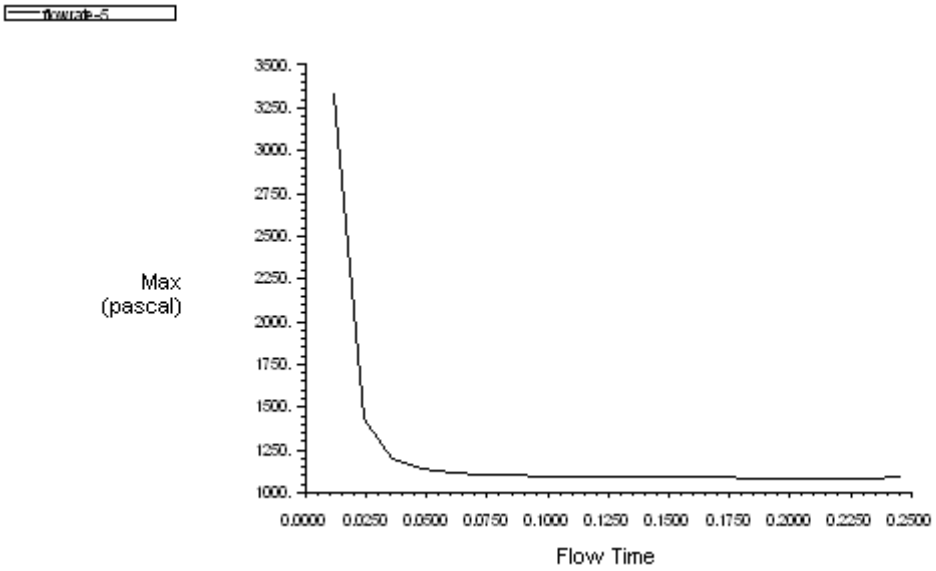

Figure C.24: Maximum pressure convergence on the proposed model (20 µl/min)

REFERENCES

[1] http://www.who.int/mediacentre/factsheets/fs282/en/

[2] Lim K.S., Allan B.D.S., and Lloyd A.W. (1998). Glaucoma drainage devices: past, present, and future. *Br J Ophthalmol*, **82**, 1083–1089.

[3] Rollet M. (1906). Le drainage au irin de la chambre anterieure contre l`hypertonie et al. douleur. *Rev Gen Ophthalmol.,* **25**, 481.

[4] Pan T., Liz Z., Brown J.D., and Ziaie B. (2003, September 17-21). Microfluidic characterization of a valved glaucoma drainage device with implications for enhanced therapeutic efficacy. *Proceedings of the 25th Annual lnternational Conference of the IEEE EMBS*. Cancun, Mexico.

[5] Pan T., Stay M.S, Barocas V.H., Brown J.D., and Ziaie B. (2005, May). Modeling and characterization of a valved glaucoma drainage device with implications for enhanced therapeutic efficacy. *IEEE Transactions on Biomedical Engineering, Vol. 52*, **5.**

[6] Pan T., Brown J.D., Ziaie B. (2002, October 23-26). A microfluid test-bed with nanopore membranes for in-vitro simulation of flow characteristics of glaucoma drainage devices. *24th Annual Conference and the Annual Fall Meeting of the Biomedical Engineering Society EMBS/BMES Conference, Proceedings of the Second Joint, Vol.3*, 1830-1831.

[7] Ho-Shing D. (2000, June). Treating Glaucoma with Drainage Devices and Pericardial Grafts. *AORN Journal, Vol. 71*, **6**, 1234-1251.

[8] Jyoti G.K. (2006, November 16). Numerical Solution of Flow Resistance In Outflow Pathway And Intravitreal Drug Delivery In Vitrectomised Eyes Mechanical Engineering. M.S. Thesis, Louisiana State University.

[9] http://www.nyee.edu/pdf/solomonaqhumor.pdf

[10] Kumar S. (2001) Numerical Solution of Ocular Fluid Dynamics. M.S. Thesis, Indian Institute of Technology.

[11] Guyton A.C., and Hall J.E. (Eds.). (1996) *Textbook of Medical Physiology*. Philadelphia, Pennsylvania: W.B. Saunders Company.

[12] Varma R., Minckler D.S. (1996) *Anatomy and Pathophysiology of the Retina and Optic Nerve: The GIaucomas.* St. Louis, Missouri: Mosby-Year Book Inc.

[13] Werner E.B. (1996) *Normal-Tension Glaucoma: The Glaucomas.* St. Louis, Missouri: Mosby-Year Book Inc.

[14] http://www.emedicine.com/oph/topic720.htm

[15] Molteno A.C.B. (1969). New implant for drainage in glaucoma: clinical trial. Br *J Ophthalmol.,* **53,** 606-615.

[16] http://www.molteno.com/technical.html

[17] Sidoti P.A., Minckler D.S., Baerveldt G., Lee P.P. and Heuer D.K. (1994). Epithelial ingrowth and glaucoma drainage implants. *Ophthalmology*, **101**, 872–875.

[18] Englert J.A., Freedman S.F., Cox T.A. (1999). The Ahmed valve glaucoma implant in refractory paediatric glaucoma. *Am J Ophthalmol.,* **127**, 34–42.

[19] Quang H.N. (2004). Avoiding and managing complications of glaucoma drainage implants. *Current Opinion in Ophthalmology*, **15**, 147–150.

[20] Ayyala R.S., Duarte J.L., Şahiner N. (2006, July). Glaucoma drainage devices: state of the art. *Expert Review of Medical Devices, Vol. 3*, **4**, 509-521.

[21] http://inhealth.org/MediaCenter/
Duke_Final_Report_F___Sensory_Diseases__Vision_.pdf

[22] Freedman J. (2006, October). Update on Tube-Shunt Procedures for Glaucoma. *Essentials in Ophthalmology*, 173-185.

[23] Krupin T., Mandell A., Ritch R., Asseff C., Podos S.M., Becker B. (1980). Filtering valve implant surgery for eyes with neovascular glaucoma. *Am J Ophthalmol.,* **89**, 338-343.

[24] http://www.ahmedvalve.com/resources/ProductBrochure.pdf

[25] biomed.brown.edu/Courses/BI108/2006108websites/group02glaucoma

[26] Hong C.H., Arosemena A., Zurakowski D., Ayyala R.S. (2005). Glaucoma drainage devices: a systematic literature review and current controversies. *Surv Ophthalmol.* **50**, 48-60.

[27] Noecker R., and Kahook M. (2006). Glaucoma drainage devices. *Techniques in Ophthalmology*, **4(2)**, 69–73.

[28] Lai J.S., Poon A.S., Chua J.K., Tham C.C., Leung A.T., and Lam D.S. (2000). Efficacy and safety of the Ahmed glaucoma valve implant in Chinese eyes with complicated glaucoma. *Br J Ophthalmol,* **84,** 718–721.

[29] Wilson M.R., Mendis U., Smith S.D., and Paliwal A. (2000). Ahmed glaucoma valve implant vs trabeculectomy in the surgical treatment of glaucoma: a randomized clinical trial. *Am J Ophthalmol.*, **130**, 267–273.

[30] Ayyala R.S., Zurakowski D., Smith J.A., Monshizadeh R., Netland P.A., Richards D.W., Layden W.E. (1998). A clinical study of the Ahmed glaucoma valve implant in advanced glaucoma. *Ophthalmology,* **105**,1968–1976.

[31] Ayyala R.S., Zurakowski D., Monshizadeh R., Hong C.H., Richards D., Layden W.E., Hutchinson B.T., and Bellows A.R. (2002). Comparison of double-plate Molteno and Ahmed glaucoma valve in patients with advanced uncontrolled glaucoma. *Ophthalmic Surg Lasers*, **33,** 94–101.

[32] Fellenbaum P.S., Almeida A.R., Minckler D.S., Sidoti P.A., Baerveldt G., and Heuer D.K. (1994). Krupin disk implantation for complicated glaucomas. *Ophthalmology*, **101,** 1178–1182.

[33] Schwartza K.S., Leeb R.K., and Geddeb S.J. (2006). Glaucoma drainage implants: a critical comparison of types. *Current Opinion in Ophthalmology,* **17**, 181–189.

[34] Kee C. (2001). Prevention of Early Postoperative Hypotony by Partial Ligation of Silicone Tube in Ahmed Glaucoma Valve Implantation. *Journal of Glaucoma,* **10**, 466–469.

[35] Prata J.A., Mermoud A., LaBree L., Minckler D.S. (1995). In vitro and in vivo flow characteristics of glaucoma drainage implants. *Ophthalmology,* **102**, 894–904.

[36] Francis B.A., Cortes A., Chen J., Alvarado J.A. (1998, September 1) Characteristics of glaucoma drainage implants during dynamic and steady-state flow conditions. *Ophthalmology, Vol. 105*, **9,** 1708-1714.

[37] The AGFID Project Team (2001). Experimental flow studies in glaucoma drainage device development. *Br J Ophthalmol*, **85**, 1231-123.

[38] Traverso C.E.,De Feo F., Messas-Kaplan A.,Denis P., Levartovsky P., Selem E.,Badalà F.,Zagorski Z., Bron A.,Beklin M. (2005). Long term effect on IOP of a stainless steel glaucoma drainage implant (Ex-PRESS) in combined surgery with phacoemulsification. *Br J Ophthalmol*, **89**, 425–429.

[39] Nyska A.,Glovinsky Y.,Belkin M., and Epstein Y. (2003). Biocompatibility of the Ex-PRESS Miniature Glaucoma Drainage Implant. *Journal of Glaucoma*, **12**, 275–280.

[40] Traverso C.E., Kaplan-Messas A., Belkin M. and The International Ex-PRESS Study Group. (2001). The Ex-PRESS miniature glaucoma implant: Intermediate results of a prospective multi-center study. *Invest Ophthalmol Vis Sci.*, **42**, 552.

[41] Wamsley S., Moster M.R., Rai S., Alvim H.S., Fontanarosa J. (2004, December). Results of the use of the Ex-PRESS miniature glaucoma implant in technically challenging, advanced glaucoma cases: A clinical pilot study. *American Journal of Ophthalmology*, *Vol. 138*, **6**, 1049-1051.

[42] http://pergatory.mit.edu/pwilloughby/docs/glaucoma_final_report.pdf

[43] Papautsky I., Amel T.A., and Frazier A.B. (2001, November). A review of laminar single-phase flow in microchannels. *ASME International Mechanical Engineering Congress & Exposition*, New York, 1-9.

[44] Aksel H. (2003, September). *Fluid Mechanics Textbook*. *Vol 1*. (3^{rd} ed.). Ankara: Department of Mechanical Engineering, METU Press.

[45] Stay M.S., Pan T., Brown J.D.,Ziaie B., and Barocas V.H. (2005). Thin-film coupled fluid-solid analysis of flow through the Ahmed glaucoma drainage device. *Journal of Biomechanical Engineering*, 1-6.

[46] McEwen W.K. (1958, August). Application of Poiseuille's law to aqueous outflow. *AMA Arch Ophthalmology*, **60**, 290-294.

[47] Shields M.B. (1992). *Textbook of glaucoma.* (3rd ed.). Maryland: Williams & Wilkins.

[48] Pan J.Y., Lin P., Maseeh F., Senturia S.D. (1990). Verification of FEM analysis of load-deflection methods for measuring mechanical properties of thin films. *IEEE Solid-State Sensor and Actuator Workshop,* 70-74.

[49] Tabata O., Kawahata K., Sugiyama S., Igarashi I. (1989, February). Mechanical property measurements of thin films using load-deflection of composite rectangular membrane. *Proc. IEEE Workshop on Microelectromechanical Systems*, 152-156.

[50] FLUENT Inc., editor. GAMBIT 2.4 Documentation: User's guide. *FLUENT Inc.*, Lebanon, 2003.

[51] FLUENT Inc., editor. GAMBIT 2.4 Documentation: Modeling guide. *FLUENT Inc.*, Lebanon, 2003.

[52] FLUENT Inc., editor. FLUENT 6.3 Documentation: User's guide. *FLUENT Inc.*, Lebanon, 2003.

[53] FLUENT Inc., editor. FLUENT 6.3 Documentation: Modeling guide. *FLUENT Inc.*, Lebanon, 2003.

[54] Geschke O., Klank H., Tellemann P. (2003). *Microsystem Engineering of Lab-on-a-chip Devices* (1st ed.). Weinheim:John Wiley & Sons, 43-44.

[55] http://www.bartels-mikrotechnik.de/downloads/GB_Microvalve_rev4.pdf

[56] Wang H.H., Liu K.C., Ko K.C., Yang L.J. (2005), The Parylene Bowed-Type Valves, *Tamkang Journal of Science and Engineering, Vol. 8,* **3**, 245-248

[57] Kwang W. O., Chong H. A. (2006), A Review of Microvalves, *J. Micromech. Microeng.* , Vol 16, R13-R16

[58] www.me.berkeley.edu/ME219/Lectures/L32ME219.pdf